

Analysis of the Ichnology, Depositional Environment of the Middle Cambrian Mount Whyte
Formation, Alberta, Canada

by

Chundi Shan

A thesis submitted in partial fulfillment of the requirements for the degree of

Master of Science

Department of Earth and Atmospheric Sciences
University of Alberta

© Chundi Shan, 2023

ABSTRACT

The Mount Whyte Formation is a prominent unit of the Middle Cambrian period in the Western Canada Sedimentary Basin (WCSB). This formation is widely distributed throughout the region and comprises both clastic and carbonate rock, deposited as part of a Middle Cambrian platform. In the Southern Rocky Mountains and Western Alberta Plains, the Mount Whyte Formation is situated unconformably on top of the Gog Group, whereas on the eastern side, it is found on top of the Basal sandstone.

The first study will specifically focus on the clastic portion of the Mount Whyte Formation and draw interpretations from the sedimentology and ichnology data available. Within these formations, several trace fossils have been identified, including *Planolites*, *Cylindrichnus*, *Teichichnus*, *Skolithos*, *Arenicolites*, *Diplocraterion*, and *Rhizocorallium*, with *Planolites* being the most representative ichnofossil present. An interpretation of the depositional environment of the Mount Whyte Formation is provided. The Mount Whyte Formation was formed by shallow marine deposits during the Middle Cambrian, which consists of shale, siltstone sandstone, interrupted by limestone beds. Based on the trace fossils suits, and sedimentological feature (lithology, grain size and structure), this formation was deposited in a zone from upper offshore to middle shoreface.

In a second study, three cores (1-6-38-15W4, 1-34-57-22W4 and 6-36-19-1W4) were logged to understand red bed distributions in these formations. Samples were subjected to both sedimentary and geochemical analyses. The former involved determining mineralogy, grain size, structure, sphericity, and ichnology data, which helped establish sedimentary facies. The resulting facies indicate a shoreface depositional environment. Meanwhile, a Principal

Component Analysis (PCA) was performed on the geochemical data, which included high-resolution measurements of redox-sensitive elements such as molybdenum (Mo) and vanadium (V) sampled at one-meter intervals. Analysis of process ichnology data, including bioturbation index, burrow diameter, diversity, and size diversity index, combined with the geochemical results, suggests that redox conditions did not exist during deposition in the Mount Whyte Formation. These findings indicate no clear correlation between redox-sensitive elements and bioturbation. As such, the formation of the red beds are ascribed to diagenesis.

PREFACE

This thesis is an original work by Chundi Shan. No part of this thesis has been previously published. The research project was designed by my supervisor M.K. Gingras.

DEDICATION

This thesis is dedicated to my family: Zhong Cao, Jucheng Shan, Lu cao and Shuxian Li.

Thanks for your love, support and encouragement.

ACKNOWLEDGMENTS

About 4 years ago, I was conducting scientific research with the Ichnology Research Group in fulfillment of my undergraduate thesis. Throughout this research, I have developed a strong interest in sedimentology and ichnology. The undergraduate project is, in essence, an interpretation of the depositional environments of the Middle Cambrian succession in East-Central plains of Alberta. I am particularly keen to join the Ichnology Research Group in the department of Earth and Atmospheric at University of Alberta, a world-leading research group in the topics I am interested in. Also, I have so many nice memories of fieldwork, lab field trips, field schools, Friday beers, road trips, short courses.

I would foremost like to thank my supervisor, Murray Gingras who believes in me, develops my geological knowledge, and most importantly, supports me finishing this work during the pandemic period. I am eternally grateful for the knowledge you have all passed onto me, and the support that has been provided through the years. Thanks to Tiffany Playter and Hilary Corlett and Kurt Konhauser for all the help.

Thank you to my office and lab mates through the years: Qi Chen, Chenyang Feng, Scott Melnyk, Arzu Acikelli, Brette Harris, Sara Biddle, Maya LaGrange Rao, Maria Rodriguez, Carolyn Marie Furlong, Waqar Ahmad, and Jiahui Gao. I will forever treasure the skills you taught me and the advice you give me.

Thanks, the members of Dan Alessi' lab for supporting me finished all of the geochemistry experiments. Especially Katherine Snihur and Konstantin Von Gunte who taught me how to do the digestion and helped me use ICP MS.

Thanks Dr. Liu, Guosheng from Heifei University of Technology for providing some opportunities for field trips in China.

TABLE OF CONTENTS

ABSTRACT.....	ii
PREFACE	iv
DEDICATION	v
ACKNOWLEDGMENTS	vi
TABLE OF CONTENTS	viii
LIST OF TABLES	x
LIST OF FIGURES	xi
LIST OF ABBREVIATIONS.....	xviii
CHAPTER 1: INTRODUCTION	1
CHAPTER 2 : ICHNOLOGY ANALYSIS FOR SEDIMENTARY FACIES OF MOUNT WHYTE FORMATION IN SOUTHWEST ALBERTA CANADA.....	6
1.Introduction.....	6
2.Geological background	7
3.Methodology	9
3.1 Field work	9
3.2 Photogrammetry.....	9
3.3 Preparing of samples	10
4.Results.....	10
4.1 Observation from outcrop	10
4.2 Observation from samples	16
5. Facies Analysis and interpretation	16
6. Discussion and Conclusion	42
CHAPTER 3: CORE AND GEOCHEMICAL ANALYSIS FOR MIDDLE CAMBRIAN MOUNT WHYTE FORMATION	44
1.Introduction.....	44
1.1 Geological Setting.....	44
2. Methodology	45
2.1 Sampling	45
2.2 Sedimentary & Ichnology Data.....	46
2.3 Geochemical Data.....	46
3. Result	48
3.1 Sedimentary and Ichnology	48

3.2 Geochemical Result	52
3.3 Relationship between elemental and ichnology data	52
3.4 Principal Component Analysis.....	56
4. Interpretation.....	69
4.1 Sedimentology and ichnology interpretation	69
4.2 Interpretation from Geochemical dataset	72
5. Conclusion	74
CHAPTER 4: SUMMARY AND CONCLUSIONS.....	75
REFERENCES	77
APPENDIX I: OBSERVATION OF OUTCROP ONE (OUTCROP CS200806A).....	81
APPENDIX II: ICHNOLOGY DATA COLLECTION FORMS	83
APPENDIX III: GEOCHEMISTRY RESULT	84
APPENDIX IV: EIGENVECTORS TABLES	85

LIST OF TABLES

Table 1. Classification and interpretation of micro-bioturbation.....	29
Table 2. Facies table of the Mount Whyte Formation in Nordegg area (Outcrop CS200806A, CS200807A and CS200808A).....	32
Table 3. Facies table of Wells 1-34-57-22W4 and 6-36-19-01W4 and 1-06-38-15W4.....	47

LIST OF FIGURES

Figure 1. Idealized stratigraphic column showing the distribution of Cambrian strata across Alberta. Note that the Mount Whyte formation is Middle Cambrian in age and is variably overlain by the Cathedral, Stephen, and Earlie formations. Modified from Slind et al. 2020.....	2
Figure 2. Paleogeographic reconstruction of Laurentia during the Middle Cambrian. The red box indicates the approximate outline of study area within present-day Alberta, Canada. From Ron Blakey (2011).....	3
Figure 3. The red marker is the approximate location of the study Area of outcrop. Reconstruction courtesy of GoogleEarth.	8
Figure 4. Litholog illustrating the sedimentological and ichnological characteristics of Outcrop CS200806A (O1). It is dominated by heavily bioturbated, planar laminated fine-grained sandstone (Facies 1) and nodular mudstone interbedded with wavy-parallel laminated fine-grained sandstone (Facies 2).	12
Figure 5. Orthomosaic of Outcrop CS200806A showing the lateral continuity of the beds and changes in bedding thickness across the outcrop.....	13
Figure 6. Litholog illustrating the sedimentological and ichnological characteristics of Outcrop CS200807A (O2). It contains massive to bioturbated fine-grained sandstone interbedded with shale (Facies 3), bioturbated, sharp-based, silty sandstone interstratified with mm-scale shale laminae (Facies 4), and sharp-based, fine-grained sandstone interbedded with shale (Facies 5).	14
Figure 7. Litholog illustrating the sedimentological and ichnological characteristics of Outcrop CS200808A (O3). It consists of bioturbated sharp-based silty sandstone interbedded with shale (Facies 4), bioturbated, sharp-based parallel laminated fine-grained sandstone interbedded with	

shale (Facies 5) and bioturbated hummocky cross-stratified fine-grained sandstone interbedded with shale (Facies 6). 15

Figure 8. Thin sections under A) PPL and B) XPL of sample SC200806A1. It is well sorted and contains curved mud-lined burrows. The burrow orientation is horizontal and filled by finer sediment. Some wavy laminations are observed. 17

Figure 9. Thin sections under A) PPL and B) XPL of sample SC200806A2. It is well sorted and contains cylindrical mud-lined burrows and curved mud-filled burrows. The burrow orientation is horizontal. The mud-lined burrows are filled by host sediment and mud-filled burrows are filled by finer sediment. 18

Figure 10. Thin sections under A) PPL and B) XPL of sample SC200806A3. It is well sorted and contains curved mud-filled burrows. They are vertical burrows and filled by finer sediment. Parallel laminations are observed on this thin section. 19

Figure 11. Thin sections under A) PPL and B) XPL of sample SC200806A5. It is well sorted and contains cylindrical mud-lined burrows and curved/sinuuous mud-filled burrows. The burrow orientation is horizontal. The mud-lined burrows are filled by host sediment and mud-filled burrows are filled by finer sediment. 20

Figure 12. Thin sections under A) PPL and B) XPL of sample SC200806A8. It is well sorted and contains cylindrical mud-lined burrows and sinuous mud-filled burrows. The mud-lined burrows are horizontal burrows and filled by host sediment. The mud-filled burrows are filled by finer sediment and have both vertical and horizontal burrow orientation. 21

Figure 13. Thin sections under A) PPL and B) XPL of sample SC200806A10 bed view. It is well sorted and contains cylindrical mud-lined burrows and sinuous mud-filled burrows. The mud-

lined burrows are horizontal burrows and filled by host sediment. The mud-filled burrows are filled by finer sediment are horizontal burrows. 22

Figure 14. Thin sections under A) PPL and B) XPL of sample SC200806A10 side view. It is well sorted and contains cylindrical mud-lined burrows and curved mud-filled burrows. The mud-lined burrows are horizontal burrows and filled by host sediment. The mud-filled burrows are filled by finer sediment and have horizontal burrow orientation. 23

Figure 15. Thin sections under A) PPL and B) XPL of sample SC200806A11. It is well sorted and contains curved mud-filled burrows. They are vertical and horizontal burrows and filled by finer sediment. 24

Figure 16. Thin sections under A) PPL and B) XPL of sample SC200807A1. It is well sorted and contains cylindrical mud-lined burrows and straight mud-filled burrows. The mud-lined burrows are horizontal burrows and filled by host sediment. The mud-filled burrows are filled by finer sediment and both vertical and horizontal burrow orientation. Weak parallel laminations are observed on this thin section. 25

Figure 17. Thin sections under A) PPL and B) XPL of sample SC200807A5 bed view. It is well sorted and contains cylindrical mud-lined burrows and sinuous mud-filled burrows. The mud-lined burrows are horizontal burrows and filled by host sediment. The mud-filled burrows are filled by finer sediment are horizontal burrows. 26

Figure 18. Thin sections under A) PPL and B) XPL of sample SC200807A5 side view. It is well sorted and contains sinuous mud-filled burrows. They are vertical and horizontal burrows and filled by finer sediment. 27

Figure 19. Thin sections under A) PPL and B) XPL of sample SC200808A2. It is well sorted and contains cylindrical mud-lined burrows and sinuous mud-filled burrows. The mud-lined burrows

are horizontal burrows and filled by host sediment. The mud-filled burrows are filled by finer sediment are horizontal and vertical burrows. 28

Figure 20. Typical cylindrical mud-lined burrows in thin section CS200806A8 under PPL. The mud-lined burrows are filled by host sediment..... 30

Figure 21. Typical cylindrical and straight mud-filled burrows in thin section CS200806A1 under PPL. The mud-filled burrows are filled by finer sediment. 30

Figure 22. Photos of A) hand sample and B) outcrop for Facies 1: Heavily bioturbated, sharp-based, planar laminated fine sandstone interbedded with bioturbated upper fine sandstone. Note that the direction of stratigraphic 'way up' differs between A and B, as it is oriented upwards in A and to the left in B. Abbreviations: *Cy* = *Cylindrichnus*, *Pl* = *Planolites*, *Pa* = *Paleophycus*..... 33

Figure 23. Photos of A) hand sample and B) outcrop for Facies 2: Nodular mudstone interbedded with sporadically bioturbated wavy-parallel lamination fine sandstone, but they only include the sandstone part. Weak wavy-parallel and planar lamination can be found in both hand sample and outcrop. Note that the direction of stratigraphic 'way up' differs between A and B, as it is oriented to the left in A and upwards in B. Abbreviations: *Pl* = *Planolites*..... 35

Figure 24. Photos of A) hand sample and B) outcrop for Facies 3: Bioturbated massive fine grain sandstone interbedded with shale. Note that the direction of stratigraphic 'way up' differs between A and B, as it is oriented to the left in A and upwards in B. Abbreviations: *Cy* = *Cylindrichnus*, *Pl* = *Planolites*. 36

Figure 25. Photos of A) hand sample and B) outcrop for Facies 4: Bioturbated, sharp-based silty sandstone interbedded with mm scaled shale. A is the hand sample for the silty sandstone part and it is heavily bioturbated. *Cy*, *Pa*, *Pl*, *Ar* are appeared. B is an outcrop photo, which shows

silty sandstone with heavily bioturbation such as Rh and Ar. Abbreviations: *Ar* = *Arenicolites*, *Cy* = *Cylindrichnus*, *Pl* = *Planolites*, *Pa* = *Paleophycus*, Rh = *Rhizocorallium*. 38

Figure 26. Photos of A) hand sample and B) outcrop for Facies 5: Bioturbated parallel laminated fine sandstone interbedded with shale. A is the hand sample for the fine sandstone part and it is heavily bioturbated. *Cy* is the most common ichno-fossiles. In the outcrop photo, which shows parallel laminated on the fine sandstone unit. Abbreviations: *Cy* = *Cylindrichnus*, *Pl* = *Planolites*, *Pa* = *Paleophycus*. 39

Figure 27. Photos of A) hand sample and B) outcrop for Facies 6: Hummocky cross laminated bioturbated fine sandstone interbedded with shale. A is the hand sample for the fine sandstone with hummock laminations. The bedding is inclined and *Pl* and *Cy* can be found in this sample. B is an outcrop photo, which shows cross-laminated on the fine sandstone unit. Abbreviations: *Ar* = *Arenicolites*, *Cy* = *Cylindrichnus*, *Pl* = *Planolites*. 41

Figure 28. Strip log illustrating the sedimentological and ichnological characteristics of Well 01-06-038-15W4. It is dominated by very fine to fine-grained sandstone interbedded with mudstone (F1) and bioturbation shows low diversity and moderate intensity. 49

Figure 29. Strip log illustrating the sedimentological and ichnological characteristics of Well 01-34-057-22W4. It is dominated by is sandstone interbedded with mudstone (F1) and mudstone interbedded with very fine sand (F2). The Bioturbation shows low diversity and high intensity. 50

Figure 30. Strip log illustrating the sedimentological and ichnological characteristics of Well 06-36-019-01W4. It is dominated by sandstone interbedded with mudstone (F1) and heavily burrowed sandy mudstone (F4). The bioturbation shows low diversity and high intensity. 51

Figure 31. Thin sections under A) PPL and B) XPL of sample 19233 with 20X magnification. It has sub rounded quartz grain with moderate sorting. 53

Figure 32. Thin sections under A) PPL and B) XPL of sample 15903 with 20X magnification. It has sub rounded quartz and glauconite grain with good sorting..... 54

Figure 33. Thin sections under A) PPL and B) XPL of sample 15962 with 20X magnification. It has sub rounded quartz grain with good sorting. 55

Figure 34. Scatter chart of iron and molybdenum versus Size and Diversity Index (SDI) for well 06-36-019-01W4. The data show a lack of a strong correlation between both elements and SDI values. 57

Figure 35. Scatter chart of iron and molybdenum verse Size and Diversity Index (SDI) for well 01-06-038-15W4, which shows a random spread..... 58

Figure 36. Scatter chart of iron and molybdenum verse Size and Diversity Index (SDI) for well 01-34-057-22W4, which shows a random spread..... 59

Figure 37. Scatter chart of iron and molybdenum verse Bioturbation Index (BI) for well 01-34-057-22W4, which shows a random spread. 60

Figure 38. Scatter chart of iron and molybdenum verse Bioturbation Index (BI) for well 06-36-019-01W4, which shows a random spread. 61

Figure 39. Scatter chart of iron and molybdenum verse Bioturbation Index (BI) for well 01-06-038-15W4, which shows a random spread. 62

Figure 40. Compare between Fe and Mo concentration versus depth and bioturbation data *versus* depth. The light green color shows the concentration has the same trend with the bioturbation and light orange color shows they have opposite trend. Both trends can be found in the core 06-36-019-01W4. 63

Figure 41. Compare between Fe and Mo concentration versus depth and bioturbation data vs. depth. The lite green color shows the concentration has the same trend with the bioturbation and

light orange color shows they have opposite trend. Both trends can be found in the core 01-06-038-15W4. 64

Figure 42. Compare between Fe and Mo concentration versus depth and bioturbation data vs. depth. The lite green color shows the concentration has the same trend with the bioturbation and light orange color shows they have opposite trend. Both trends can be found in the core 01-06-038-15W4. 65

Figure 43. PCA result of Well 1-34-57-22W4 by using Eigenvectors 2 versus Eigenvectors 1. For PCA, the distance between two data points on the X-axis will determine the relationship between data points. Thus, in this well, compared to Mo and Cd, Fe has weaker relationship to SDI. 66

Figure 44. PCA result of Well 6-36-19-1W4 by using Eigenvectors 2 versus Eigenvectors 1. For PCA, the distance between two data points on the X-axis will determine the relationship between data points. Thus, in this well, compared to Mo and Cd, Fe has stronger relationship to SDI..... 67

Figure 45. PCA result of Well 1-6-38-15W4 by using Eigenvectors 2 vs Eigenvectors 1. For PCA, the distance between two data points on the X-axis will determine the relationship between data points. Thus, in this well, compared to Mo and Cd, Fe has weaker relationship to SDI. 68

LIST OF ABBREVIATIONS

ICHNOFOSSILS

Ar *Arenicolites*

Cy *Cylindrichnus*

Di *Diplocraterion*

Pl *Planolites*

Pa *Palaeophycus*

Ph *Phycosiphon*

Rh *Rhizocorallium*

Sk *Skolithos*

Te *Teichichnus*

Cr *Cruziana*

Mo *Monocraterion*

Ps *Psilonichnus*

CHAPTER 1: INTRODUCTION

The Western Canada Sedimentary Basin consists of a Phanerozoic wedge overlying a Precambrian crystalline basement (Mossop and Shetsen, 1994). According to Mossop and Shetsen (1994), the basin exhibits a northeastward tapering towards a zero-edge that abuts the Canadian Shield, while the strata within the basin are being cannibalized by the westward deformation front of the Cordillera. As a result, numerous subsurface equivalent layers have been exposed in the Canadian Rockies Mountains.

For The Mount Whyte Formation, only regional-scale research had been publicly available, which unfortunately lacked high-resolution facies analyses that incorporate ichnological observations. Slind et al. (2020) described a substantial sedimentary package deposited as a Middle Cambrian shallow marine system (Fig. 1). The formation is observed to unconformably rest on the Gog Formation in the western area, followed by deposition of the Cathedral Formation. On the other hand, in the eastern plains of Alberta, the Mount Whyte Formation transitions to the Earlie Formation above the Basal Sandstone unit (Slind et al., 2020).

The Mount Whyte Formation in the study area is observed to unconformably overlie the Gog Group and is conformably overlain by the Cathedral Formation, with the Stephen Formation on top, as described by Slind et al. (2020). There is no evidence of material from the Earlie Formation in the outcrop or drill cores. The sediments of the Alberta Plains during the Middle Cambrian period were deposited in a partially confined, epicontinental setting, with large amounts of siliciclastic material entering the shallow marine environment, as suggested by Aitken (1997) (Fig. 2). The interpretation of the depositional environment in this study supports

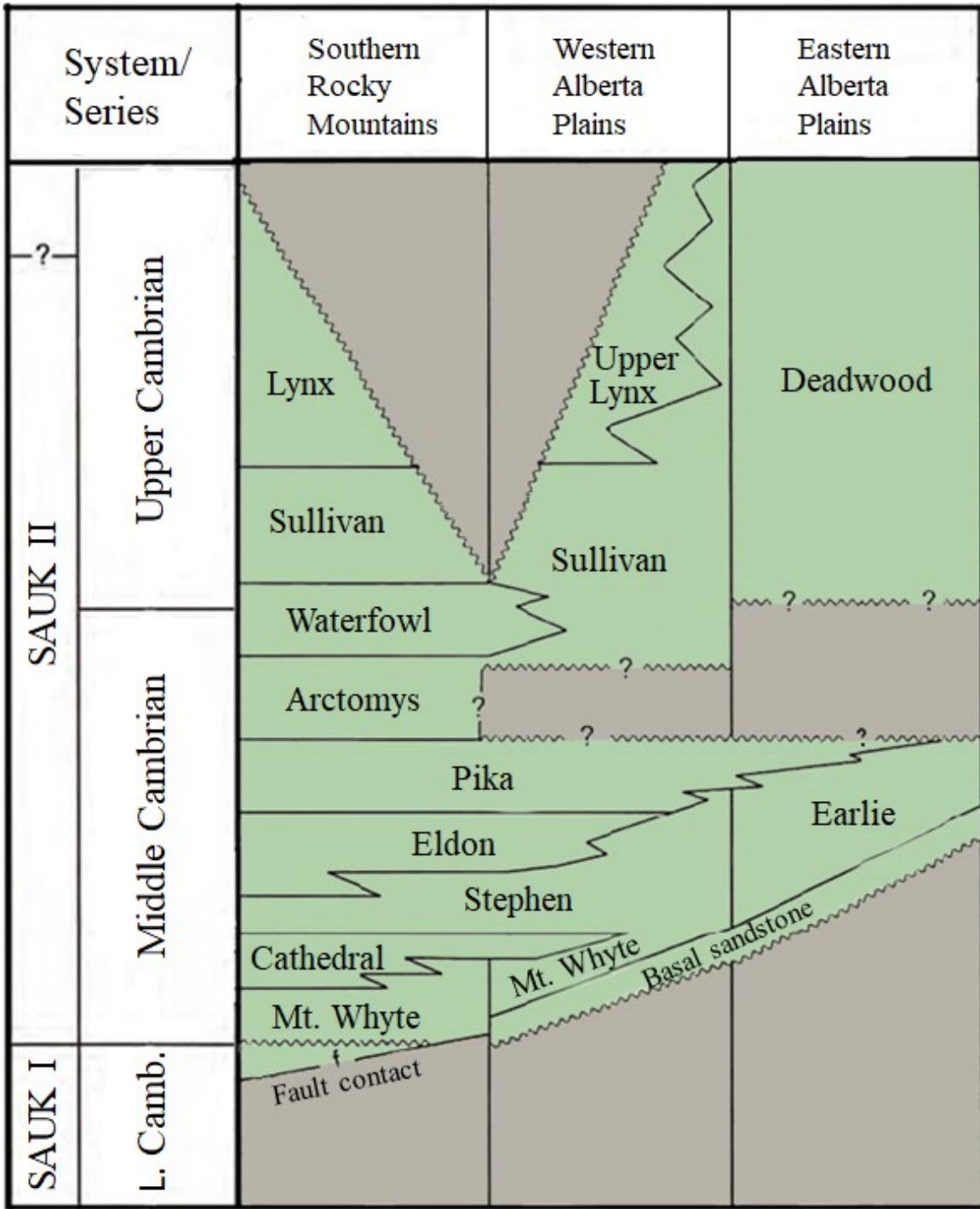


Figure 1. Idealized stratigraphic column showing the distribution of Cambrian strata across Alberta. Note that the Mount Whyte formation is Middle Cambrian in age and is variably overlain by the Cathedral, Stephen, and Earlie formations. Modified from Slind et al. 2020.

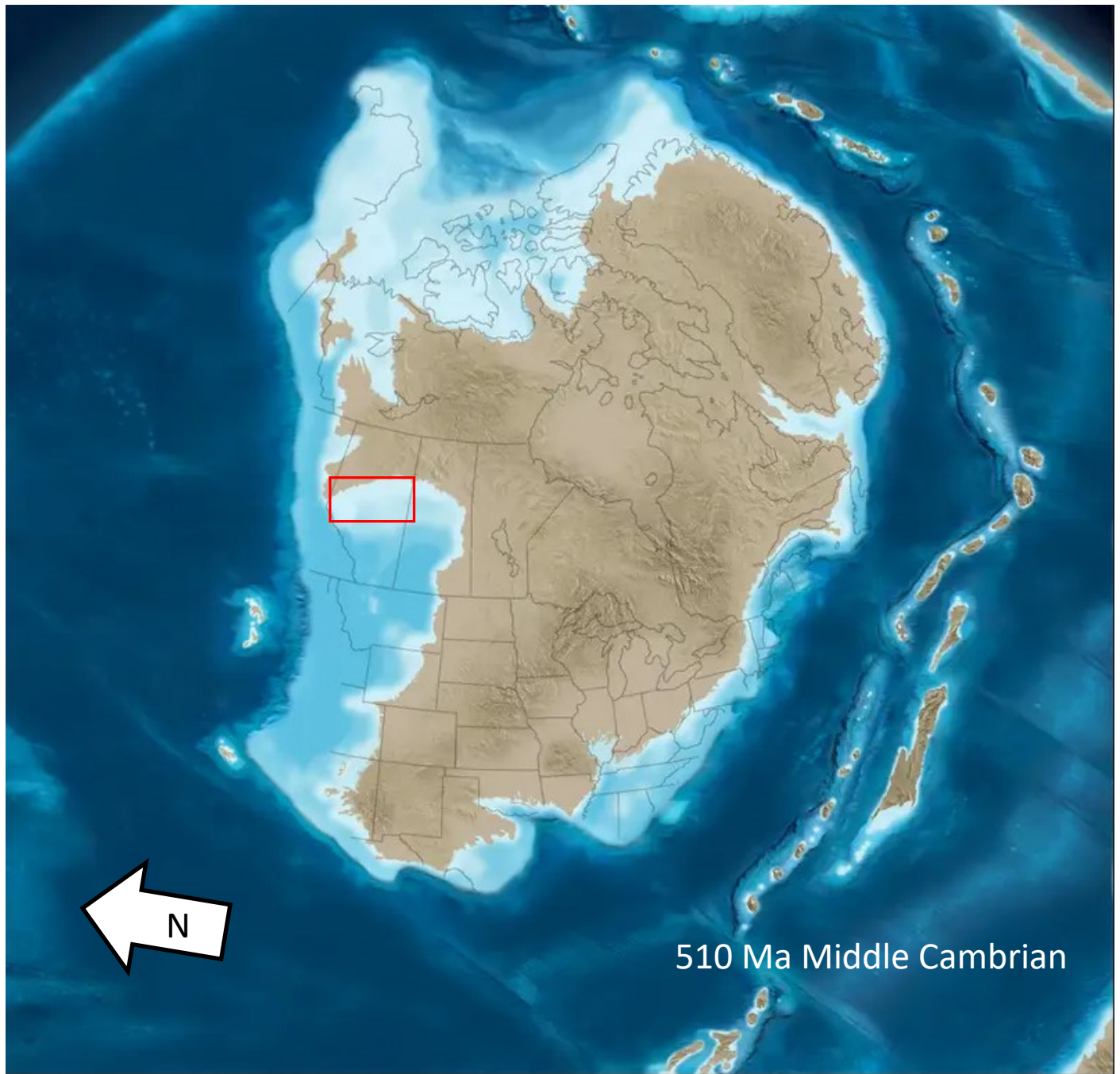


Figure 2. Paleogeographic reconstruction of Laurentia during the Middle Cambrian. The red box indicates the approximate outline of study area within present-day Alberta, Canada. From Ron Blakey (2011).

the idea that the Mount Whyte Formation was deposited in a proximal offshore to shoreface environment.

The study of fossil tracks and traces made by organisms in their ecosystems is known as ichnology, which is crucial for understanding sedimentology and analyzing hydrocarbon reservoirs (Pemberton et al., 2001). It is a valuable tool that can aid in solving various sedimentological problems. Ichnology has also become a valuable tool for understanding the physical and chemical variables of an ecosystem during and after deposition, as noted by Gingras et al. (2011).

The main objective of Chapter 2 is to use trace fossils as a means of interpreting depositional environments. This will be accomplished by employing a combination of physical sedimentology, such as lithology, grain size, and sedimentary structures, along with ichnology observations, including bioturbation intensity, ichnogenera, and ichno-diversity (Seilacher, 1978; Pemberton et al., 1992a; MacEachern, et al., 2010). The goal is to provide a higher resolution interpretation of specific paleo-environments.

Chapter 2 focuses on a depositional environment analysis of the trace fossil assemblages found in the outcrop datasets of the Mount Whyte Formation, utilizing both sedimentological and ichnological methods to interpret the clastic unit. The study area is located in the Nordegg region, situated in the southern Rocky Mountains of southwestern Alberta. The Mount Whyte Formation is observed to overlie the Lower Cambrian Gog Group with a distinct abrupt contact.

Chapter 3 focuses on analyzing data from three drill cores that cover formations from the Mount Whyte Formation to the Stephen Formation. Specifically, the study examines wells 1-34-57-22W4 and 6-36-19-01W4, which contain sedimentary material from the Mount Whyte

Formation, and well 1-06-38-15W4, which contains units from the Stephen and Cathedral Formations. The goal of this chapter is to interpret the depositional environments present in the drill cores, which represent a succession of shoreface environments influenced by storms, ranging from upper offshore to foreshore. Additionally, the chapter investigates whether there is a relationship between redox sensitive elements and bioturbation, using geochemical and sedimentological data to explain the formation of red beds.

CHAPTER 2 : ICHNOLOGY ANALYSIS FOR SEDIMENTARY FACIES OF MOUNT WHYTE FORMATION IN SOUTHWEST ALBERTA CANADA

1. Introduction

Ichnofacies is a term used to describe a group of trace fossils that are found together in a particular sedimentary environment and are indicative of specific environmental conditions. These trace fossils can be used to interpret the paleoenvironmental conditions and processes that existed during deposition (Seilacher, 1962, 1978). Ichnofacies is useful to describe the depositional environment from shallow marine to deep water; furthermore, it can provide a high-resolution sedimentological interpretation (Gingras et al., 2011). The concept of "process ichnology" involves using observations of biogenic sedimentary structures to interpret or estimate physical and chemical stresses in the sedimentary environment, as outlined by Gingras et al. (2011). These stresses can be either physical, such as sedimentation rates and substrate consistency, or chemical, such as salinity and oxygen levels. Important observations include bioturbation characteristics such as diversity, intensity, burrow size, and burrow lining, which can be used to calculate a Bioturbation Index (BI) that ranges from 0 (unburrowed) to 6 (biogenic homogenization). In addition, a Size Diversity Index (SDI) can be calculated by multiplying diversity by the largest observed burrow diameter, which is generally used as a proxy for salinity and oxygen stress (Wignall and Myers, 1988; Hauck et al., 2009).

The Mount Whyte Formation outcrop in eastern Alberta primarily comprises clastic rocks like sandstone, mudstone, and shale, exhibiting sedimentary structures and trace fossils that indicate a marine depositional environment. This makes it an ideal candidate for ichnological analysis to study facies and depositional environments. Various types of trace fossils are

identified in the Mount Whyte Formation, with some appearing sporadically and others commonly found in most rock units. There are some common ichnofossil (trace fossil) in Mount Whyte formation: *Skolithos*, *Planolites*, *Diplocraterion*, *Cylindrichnus*, *Teichichnus*, *Palaeophycus*, *Rhizocorallium*, *Phycosiphon*, *Arenicolites*. Also, there are some undiagnosed hook-like mud-lined burrows that bear similarities to small *Cylindrichnus*. Previous studies on Mount Whyte Formation have mainly focused on carbonate rocks in southern Alberta, and none of them have utilized the ichnology method to aid in facies identification and the interpretation of ancient depositional environments. The present study aims to provide such an interpretation for the clastic unit of Mount Whyte formation by employing both sedimentology and ichnology.

2. Geological background

The Mount Whyte Formation is located in the Western Canada Sedimentary Basin which was formed by shallow marine deposits during the Middle Cambrian and it is a mappable unit consisting of shale, siltstone, sandstone and limestone (Aitken, 1997). It belongs to a thick sedimentary package that was deposited as a Middle Cambrian platform (Slind et al., 2020). The formation can be subdivided into three distinct members: the upper member consists of shale interbedded with oolitic limestone; the middle member consists of shale containing thinly bedded sandstone and conglomerate that transitions to impure limestone at its upper boundary; and the basal member is characterized by thinly bedded limestone and sandy limestone with lenticular deposits of pebbly sandstone and shale interbeds (Chrisite et al., 1981). The geological setting of Mount Whyte Formation is unconformably on the top of the Gog Group, and conformably overlain by the Cathedral Formation (Slind et al., 2020). The study area is in the Nordegg area, which is located in the southern Rocky Mountains of southwestern Alberta (Fig. 3). The studied outcrops of the Mount Whyte Formation overlie the Lower Cambrian Gog Group with a sharp

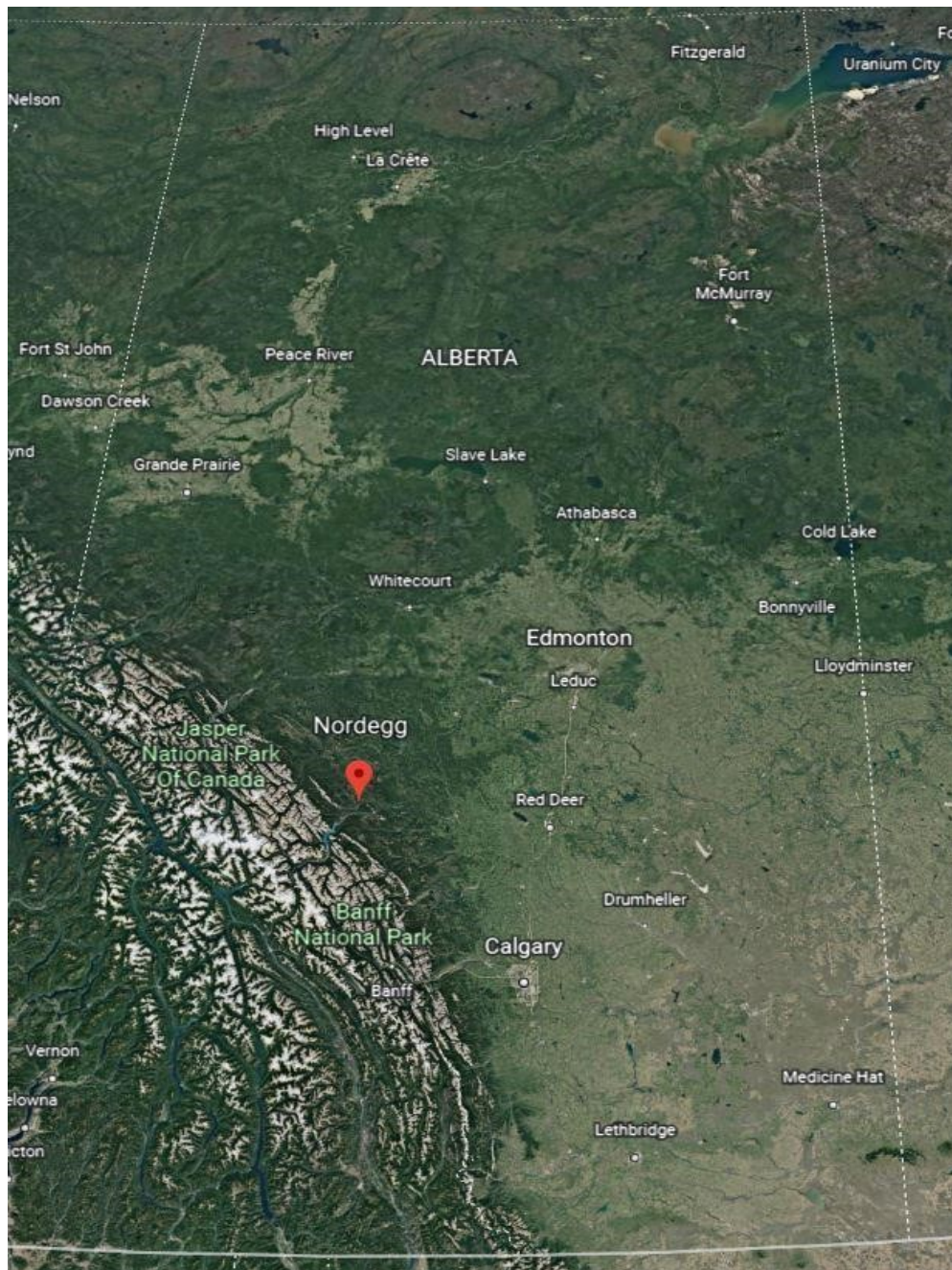


Figure 3. The red marker is the approximate location of the study Area of outcrop. Reconstruction courtesy of GoogleEarth.

contact and the (upper) Cathedral Formation contact is not observed. The outcrops that are discussed in this study should form the Basal member of the Mount Whyte Formation.

3. Methodology

3.1 Field work

In the field, three outcrops are observed, and they are CS200806A, CS200807A and CS200808A. For each location, outcrop was studied for color, grain size, sedimentary structure, bioturbation, bedding thickness, contact and accessory sedimentary features. A litho-log is provided for each outcrop. The strip log summarizes the lithology, grain size, and sedimentary structures for each outcrop, as well as information on biogenic structures such as the Bioturbation Index (BI) and ichnofossil species. In addition, sedimentary facies were identified for this formation.

Each outcrop is sampled by selecting samples containing typical trace fossils or sedimentary structures. Digital photos are taken of specific features such as trace fossils and sedimentary structures for each outcrop using a digital camera, while panorama photos of the entire outcrop CS200806A are taken using a DJI Mavic Pro quadrotor drone.

3.2 Photogrammetry

A 3D model of outcrop CS200806A was created using Agisoft Metashape Professional © modeling software. Photos and panorama photos of the outcrop were taken with a digital camera and DJI Mavic Pro quadrotor drone. The point dense cloud technique was used to align photos and generate meshes, which were then textured. An orthomosaic was created, resulting in a complete 3D model. To measure strike and dip data of each bedding plane, dense markers were

added to label each bed on the model. These measurements could then be compared to those taken in the field.

3.3 Preparing of samples

Twenty-one rock samples were collected from the outcrops and hand samples were prepared from them. To prepare hand samples, a rock saw was used to cut a flat surface along both parallel and perpendicular directions to the bedding surface. Then, these surfaces were polished using a grinding machine. High-resolution photos were taken using a Digital Single Lens Reflex camera and a scanner to record both sedimentary and biogenic structures. However, some small sedimentary structures and cryptical bioturbation cannot be observed in the field or by using hand samples. Therefore, twelve thin sections were made to observe these features in detail at the micro-level. If a hand sample did not have clear beddings or other sedimentary structures, and it was not possible to observe biogenic structures, this sample was considered to have a high BI value (around 6) or cryptical bioturbation. The thin sections were prepared by cutting and polishing the remaining parts of the hand samples, and no dyeing methods were applied. Photos were taken by scanning these thin sections to make observations.

4. Results

4.1 Observation from outcrop

Description of Outcrop CS200806A (O1): For outcrop one, CS200806A, (O1), data was collected meter to meter and there are 18 data points, from the bottom to the top, because the thickness of O1 is too thick to collect data from every bed (Table. 4, in the appendix). O1 has a fining upward trend of grain size and consists of fine sandstone at the bottom and the mudstone with fine sandstone interbeds. The bioturbation does not appear in all beds to show the feature of

low diversity, but if a bed contains burrows, it will have a moderate to high bioturbation intensity (BI>3). The most common sedimentary structure is planar lamination/bedding (Fig. 4). A Photogrammetric Model (Fig. 5) shows bedding, lateral continuity of beds, bed thickness variations laterally and vertically, and some aspects of structure (Fig. 5).

Description of Outcrop CS200807A (O2): Outcrop CS200807A (O2) of the Mount Whyte Formation can be described as having a greenish grey color with rust color weathering on the surface. The formation can be observed to start from a thin shale layer overlying the Gog sandstone with a sharp contact and then gradually changes to silty sandstone interbedded with shale. Further up, it changes to fine sandstone interbedded with silty sandstone and shale, and finally ends with shale interbedded with fine sandstone. Planar lamination/bedding is the most common sedimentary structure observed, with some parallel wavy lamination present in O2. The bioturbation is not obvious on the side view, with only Ar, Ph and some dark color unknown burrows being found. However, Pl can be observed in abundance on the top view, indicating heavy burrowing in some parts. Like O1, nodules also appear in silty sandstone (Refer to Fig. 6 for more details).

Description of Outcrop CS200808A (O3): The outcrop displays a greenish grey color with rust-colored weathering on the surface. The lowermost layer consists of fine-grained sandstone with muddy lamination. Above it, there is a shale layer followed by a layer of burrowed fine-grained sandstone. Further up, a silty sandstone with wavy lamination can be observed. The dominant lithology from here to the top is fine-grained sandstone interbedded with shale, with muddy parallel wavy lamination prevailing.

The O3 is characterized by planar-to-wavy-parallel lamination, while clear hummocky cross lamination and cross lamination can be observed towards the top of the outcrop. In terms of

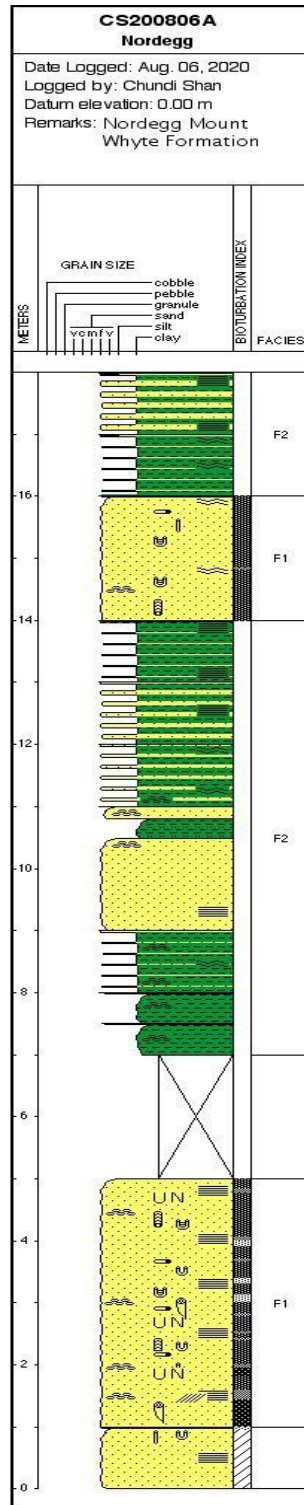


Figure 4. Litholog illustrating the sedimentological and ichnological characteristics of Outcrop CS200806A (O1). It is dominated by heavily bioturbated, planar laminated fine-grained sandstone (Facies 1) and nodular mudstone interbedded with wavy-parallel laminated fine-grained sandstone (Facies 2).



Figure 5. Orthomosaic of Outcrop CS200806A showing the lateral continuity of the beds and changes in bedding thickness across the outcrop.

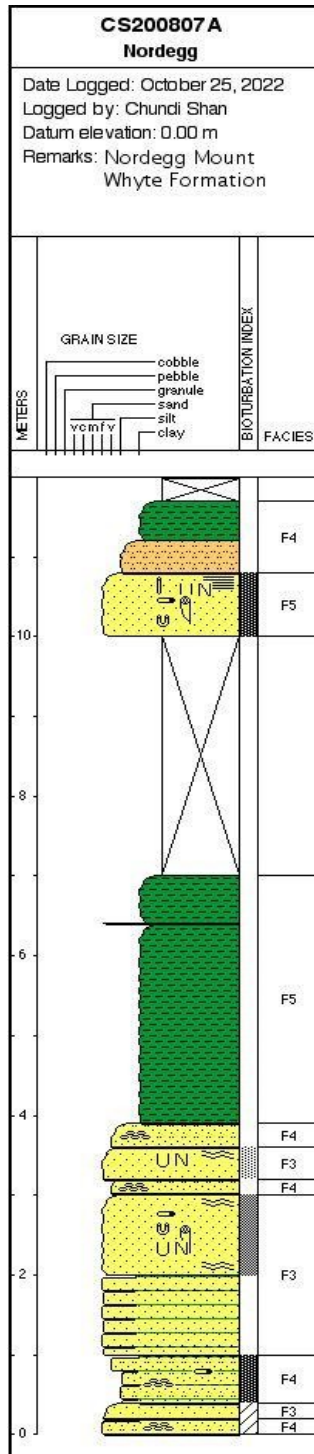


Figure 6. Litholog illustrating the sedimentological and ichnological characteristics of Outcrop CS200807A (O2). It contains massive to bioturbated fine-grained sandstone interbedded with shale (Facies 3), bioturbated, sharp-based, silty sandstone interstratified with mm-scale shale laminae (Facies 4), and sharp-based, fine-grained sandstone interbedded with shale (Facies 5).

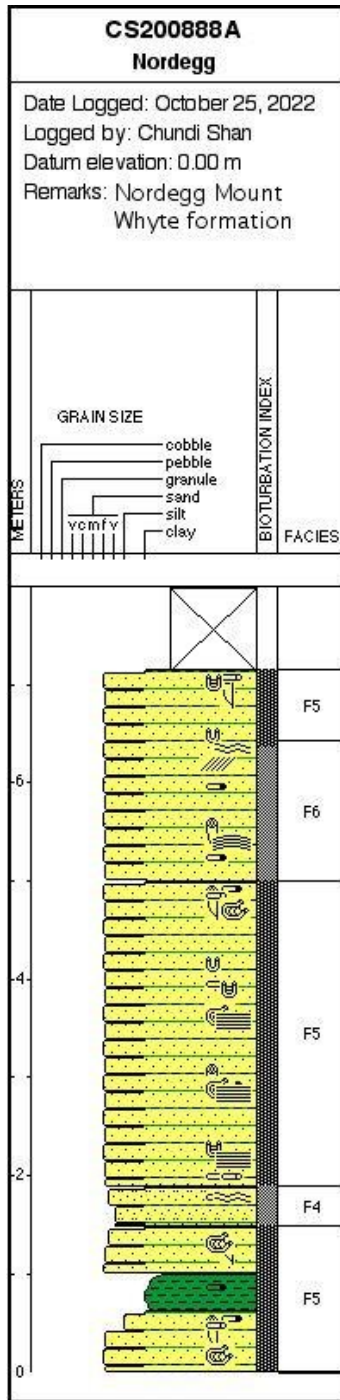


Figure 7. Litholog illustrating the sedimentological and ichnological characteristics of Outcrop CS200808A (O3). It consists of bioturbated sharp-based silty sandstone interbedded with shale (Facies 4), bioturbated, sharp-based parallel laminated fine-grained sandstone interbedded with shale (Facies 5) and bioturbated hummocky cross-stratified fine-grained sandstone interbedded with shale (Facies 6).

bioturbation, most beds in O3 exhibit heavy bioturbation ($BI \geq 4$), and the diversity of bioturbation is greater than that of O2. On the side view, Pl, Pa, Rh, and Cy can be easily identified, while on the top view, Ar and Di can be observed (Fig. 7).

4.2 Observation from samples

A total of 21 hand samples were obtained from the outcrop, providing more detailed information for the observations made in the field. The trace fossils found in the samples were of particular importance. Most of the samples contained bioturbation, with Pl, Cy, and Te being the most commonly observed ichnofossil types. The lithology of the samples ranged from silty sandstone to fine sandstone, and showed distinct planar lamination and cross-lamination.

Thin sections were prepared (as shown in Fig. 8 to Fig. 19) to identify cryptic/micro bioturbation and mineralogy under both Plain Polarized Light (PPL) and Crossed Polarized Light (XPL). Quartz was found to be the most common mineral, with calcite cement present between quartz grains. Two main types of micro-burrows were identified in the Mount Whyte formation. The first type, mud-lined burrows, were the most common in thin sections. These burrows had a relatively large diameter and contained brown mud sediment. The second type, mud-filled burrows, were less common but still present in some thin sections, appearing as small brown mud dots of varying sizes. All thin sections showed very-well sorting and no sedimentary structures, suggesting they were completely homogenized and indicating slow or episodic sedimentation rates. The presence of micro-burrows did not appear to indicate any significant physical or chemical stress (Table 1 and Fig. 20 and Fig. 21).

5. Facies Analysis and interpretation

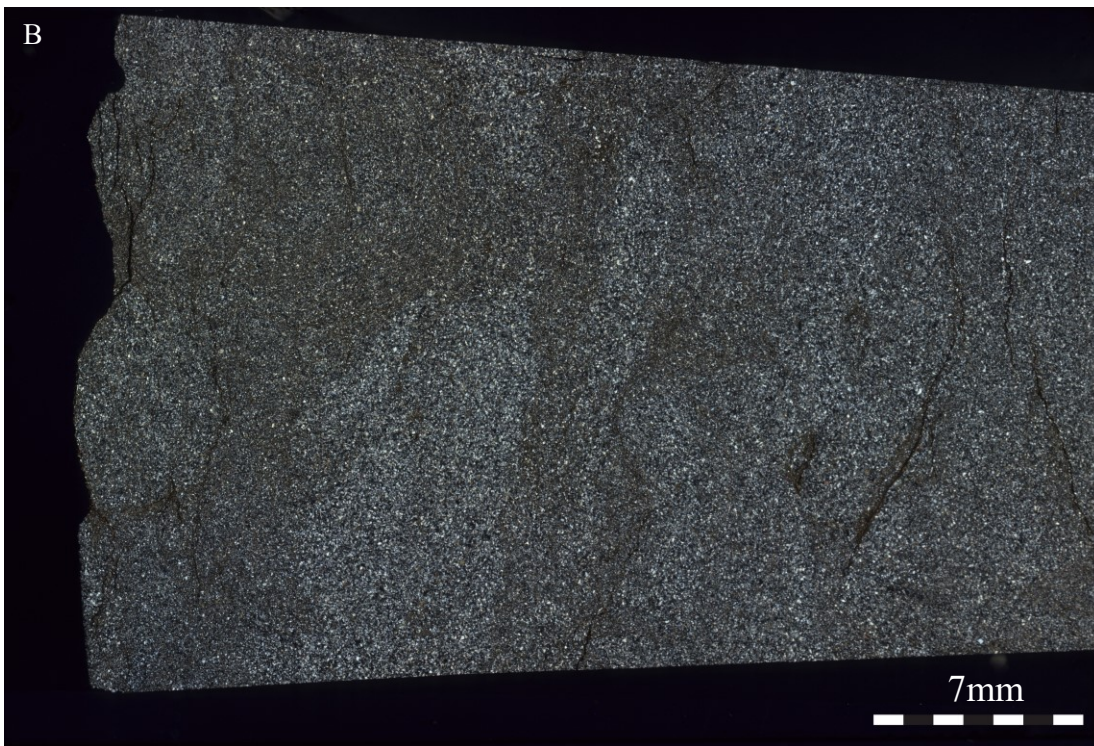
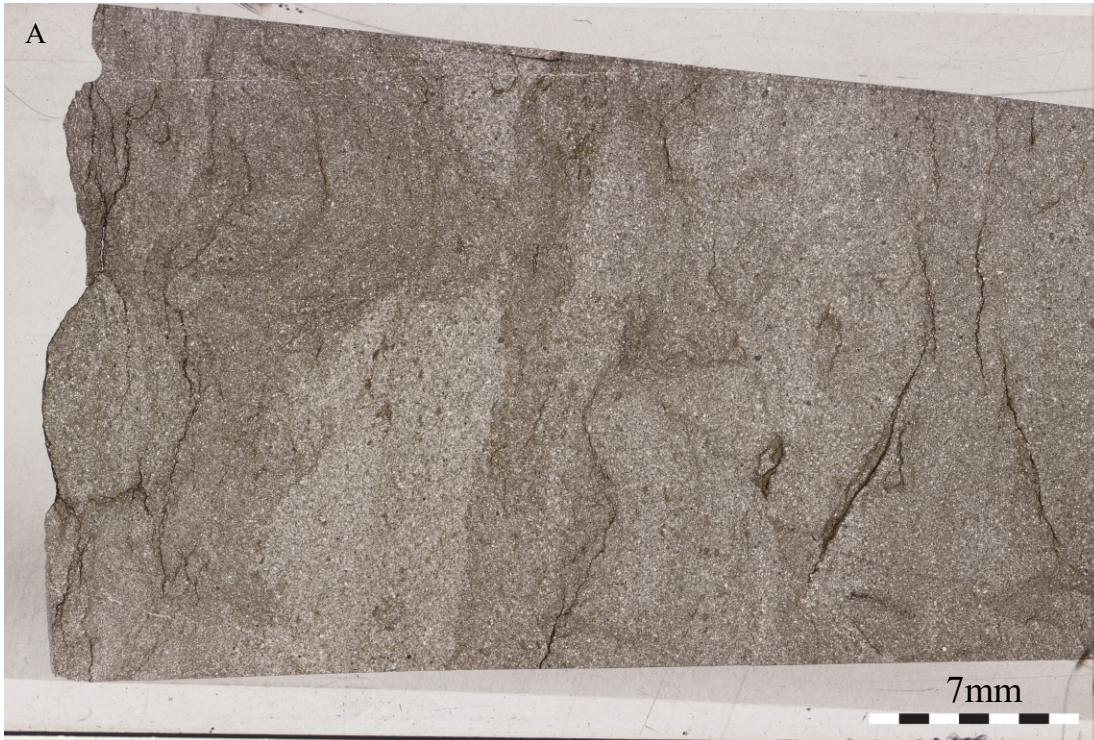


Figure 8. Thin sections under A) PPL and B) XPL of sample SC200806A1. It is well sorted and contains curved mud-lined burrows. The burrow orientation is horizontal and filled by finer sediment. Some wavy laminations are observed.

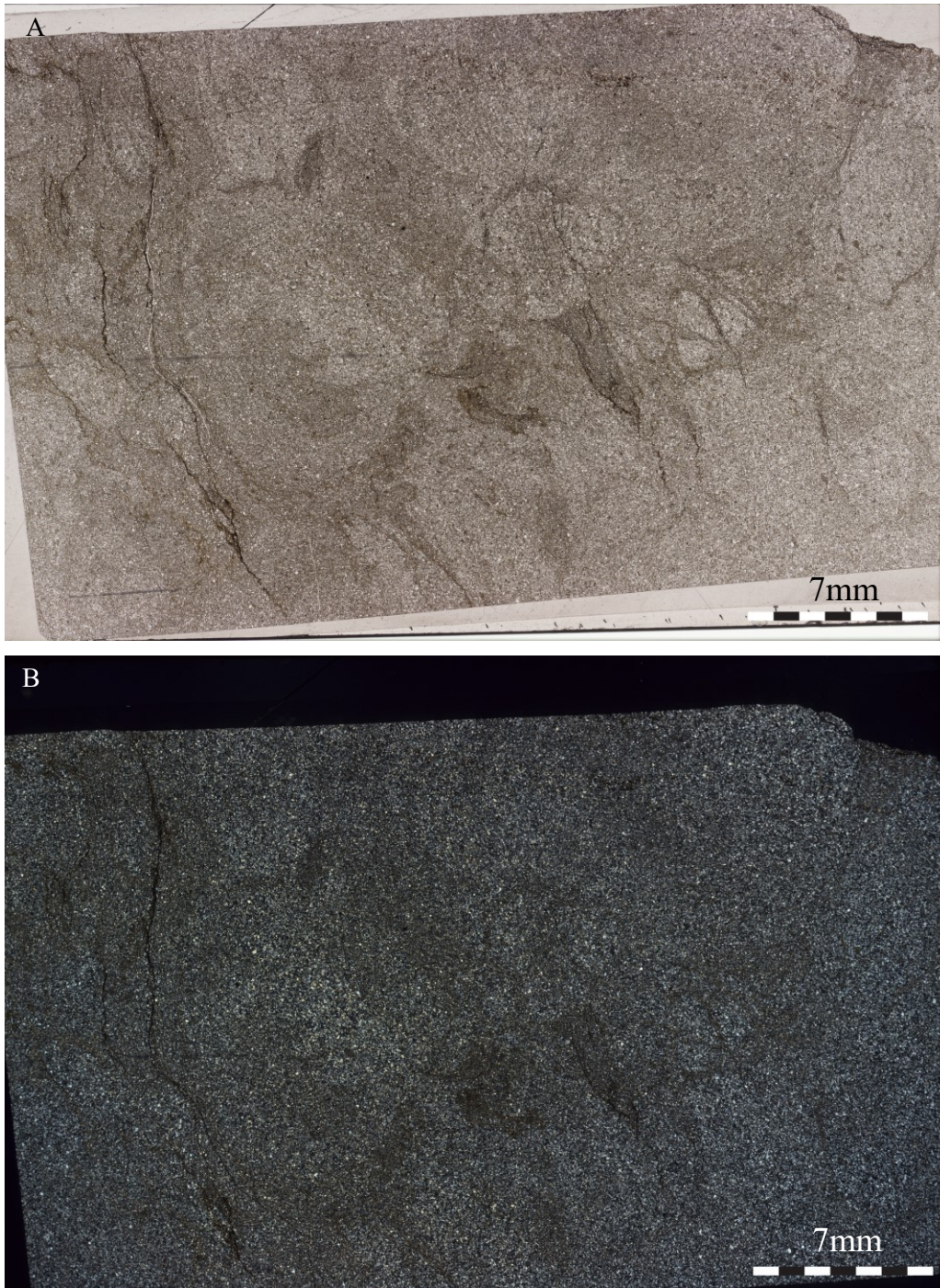


Figure 9. Thin sections under A) PPL and B) XPL of sample SC200806A2. It is well sorted and contains cylindrical mud-lined burrows and curved mud-filled burrows. The burrow orientation is horizontal. The mud-lined burrows are filled by host sediment and mud-filled burrows are filled by finer sediment.

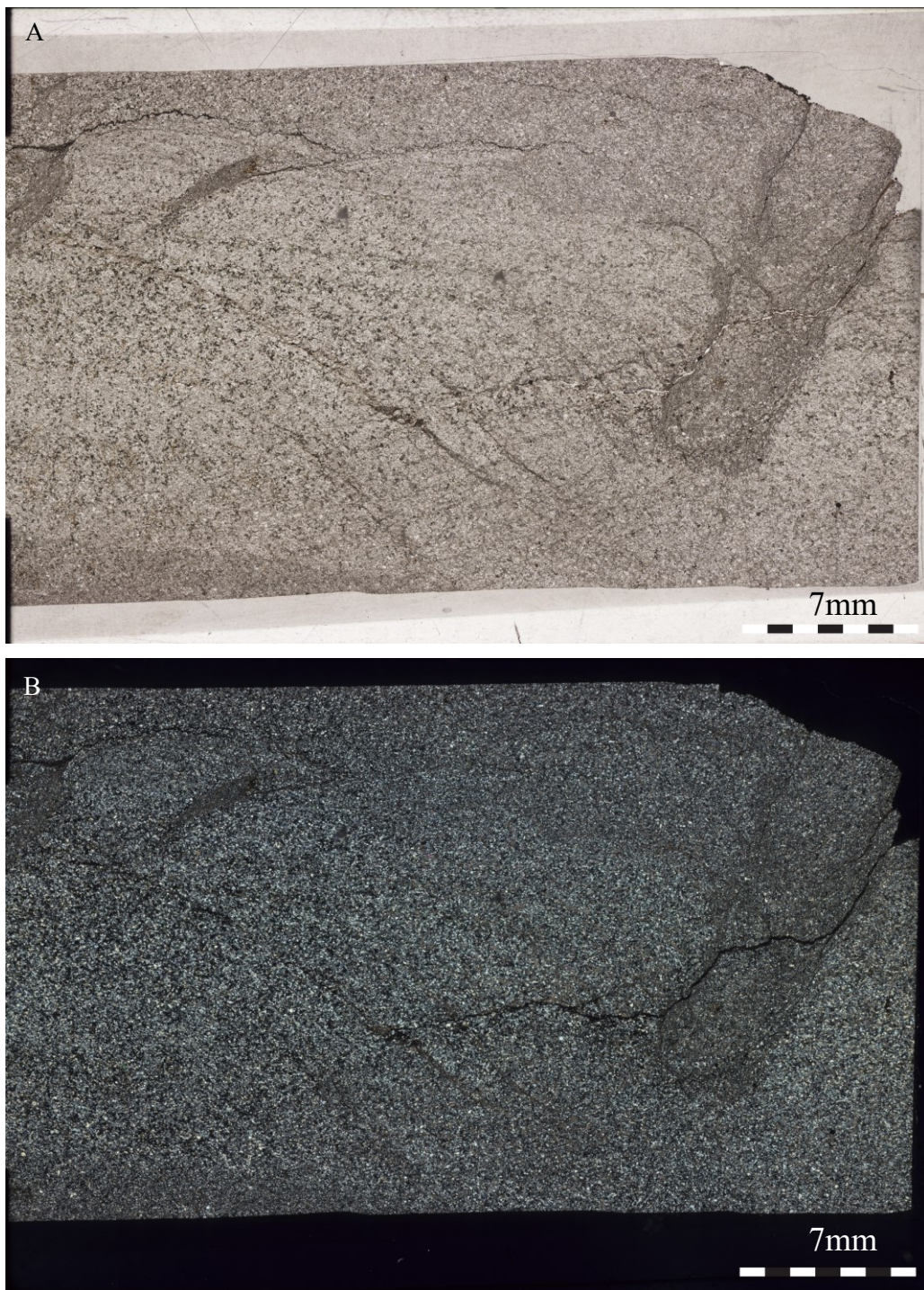


Figure 10. Thin sections under A) PPL and B) XPL of sample SC200806A3. It is well sorted and contains curved mud-filled burrows. They are vertical burrows and filled by finer sediment. Parallel laminations are observed on this thin section.

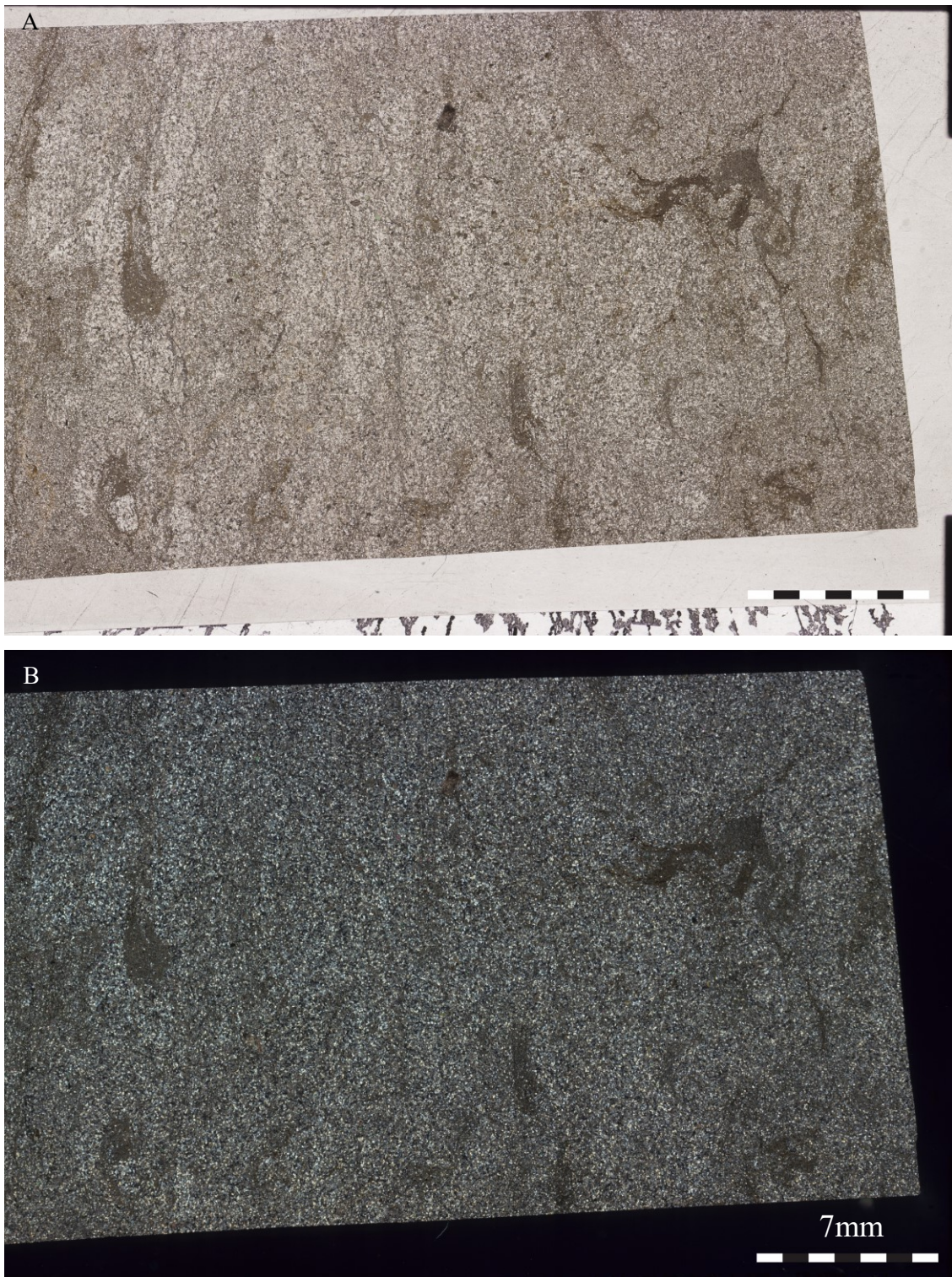


Figure 11. Thin sections under A) PPL and B) XPL of sample SC200806A5. It is well sorted and contains cylindrical mud-lined burrows and curved/sinuuous mud-filled burrows. The burrow orientation is horizontal. The mud-lined burrows are filled by host sediment and mud-filled burrows are filled by finer sediment.

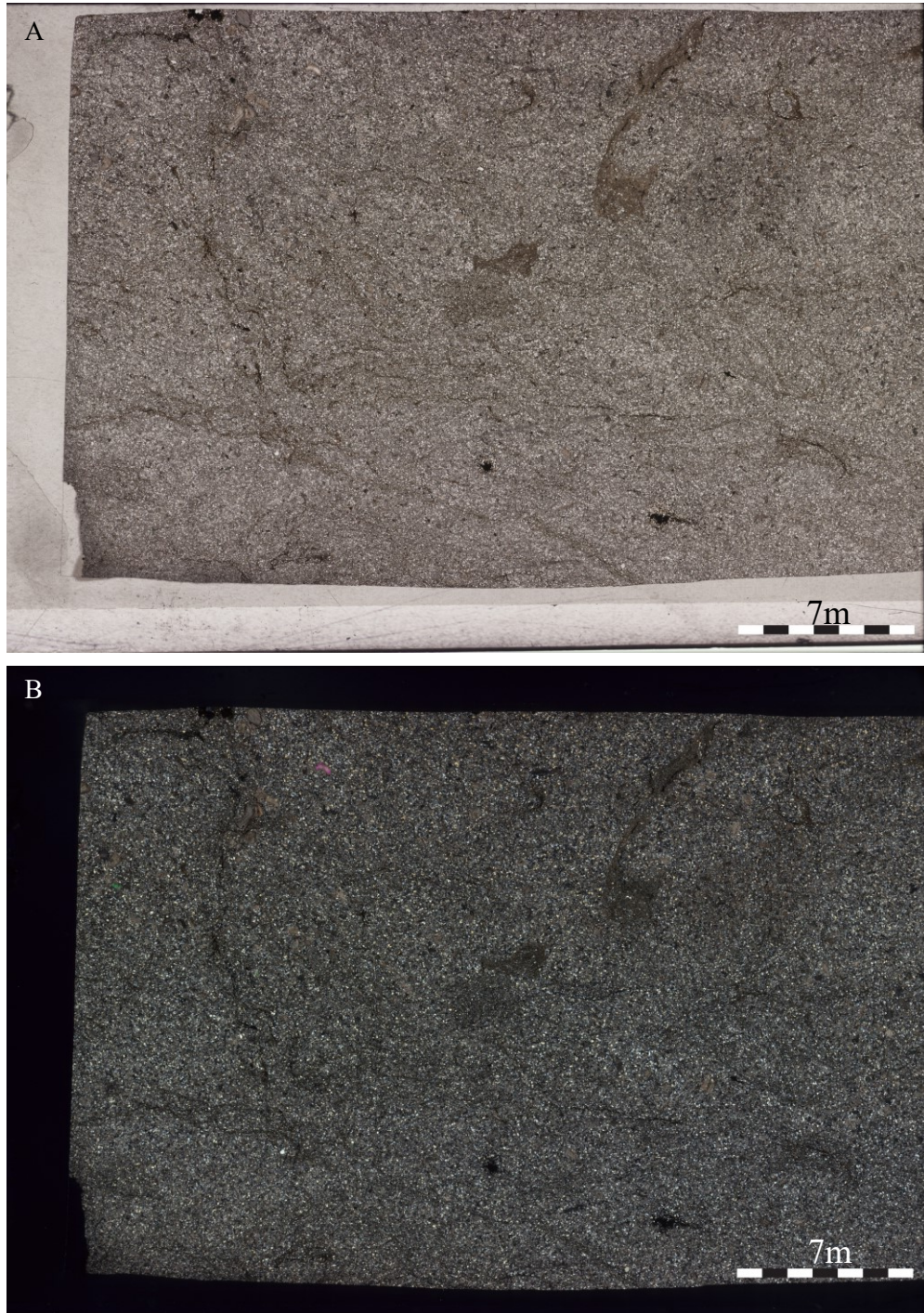


Figure 12. Thin sections under A) PPL and B) XPL of sample SC200806A8. It is well sorted and contains cylindrical mud-lined burrows and sinuous mud-filled burrows. The mud-lined burrows are horizontal burrows and filled by host sediment. The mud-filled burrows are filled by finer sediment and have both vertical and horizontal burrow orientation.

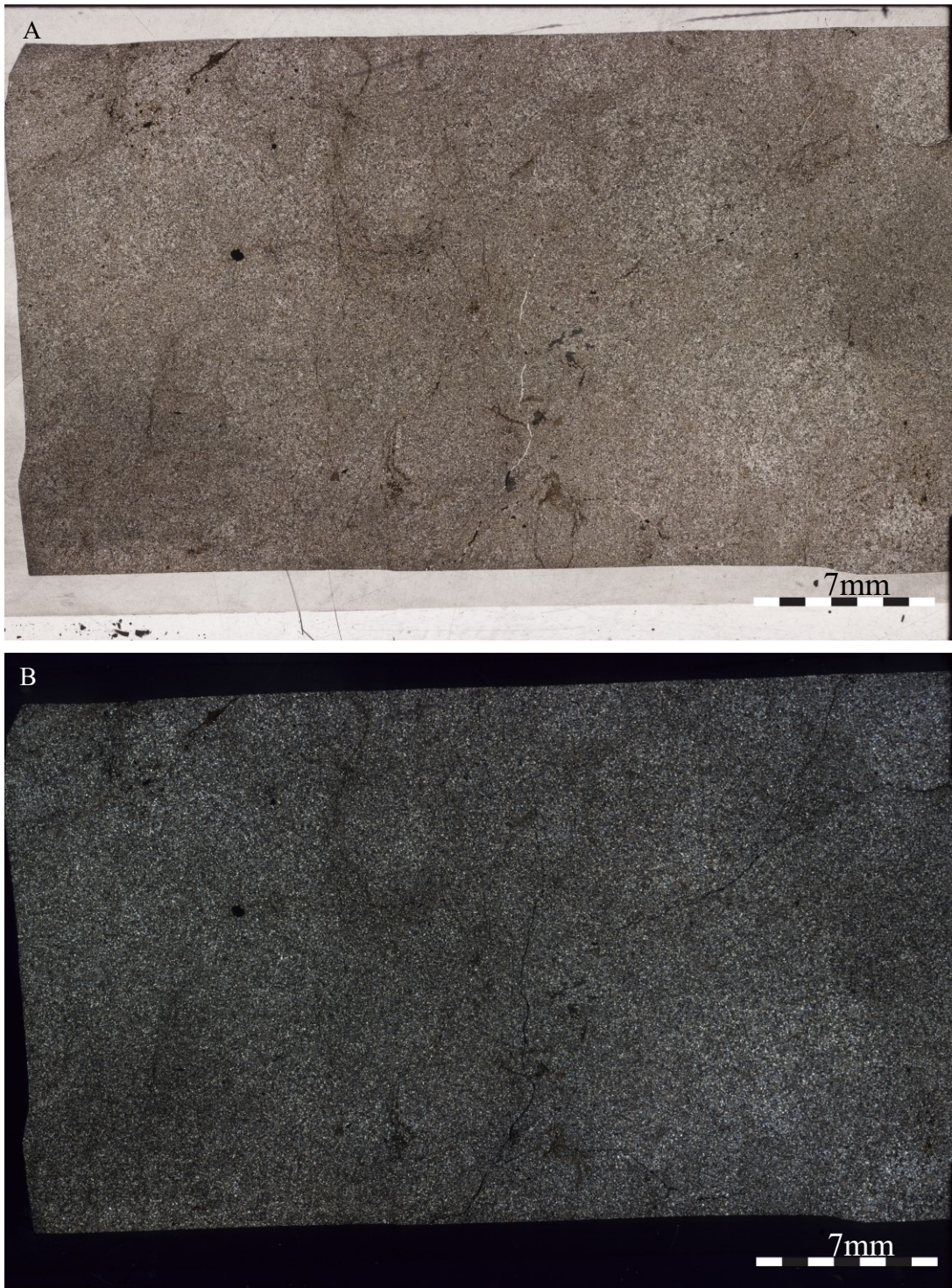


Figure 13. Thin sections under A) PPL and B) XPL of sample SC200806A10 bed view. It is well sorted and contains cylindrical mud-lined burrows and sinuous mud-filled burrows. The mud-lined burrows are horizontal burrows and filled by host sediment. The mud-filled burrows are filled by finer sediment are horizontal burrows.

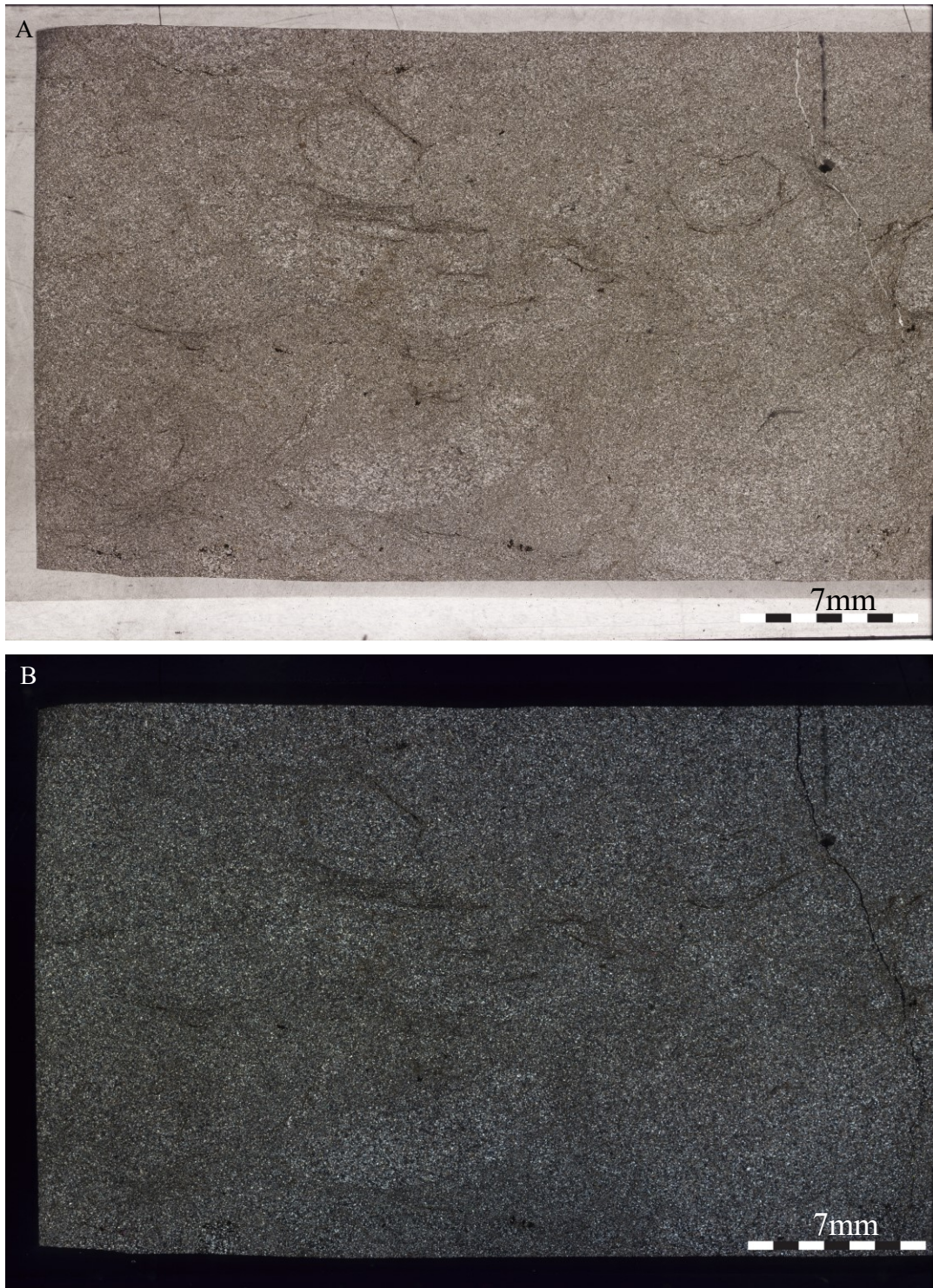


Figure 14. Thin sections under A) PPL and B) XPL of sample SC200806A10 side view. It is well sorted and contains cylindrical mud-lined burrows and curved mud-filled burrows. The mud-lined burrows are horizontal burrows and filled by host sediment. The mud-filled burrows are filled by finer sediment and have horizontal burrow orientation.

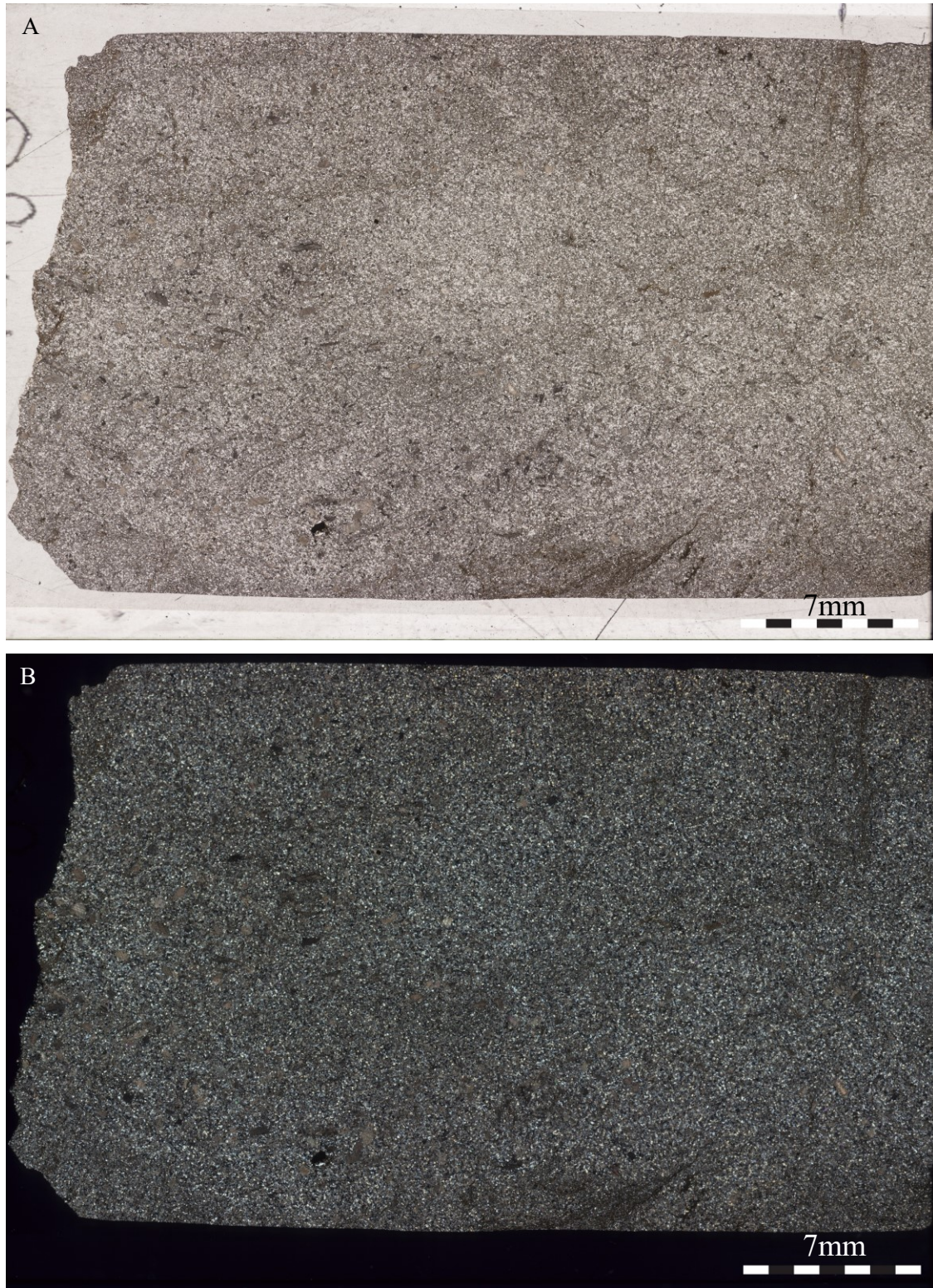


Figure 15. Thin sections under A) PPL and B) XPL of sample SC200806A11. It is well sorted and contains curved mud-filled burrows. They are vertical and horizontal burrows and filled by finer sediment.

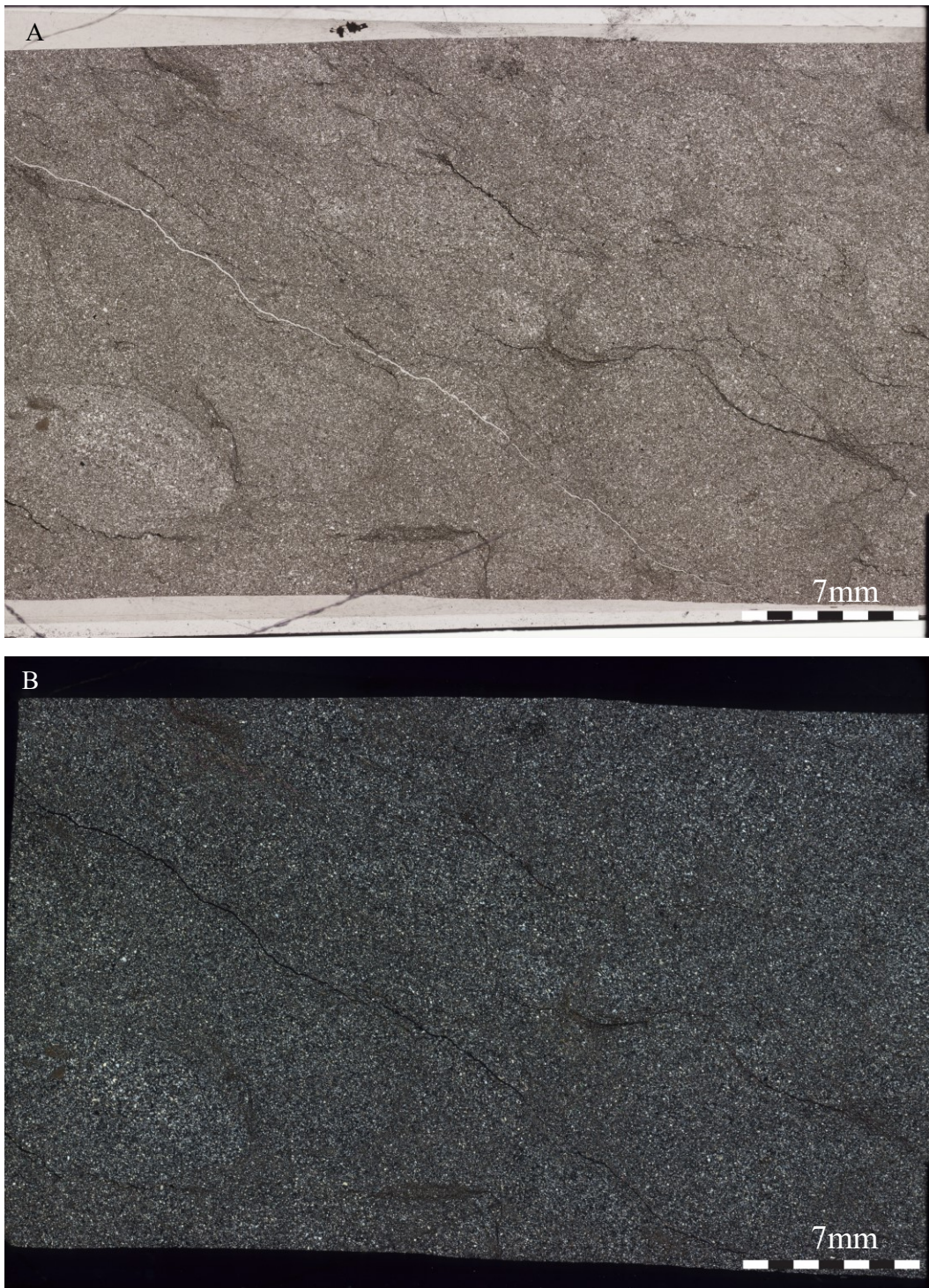


Figure 16. Thin sections under A) PPL and B) XPL of sample SC200807A1. It is well sorted and contains cylindrical mud-lined burrows and straight mud-filled burrows. The mud-lined burrows are horizontal burrows and filled by host sediment. The mud-filled burrows are filled by finer sediment and both vertical and horizontal burrow orientation. Weak parallel laminations are observed on this thin section.

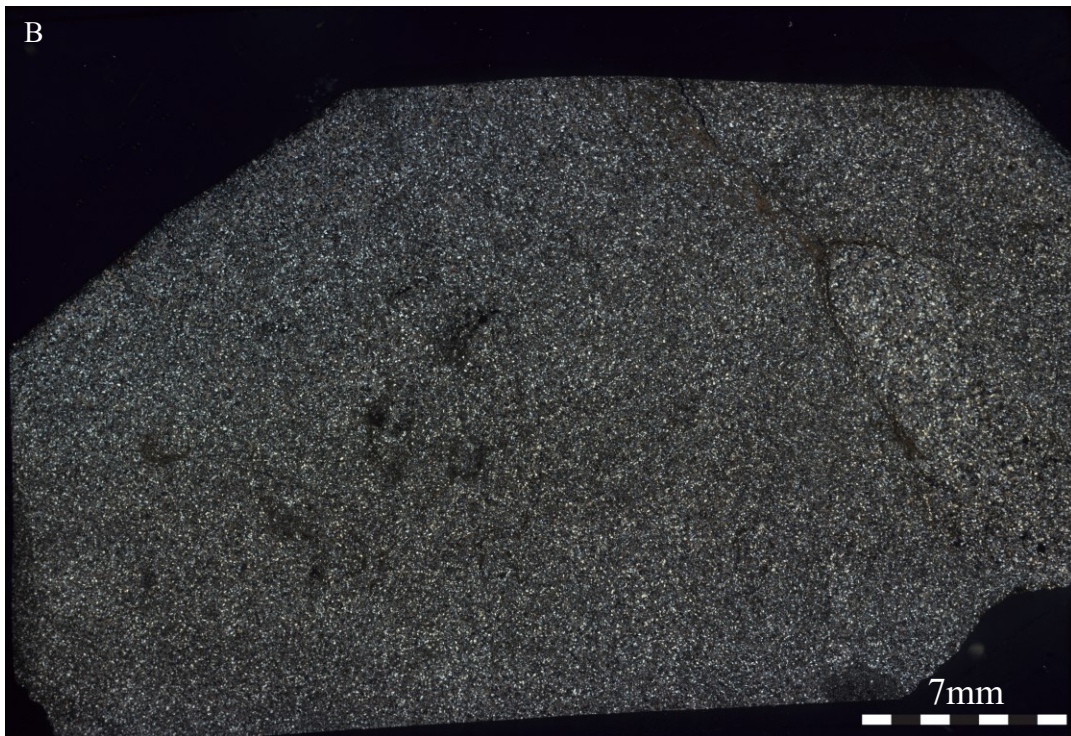
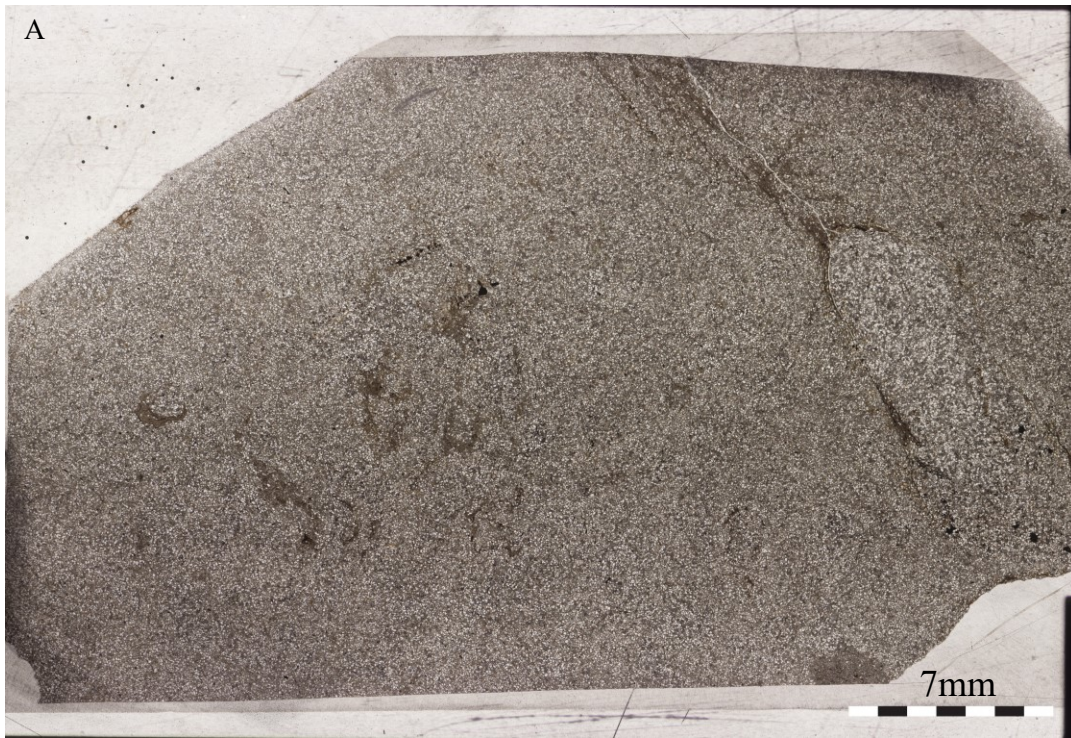


Figure 17. Thin sections under A) PPL and B) XPL of sample SC200807A5 bed view. It is well sorted and contains cylindrical mud-lined burrows and sinuous mud-filled burrows. The mud-lined burrows are horizontal burrows and filled by host sediment. The mud-filled burrows are filled by finer sediment are horizontal burrows.

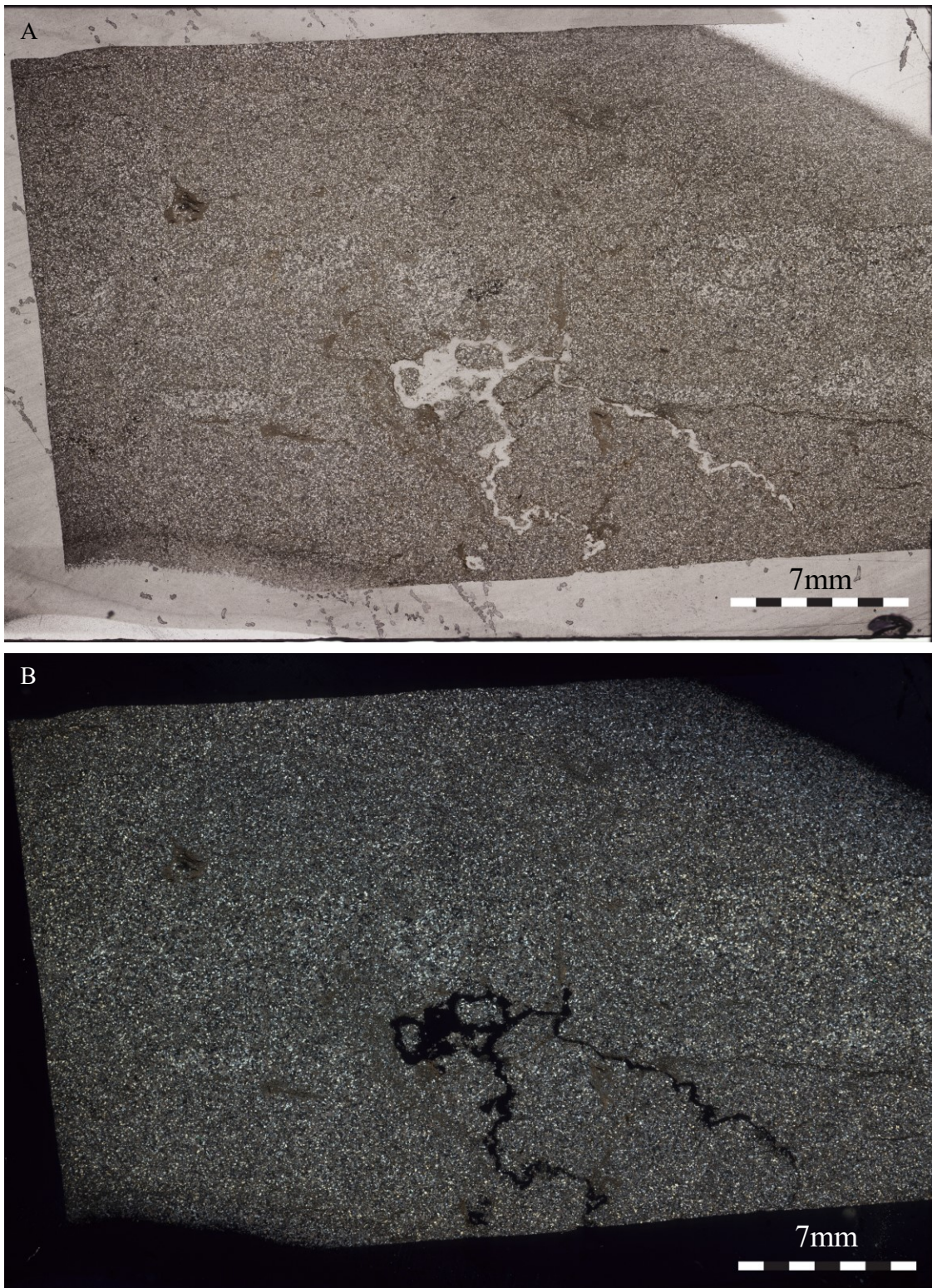


Figure 18. Thin sections under A) PPL and B) XPL of sample SC200807A5 side view. It is well sorted and contains sinuous mud-filled burrows. They are vertical and horizontal burrows and filled by finer sediment.

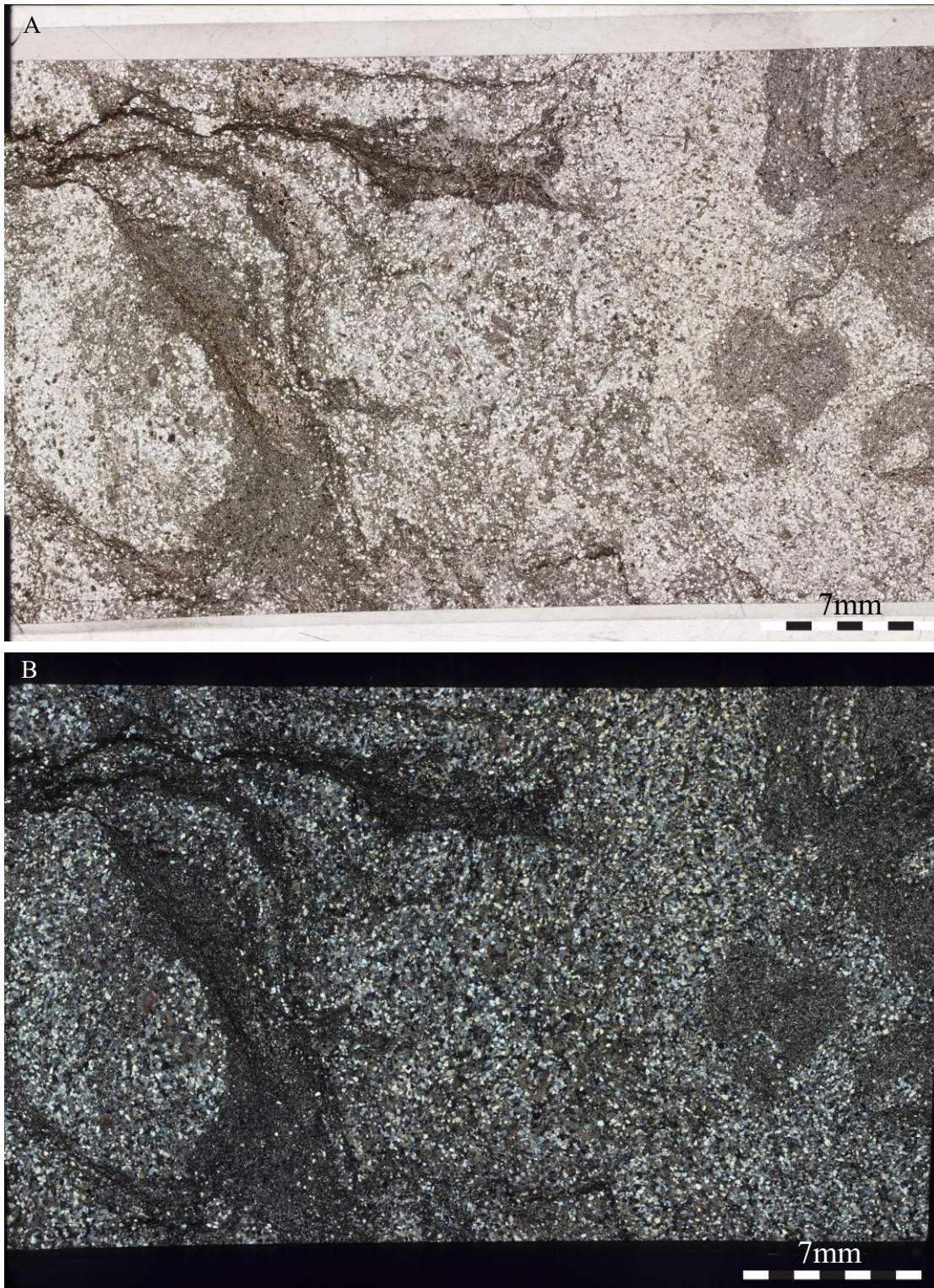


Figure 19. Thin sections under A) PPL and B) XPL of sample SC200808A2. It is well sorted and contains cylindrical mud-lined burrows and sinuous mud-filled burrows. The mud-lined burrows are horizontal burrows and filled by host sediment. The mud-filled burrows are filled by finer sediment are horizontal and vertical burrows.

Kinds	Mud lined burrows	Mud-filled burrows
Features	<ul style="list-style-type: none"> • Relatively large • Concentration of brown mud around burrow • Well sorted silt minerals filled 	<ul style="list-style-type: none"> • Fill appears brown-colored mud. • Different size
Intensity	<ul style="list-style-type: none"> • Most common in thin sections and high intensity 	<ul style="list-style-type: none"> • Relatively high intensity but less common than Mud lined burrows
Interpretation	<ul style="list-style-type: none"> • Completely homogenized thin sections indicate sedimentation rates are slow/episodic enough to allow complete reworking. • Size of burrows appears to be attributed to macrofauna not meiofauna – no real indication of oxygen stress other than low ichnogenera diversity. • Support the point of view for a shoreface depositional environment. 	

Table 1. Classification and interpretation of micro-bioturbation

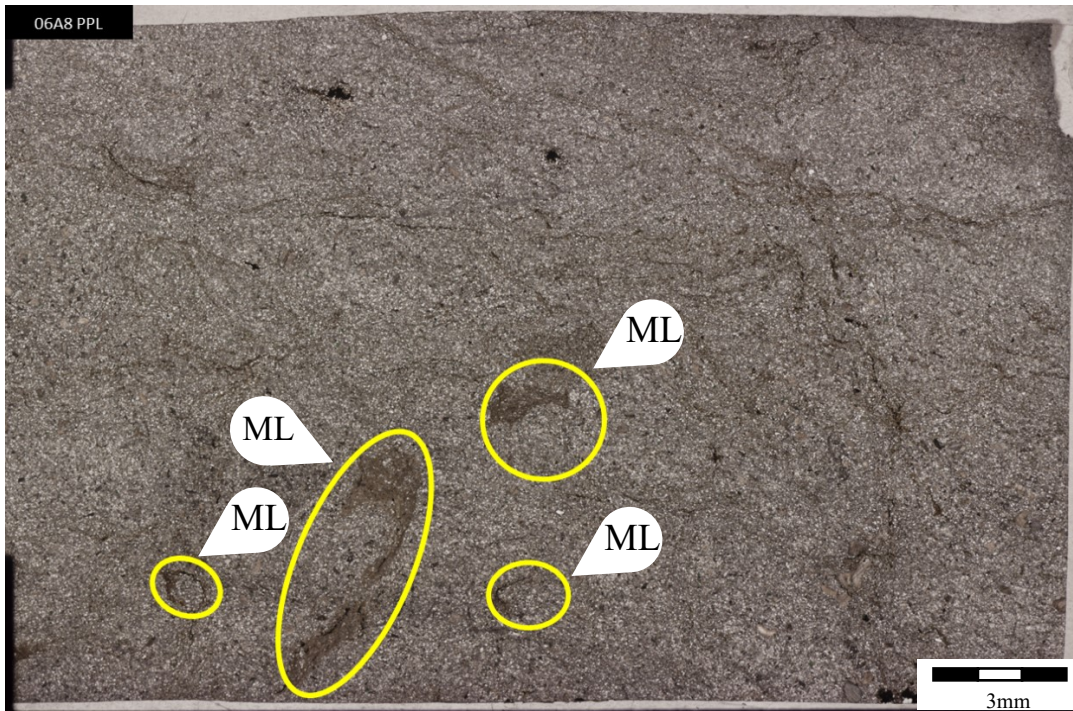


Figure 20. Typical cylindrical mud-lined burrows in thin section CS200806A8 under PPL. The mud-lined burrows are filled by host sediment.

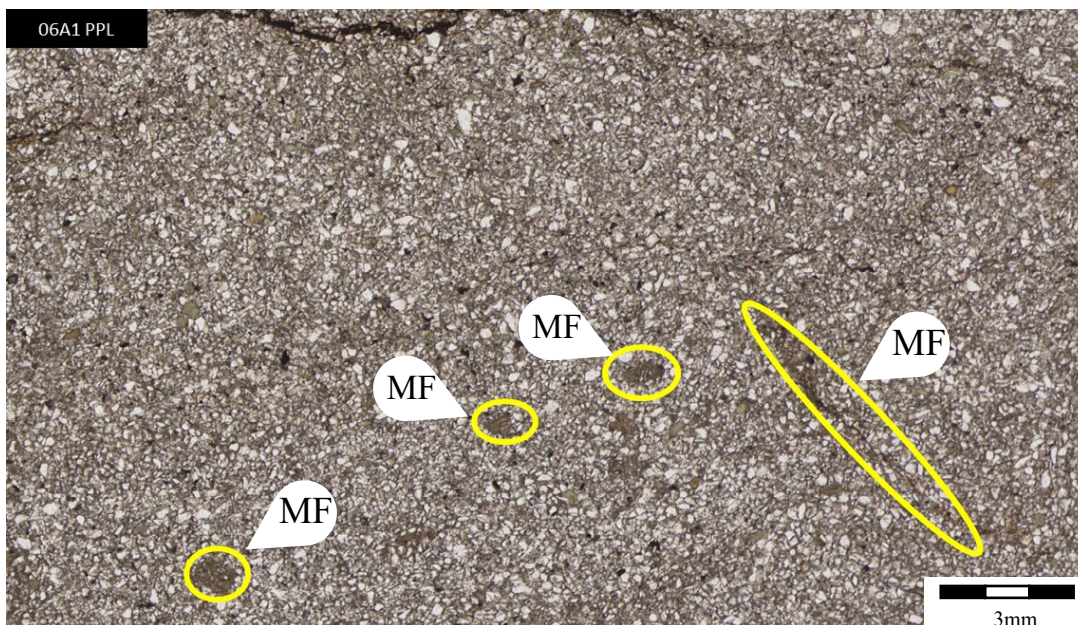


Figure 21. Typical cylindrical and straight mud-filled burrows in thin section CS200806A1 under PPL. The mud-filled burrows are filled by finer sediment.

The study area is characterized by six facies (Table 2), each with distinct lithology, sedimentary structures, and ichnological characteristics. Based on these features, the depositional environment of each facies is interpreted as ranging from upper offshore to middle shoreface environment. The details of each facies are as follows:

Facies 1 (F1) is composed of heavily bioturbated, planar-laminated fine sandstone interbedded with bioturbated upper fine sandstone, with laminae at the millimeter scale (Fig. 22). The grain size ranges from fine to upper fine, and there is less heterolithic stratification. Some parallel planar laminations appear in the fine-sand layer, while heavily bioturbated ($BI \geq 4$) structures can be found within each bed, and cross bedding is less common. The bioturbation shows high diversity but moderate to low intensity, with both fine sandstone and upper fine sandstone containing bioturbations. The upper fine sandstone may also have cryptic bioturbation. Nodules appear in some fine sandstone layers.

The presence of planar lamination and bioturbation suggests a moderate to high-energy environment, possibly representing tempestites. Trace fossils identified include Di, Ar, Te, Cy, Sk, Pl, Pa, and Rh, with an ichnofacies between *Skolithos* and *Cruziana* (MacEachern et al., 1999; Pemberton and MacEachern, 1995). The diversity of trace fossils is high, but the intensity is moderate to low, likely due to periodic storm weather and high sedimentation rates as the main stressors in this environment (Pemberton et al., 1997; MacEachern et al., 2005), alternating with periods of low stress (fairweather). The depositional environment is interpreted as a proximal lower shoreface.

Facies	F1	F2	F3	F4	F5	F6
Lithologic description	Heavily bioturbated, sharp-based, planar laminated fine sandstone interbedded with bioturbated upper fine sandstone	Nodular mudstone interbedded with sporadically bioturbated wavy-parallel lamination fine sandstone	Bioturbated massive fine grain sandstone interbedded with shale	Bioturbated dm scaled, sharp-based silty sandstone interbedded with mm scaled shale	Bioturbated parallel laminated, sharp-based fine sandstone interbedded with shale	Hummocky cross laminated bioturbated fine sandstone interbedded with shale
Appears	O1	O1	O1 and O2	O2 and O3	O2 and O3	O3
Ichnological assemblage	Di, Ar, Te, Cy, Sk, Pl, Pa, Rh	Pl and Te	Ar, Pl	Ar, Pl, and Ph	Pl, Rh, Pa, Cy, Di and Ar	Di and Ar
Bioturbation Index	4	1~2	4	4	4	2-3
Primary physical structure	Planner lamination and cross lamination	Wavy-parallel lamination	Rare wavy-parallel lamination	None observed	Parallel-wavy lamination	Hummocky cross lamination and cross lamination
Grain size	Fine & upper fine sand dominated	Mud dominated and fine sand	Fine sand & Mud	Silty sand & Mud	Fine sand & Mud	Fine Sand and Mud

Table 2. Facies table of the Mount Whyte Formation in Nordegg area (Outcrop CS200806A, CS200807A and CS200808A).

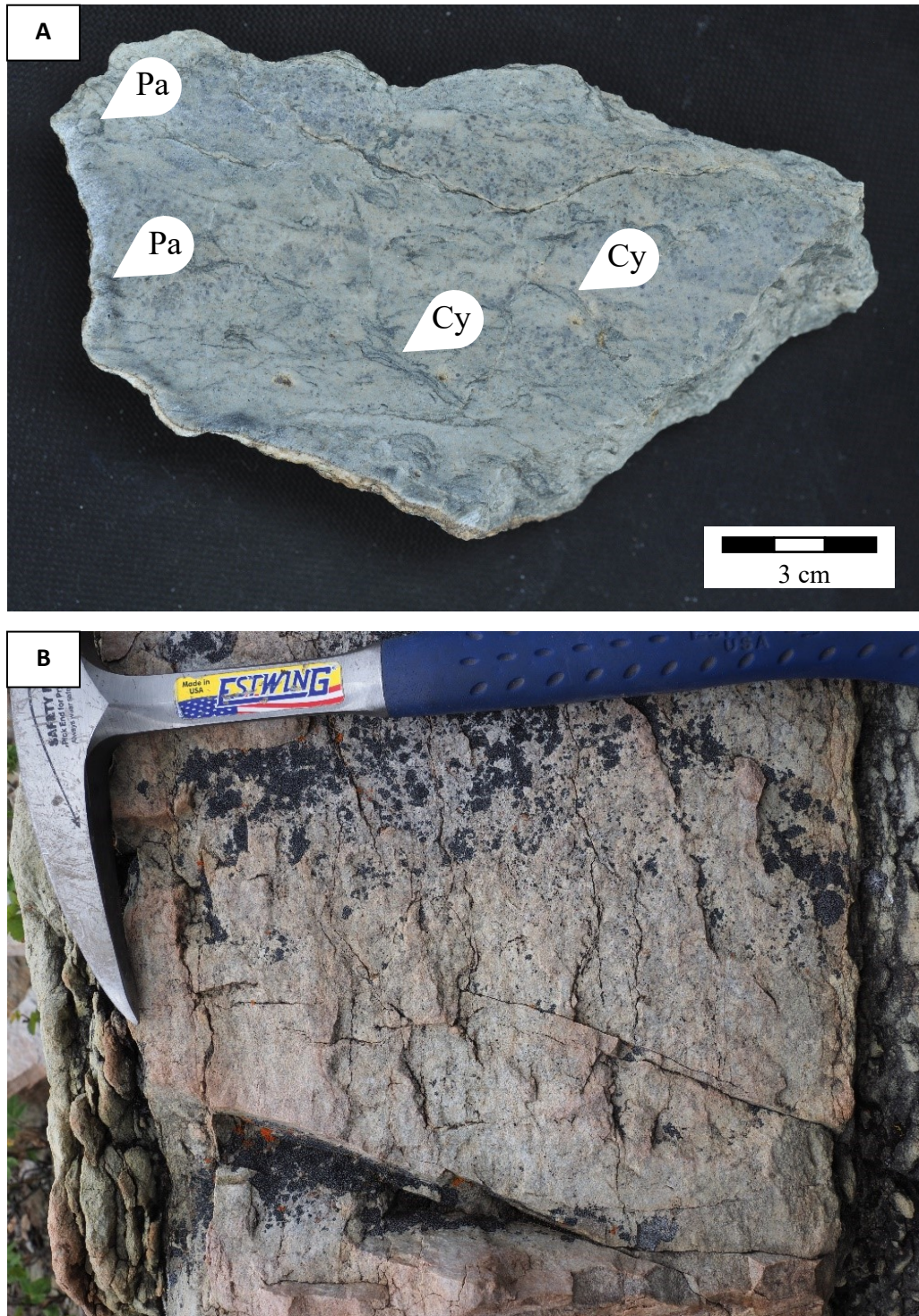


Figure 22. Photos of A) hand sample and B) outcrop for Facies 1: Heavily bioturbated, sharp-based, planar laminated fine sandstone interbedded with bioturbated upper fine sandstone. Note that the direction of stratigraphic 'way up' differs between A and B, as it is oriented upwards in A and to the left in B. Abbreviations: *Cy* = *Cylindrichnus*, *Pl* = *Planolites*, *Pa* = *Paleophycus*.

Facies 2 (F2) is characterized by nodular mudstone interbedded with sporadically bioturbated wavy-parallel laminated fine sandstone (Fig. 23). This facies exhibits heterolithic stratification with thin (cm scale) fine sandstone layers intercalated within decimeter-scale mudstone. Weak wavy-parallel and planar laminations are observed in the sharp-based sandstone layers, while some layers are massive. A large number of nodules are present in some mudstone beds. Bioturbation in this facies is very rare, with only a few suspected Pl and Te traces found in sandstone layers, while most units are non-bioturbated.

The fine clay and sand grain size suggests a very low-energy depositional environment for Facies 2. The rarity of bioturbation suggests a high-stress environment, likely due to low oxygen levels in the deep water environment (Gingras et al., 2011). The presence of thin, fine sandstone layers may indicate a high-energy tempestite. Therefore, this facies likely represents a lower offshore environment.

Facies 3 (F3) consists of massive fine-grained sandstone interbedded with shale that shows heterolithic stratification. The shale beds are thin and fissile, with no apparent sedimentary structure. In the sandstone beds, there are sharp-based mm scale fissile shale interbedded with dm scale fine sandstone, which mostly have a massive appearance, but rare wavy-parallel lamination can be observed (Fig. 24). The bioturbation in this facies is low to moderate, with typical Pl and Ar on the top view, but trace fossils are rare. However, on the top of this facies, there is a sandstone bed containing intensive bioturbation (BI=4). Facies 3 is characterized by interbedded fine-grained sandstone and millimeter-scale mudstone. The thin mud beds suggest a low-energy fair-weather period, indicating a lower stress environment. Ar and Pl indicate the *Cruziana* ichnofacies. The moderate to high intensity of bioturbation indicates

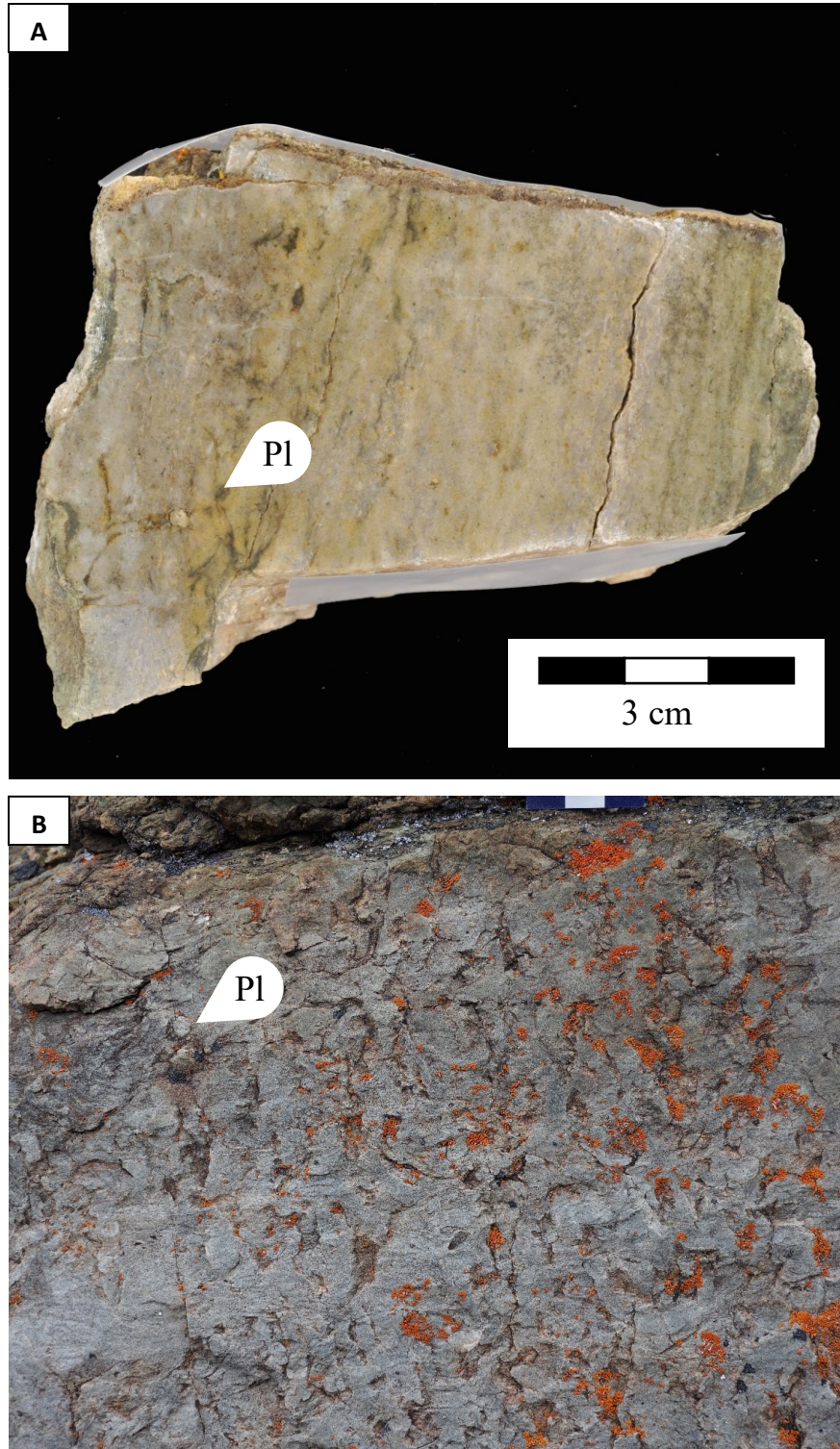


Figure 23. Photos of A) hand sample and B) outcrop for Facies 2: Nodular mudstone interbedded with sporadically bioturbated wavy-parallel lamination fine sandstone, but they only include the sandstone part. Weak wavy-parallel and planar lamination can be found in both hand sample and outcrop. Note that the direction of stratigraphic 'way up' differs between A and B, as it is oriented to the left in A and upwards in B. Abbreviations: Pl = Planolites.

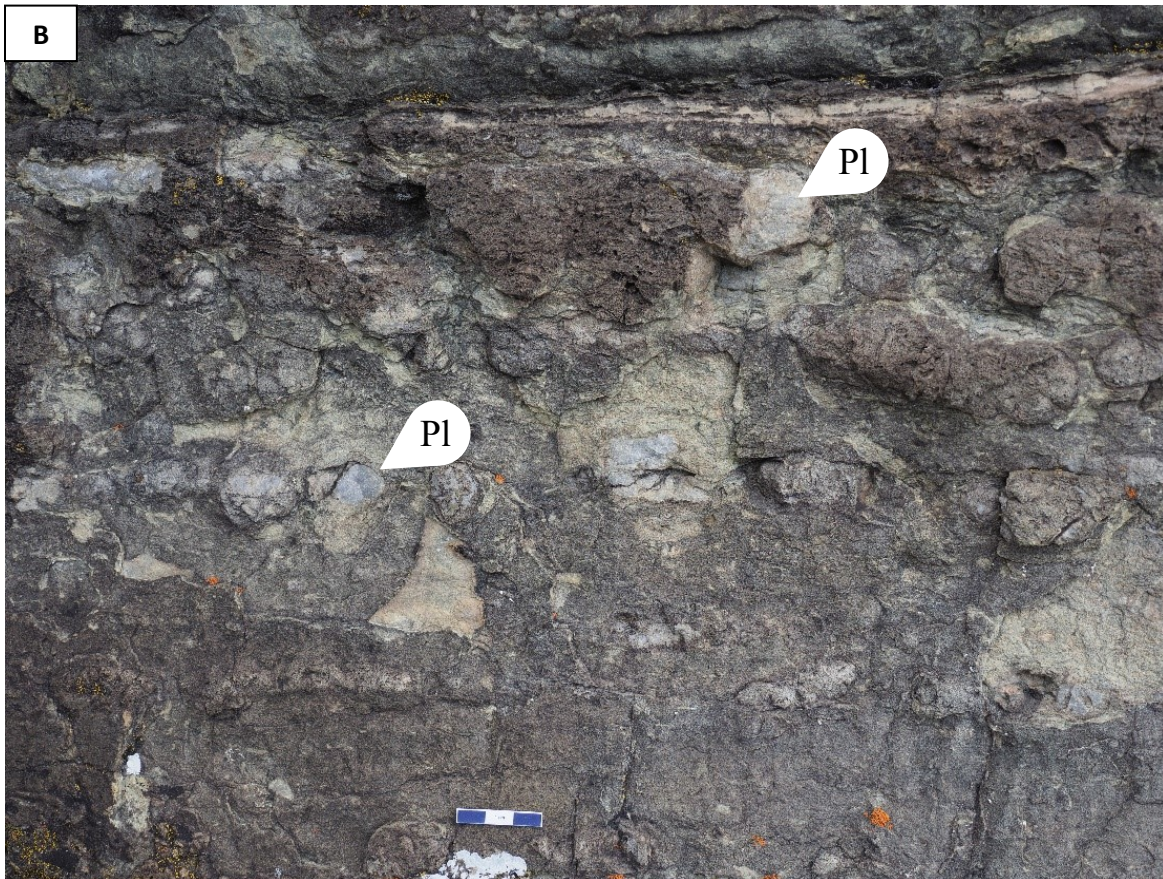
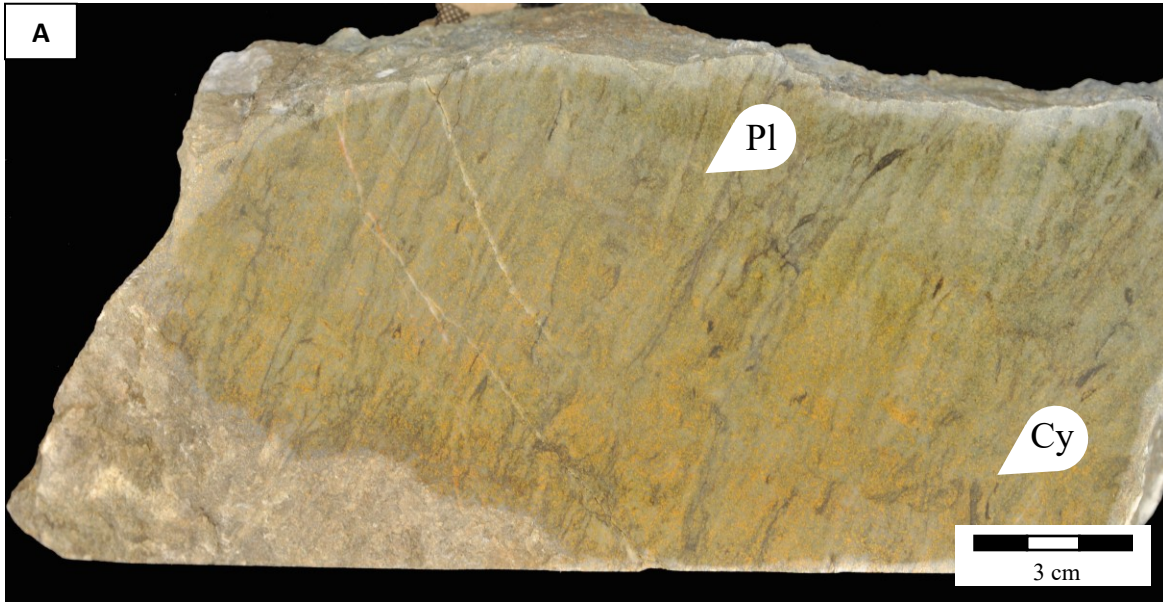


Figure 24. Photos of A) hand sample and B) outcrop for Facies 3: Bioturbated massive fine grain sandstone interbedded with shale. Note that the direction of stratigraphic 'way up' differs between A and B, as it is oriented to the left in A and upwards in B. Abbreviations: *Cy* = *Cylindrichnus*, *Pl* = *Planolites*.

a low stress environment. Therefore, this unit may have been deposited in a distal lower shoreface environment with low storm influence.

Facies 4 (F4) is composed of heavily bioturbated ($BI \geq 4$) sharp-based silty sandstone interbedded with mm-scaled shale (Fig. 25). This facies lacks obvious sedimentary structures, making it difficult to identify ichnogenera despite its high diversity.

The grain size of F4 suggests a low-energy environment, and the absence of significant biological reprocessing implies a low-stress habitat. The structureless and bioturbated beds further support the interpretation of a fully marine, low-stress environment. The trace fossils observed in this facies indicate a transition from the *Cruziana* ichnofacies to the *Zoophycos* ichnofacies, with Ar, Pl, and Ph being present. Based on these observations, the depositional environment of Facies 4 is interpreted as upper offshore (Pemberton et al., 2012).

Facies 5 (F5) is composed of sharp-based, bioturbated fine sandstone interbedded with shale, exhibiting parallel lamination and physical structures such as planar and parallel-wavy lamination (Fig. 26). The sandstone beds range in thickness from 15 to 155 cm, while the shale layers are in mm to cm scale. This facies is heavily bioturbated ($BI \geq 4$), and ichnofossils are abundant in both sandstone and mudstone beds, indicating a diverse and low-stress environment.

Despite the presence of parallel lamination suggesting high-energy storm influence, the appearance of Pl, Rh, Pa, Cy, Di and Ar indicate the *Cruziana* ichnofacies (MacEachern et al., 2008), characteristic of a low-stress environment. The high sedimentation rate caused by short-period storm events may have been the primary stress in the depositional environment. Nevertheless, these storms were unable to significantly affect the sediment at the depth of the seafloor. This unit is likely deposited in a distal lower shoreface environment.

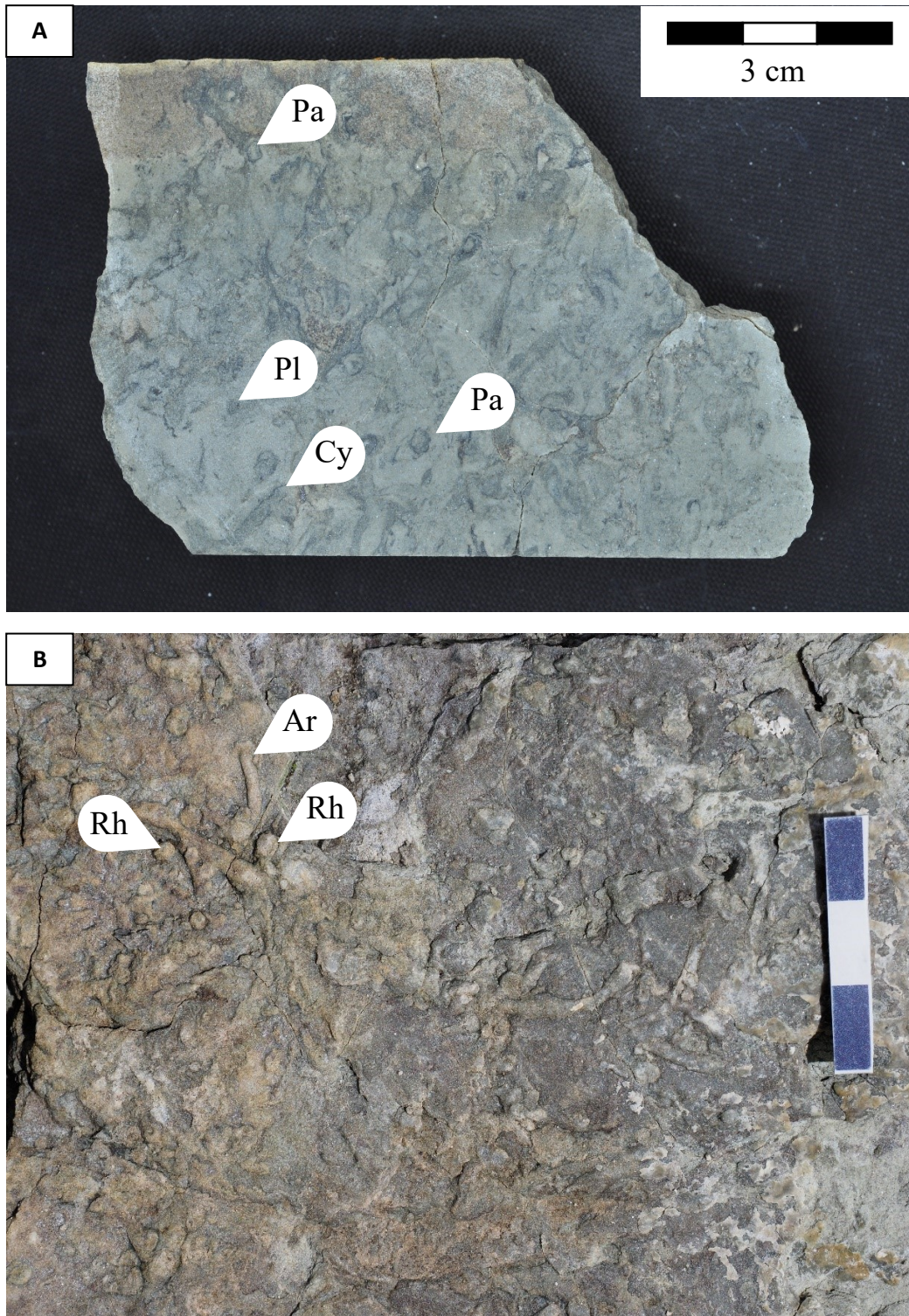


Figure 25. Photos of A) hand sample and B) outcrop for Facies 4: Bioturbated, sharp-based silty sandstone interbedded with mm scaled shale. A is the hand sample for the silty sandstone part and it is heavily bioturbated. Cy, Pa, Pl, Ar are appeared. B is an outcrop photo, which shows silty sandstone with heavily bioturbation such as Rh and Ar. Abbreviations: *Ar* = *Arenicolites*, *Cy* = *Cylindrichnus*, *Pl* = *Planolites*, *Pa* = *Paleophycus*, *Rh* = *Rhizocorallium*.

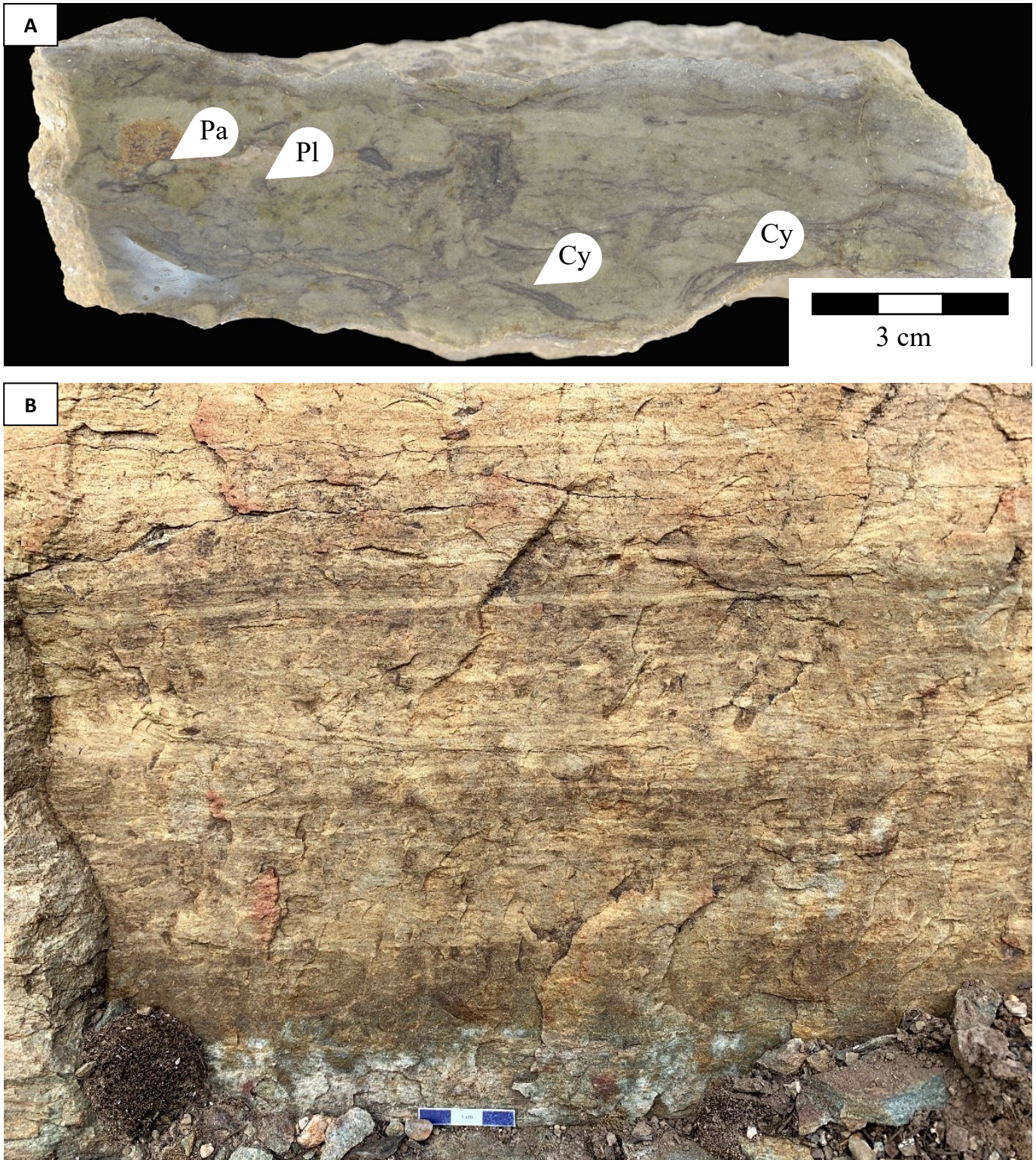


Figure 26. Photos of A) hand sample and B) outcrop for Facies 5: Bioturbated parallel laminated fine sandstone interbedded with shale. A is the hand sample for the fine sandstone part and it is heavily bioturbated. Cy is the most common ichno-fossiles. In the outcrop photo, which shows parallel laminated on the fine sandstone unit. Abbreviations: *Cy* = *Cylindrichnus*, *Pl* = *Planolites*, *Pa* = *Paleophycus*.

Facies 6 (F6) is characterized by hummocky cross-laminated sandstone, which suggests a high-energy environment caused by storm/tempest weather events (Fig. 27). The high sedimentation rate resulting from this environment can cause a high physical stress to the biological community. However, despite the high energy environment, burrows can still be found in this unit and the trace fossil suites of Di and Ar reflect the *Skolithos* ichnofacies (Pemberton and MacEachern, 1995). This suggests that there were episodes of low stress between the storm events, such as appropriate sedimentation rates, salinity, and sufficient oxygen supply. Therefore, the depositional environment of facies 6 is assigned to the middle shoreface (MacEachern and Pemberton, 1992).

The facies observed in the outcrops indicate a transition from an upper offshore to a middle shoreface environment, with evidence of storm influence throughout. The first outcrop shows a fining-upward trend that could indicate a transgression. The trace fossils in the sandstone unit show moderate to high diversity and low to moderate intensity, indicating some stress in the environment, likely due to sedimentation rate. The second outcrop is in a transition zone with heavily bioturbated sandstone indicating a less stressed environment, potentially due to more oxygen or nutrients. The third outcrop is in the lower to middle shoreface with hummocky cross laminated bioturbated sandstone on top of parallel laminated sandstone, potentially indicating a regression or larger storm event. All units in the outcrops show high ichnodiversity, high bioturbation intensity, and larger sizes, indicating stable salinity, adequate oxygen levels, and reduced wave energy during deposition (Gingras et al., 2011). Facies 2 is the only one that indicates a deep-water environment, potentially with high chemical stress due to low oxygen levels.

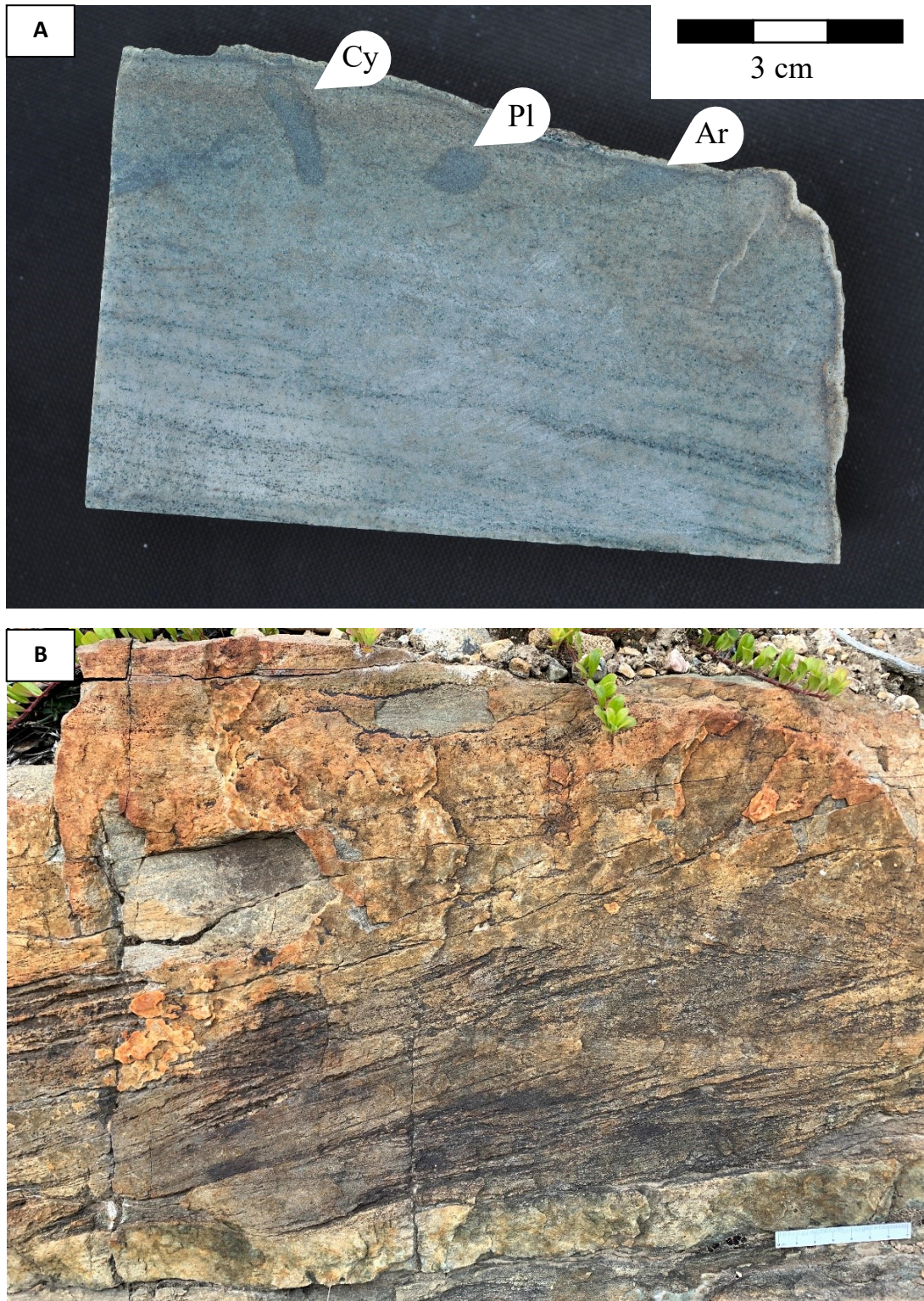


Figure 27. Photos of A) hand sample and B) outcrop for Facies 6: Hummocky cross laminated bioturbated fine sandstone interbedded with shale. A is the hand sample for the fine sandstone with hummock laminations. The bedding is inclined and Pl and Cy can be found in this sample. B is an outcrop photo, which shows cross-laminated on the fine sandstone unit. Abbreviations: *Ar* = *Arenicolites*, *Cy* = *Cylindrichnus*, *Pl* = *Planolites*.

6. Discussion and Conclusion

It is important to note that while the absence of carbonate outcrops and the lack of clear evidence for episodic deposits may suggest a different depositional mechanism for the Mount Whyte Formation than previously suggested, it is also possible that the outcrop thickness simply does not allow for the identification of these features. Further research may be needed to fully understand the depositional history of the formation.

That being said, the consistent identification of the facies as belonging to a shallow marine system, as well as the presence of a deeper water facies (F2), supports the previous studies' conclusions that the Mount Whyte Formation was deposited in part in a shallow marine setting.

The Mount Whyte formation, which is deposited in a shallow marine environment, bears a strong resemblance to the Early and Middle Cambrian Mount Clark and Mount Cap formations in northwestern Canada. Both the Mount Clark and Mount Cap formations also exhibit depositional environments that can be classified as shoreface environments and are dominated by the *Cruziana* and *Skolithos* Ichnofacies (Matthew, 2018; Herbers, 2016). Bioturbation distribution is generally influenced by episodic storms, but not by salinity or oxygen variations. Furthermore, like the Mount Whyte formation, the Mount Cap and Mount Clark Formations were deposited in an offshore to shoreface setting.

In summary, the Mount Whyte formation in the Nordegg area of Alberta during the Middle Cambrian period spans from offshore to middle shoreface. By examining the sedimentary and biogenetic features, six distinct facies have been identified, which collectively indicate a transition from an offshore to a shoreface environment. Throughout most of the outcrop, the

bioturbation shows characteristics of low diversity, high bioturbation intensity, and moderate burrow size, suggesting a fully marine environment with minimal influence from storms. Furthermore, observations of micro-bioturbation in thin sections suggest that at several levels sedimentation rates were slow and episodic, allowing for complete reworking, with no was no evidence of oxygen stress beyond low ichnogenera diversity.

CHAPTER 3: CORE AND GEOCHEMICAL ANALYSIS FOR MIDDLE CAMBRIAN MOUNT WHYTE FORMATION

1. Introduction

Red beds refer to sedimentary rocks with a reddish hue that can contain both clastic and carbonate materials and can be found in various depositional environments (Eren et al., 2013). The reddish color is typically due to the presence of hematite, an oxidized form of iron that appears in the sediment matrix. Hematite can originate from bacterial activity during diagenesis (Eren et al., 2013), or it can be a product of deposition (Turner, 1979).

The aim of this study is to utilize sedimentological and geochemical data from three drill cores to examine the formation of red beds and investigate any possible relationship between bioturbation and redox-sensitive elements in the Cambrian Mount Whyte, Cathedral, and Stephen formations. The wells 1-34-57-22W4 and 6-36-19-01W4 belong to the Mount Whyte formation, while well 1-06-38-15W4 is from the Stephen and Cathedral formations. Iron (Fe) is a redox-sensitive element, and its distribution in sedimentary rocks is typically influenced by oxygen distribution at the seafloor. Given that the geochemical data from the three cores exhibit notable Fe enhancement and bioturbation, it may be possible to use the distribution of bioturbation as a proxy for bottom water oxygen content to explore the relationship between Fe and O₂ distribution. By identifying any correlations, we can propose potential mechanisms for Fe sequestration within the sedimentary layers, which can aid in the development of red beds.

1.1 Geological Setting

The research area is situated in eastern Alberta's Western Canada Sedimentary Basin, comprising three formations - Mount Whyte, Cathedral, and Stephen - that were deposited

during the Middle Cambrian as a platform (Slind et al., 2020). In the western part, these strata sit unconformably on the Gog Group, while on the eastern side, they rest on the Basal sandstone unit (Slind et al., 2020). The lowermost Mount Whyte Formation is composed of mixed fine-grain sandstone with mudstone, overlain unconformably by the Cathedral Formation, dominated by limestone, and situated between Mount Whyte and the Stephen Formation. The Stephen Formation, mostly consisting of mudstone, can be split into a "thin Stephen" in the eastern platform region and a "thick Stephen" in the western portion (Slind et al., 2020). The Eldon Formation rests on top of the Stephen Formation (Slind et al., 2020). While the Alberta Geological Survey found these formations to be mostly composed of massive carbonates, core observations in the study area suggest that clastic sediments are more prevalent.

2. Methodology

2.1 Sampling

For this research, three Middle Cambrian drill cores from the Mount Whyte Formation, Cathedral Formation, and Stephen Formation were logged and sampled at the Alberta Core Research Centre. As all three cores are composed of shale and sandstone, gamma ray logs were used to identify the formations. The Mount Whyte Formation should exhibit a high gamma ray value, with a clean shoulder at the top indicating the separation from the Cathedral Formation. Therefore, Wells 1-34-57-22W4 and 6-36-19-01W4 are mainly from the depth of Mount Whyte Formation, while Well 1-06-38-15W4 is above the Mount Whyte Formation and is from the Stephen and Cathedral Formation.

Samples of approximately 1 g were collected every 50 cm from each core, with each sample being small pebble-sized sandstone or mudstone. These samples were then powdered

using a ShatterBox, and some of them were made into thin sections, which were prepared as polished sections.

2.2 Sedimentary & Ichnology Data

AppleCore© software was used to log each of the three cores, which enabled recording of the lithology, sedimentary structures, and grain size. These logs also provided valuable information regarding ichnological features, such as Bioturbation Index (BI) and ichnospecies. BI, which measures the degree of bioturbation in the sedimentary unit on a scale of 0 (unburrowed) to 6 (biogenic homogenization) (Gingras et al., 2011), was used in this study.

The sedimentological and ichnological analysis of the core resulted in the identification of nine facies, which are listed in Table 3. Core photos were used to collect additional data for ichnological analysis, and Photoshop was used to measure the burrow size (diameter) using the length of the core box (75 cm) as a reference. The diversity of trace fossils was also counted from core photos, and a Size Diversity Index (SDI) was calculated as Diversity multiplied by Size, which is the largest observed diameter. The Variability of the burrow was determined by calculating the difference between the maximum and minimum BI at a given depth. The Size-diversity index is commonly used as a proxy for salinity and oxygen stress (Wignall and Myers 1988; Hauck et al., 2009). Finally, thin sections from each core were examined under a microscope to identify mineralogy, grain size, and sphericity.

2.3 Geochemical Data

Rock samples were fully dissolved by a microwave digestion method using hydrofluoric acid (HF), which assists in dissolving aluminosilicate minerals (Wilson et al. 2006). A Teflon tube heater was used in place of a high-performance microwave, which resulted in a longe

Facies	F1a	F1b	F2a	F2b	F2c	F3	F4	F5	F6
Lithologic description	Burrowed sandstone with mudstone interbeds	Sporadically burrowed sandstone with mudstone interbeds	Lightly burrowed mudstone with sandstone interbeds	Burrowed mudstone and sandy mudstone with sandstone interbeds	Sporadically burrowed cross bedded mudstone with sandstone interbeds	Fine to medium massive sandstone	Heavily burrowed Sandy mudstone and mudstone	Anhydrite dolostone	Bioclastic Sandstone
Appears	Core 1, 2 and 3	Core 1, 2 and 3	Core 1 and 3	Core 1 and 2	Core 1	Core 1, 2 and 3	Core 1 and 2	Core 3	Core 3
Ichnological assemblage	Pl, Cy, Ar, As, Gy, Li, Pa, Ps	Op, Pl, Ar, Cy, Gy, Cr, Mo	Pl	Pl, Cy, Ar, As, Gy, Di,	Te, Gy, Pl	None observed	Pl, Cy, Ar	None observed	Ar
Bioturbation Index	3~4	0~3	1~2	3~5	0~4	0	4~6	0	About 0
Primary physical structure	Planner to Low angle planner bedding and cross bedding	Low angle Planner bedding; cross bedding; Synaeresis Cracks	Planner bedding	Mostly massive appearance with little Planner bedding	Cross bedding and planner bedding	Massive Appearance	Mostly massive Appearance	Massive Appearance	Massive Appearance
Lithological accessories	Shell fragments; Rip-up clasts; Soft-sediment deformation	Shell fragments; Soft-sediment deformation	Soft-sediment deformation	Soft-sediment deformation; Shell fragments; Detrital organic material	None observed	Shell fragments	Detrital organic material	None observed	None observed
Grain size	Very fine & fine sand dominated	Fine sand dominated	Fine sand & Mud	Fine sand & Mud	Fine sand & Mud	Fine to medium Sand	Mud dominated	N/A	Medium to coarse sand
Remarks	Intermittent bioclastic units: cm scale	Trace confined in mudstone	Trace mostly in mudstone	Intermittent bioclastic units	Higher sand content, more sedimentary structure	Some parts Irons stained; intermittent bioclastic units	Some parts Iron stained; small amount fine grain sand can be found	N/A	Shell bed matrixed with sand

Table 3. Facies table of Wells 1-34-57-22W4 and 6-36-19-01W4 and 1-06-38-15W4.

heating process. There are three steps for digestion. First, 4 mL of Nitric acid (HNO_3) and 4 mL of Hydrogen peroxide (H_2O_2) were mixed with 0.1 g rock powder and then, the mixture was heated. Second, 2 mL of HF was added into the mixture, and finally, 20 mL of boric acid (H_3BO_3) was added to neutralize the HF. The solution was heated at 150°C in each step. Before samples were analyzed by inductively coupled plasma mass spectrometry (Agilent 8800 Triple quadrupole ICP-MS/MS), they should be diluted with Milli-Q water to a total volume of 100 mL.

In examining the relationship between redox and bioturbation, certain elements were selected based on their sensitivity to changes in oxygen-deficient environments. Iron (Fe) and molybdenum (Mo) in particular are selected in this study on the basis of their redox sensitive property and good recovery. Also, all data are charted and plotted by using Microsoft Excel© and Datadesk©. Datadesk© is used for Pearson Product-Moment and Principal Component Analysis (PCA), which commonly contributes to reducing the size of the dataset and establishing correlations between different elements. Eigen Vector one and two were chosen to plot, based on their ability to account for all variability in the dataset. Fourteen elements have been selected based on the Pearson Product-Moment Correlation, mainly including Na, Al, Si, P, S, Ca, V, Fe, Zn, Sr, Mo, Cd, Ba and U. In addition, the SDI data has been selected from ichnology data because of its representativeness. Three scatter diagrams are generated based on the Eigenvectors from Principal Component Analysis.

3. Result

3.1 Sedimentary and Ichnology

Figures 28, 29, and 30 provide a summary of the lithology, physical sedimentary structures, and trace fossils identified in each drill core. A more detailed ichnological analysis,

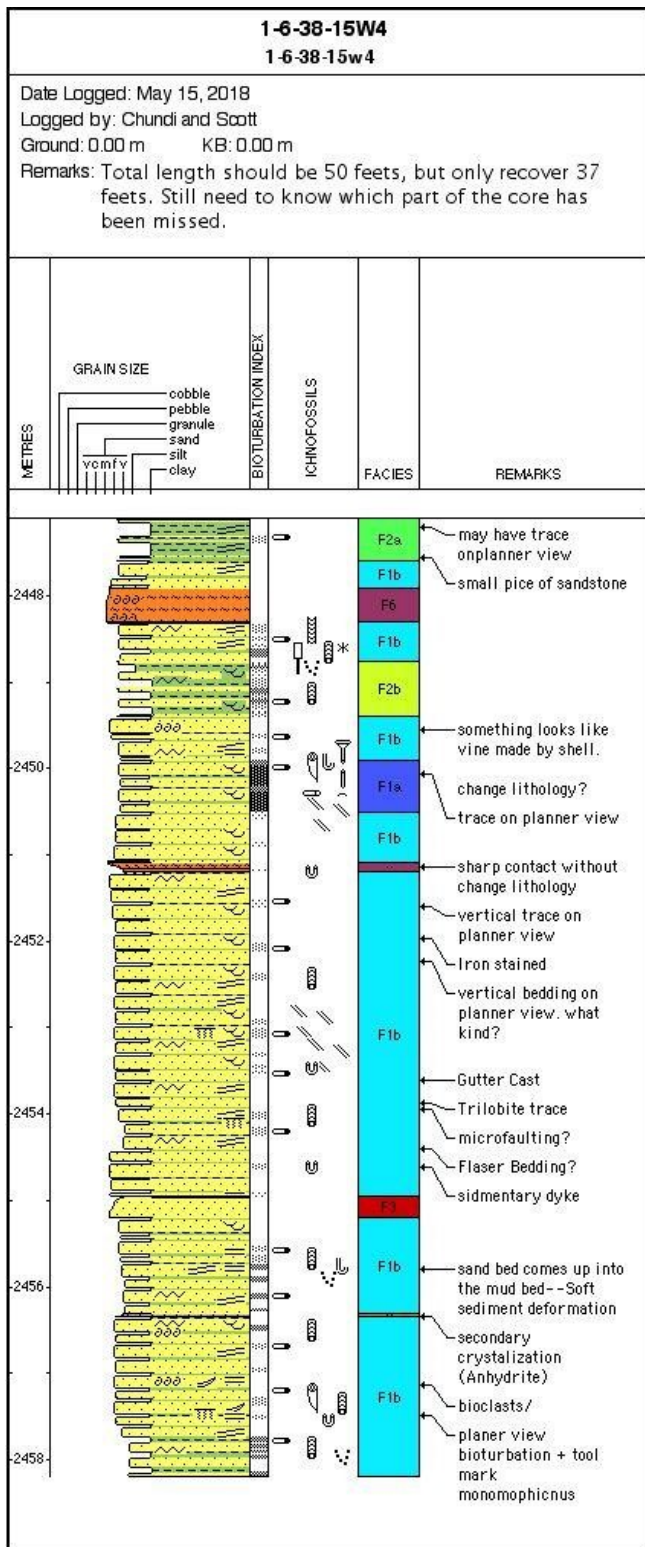


Figure 28. Strip log illustrating the sedimentological and ichnological characteristics of Well 01-06-038-15W4. It is dominated by very fine to fine-grained sandstone interbedded with mudstone (F1) and bioturbation shows low diversity and moderate intensity.

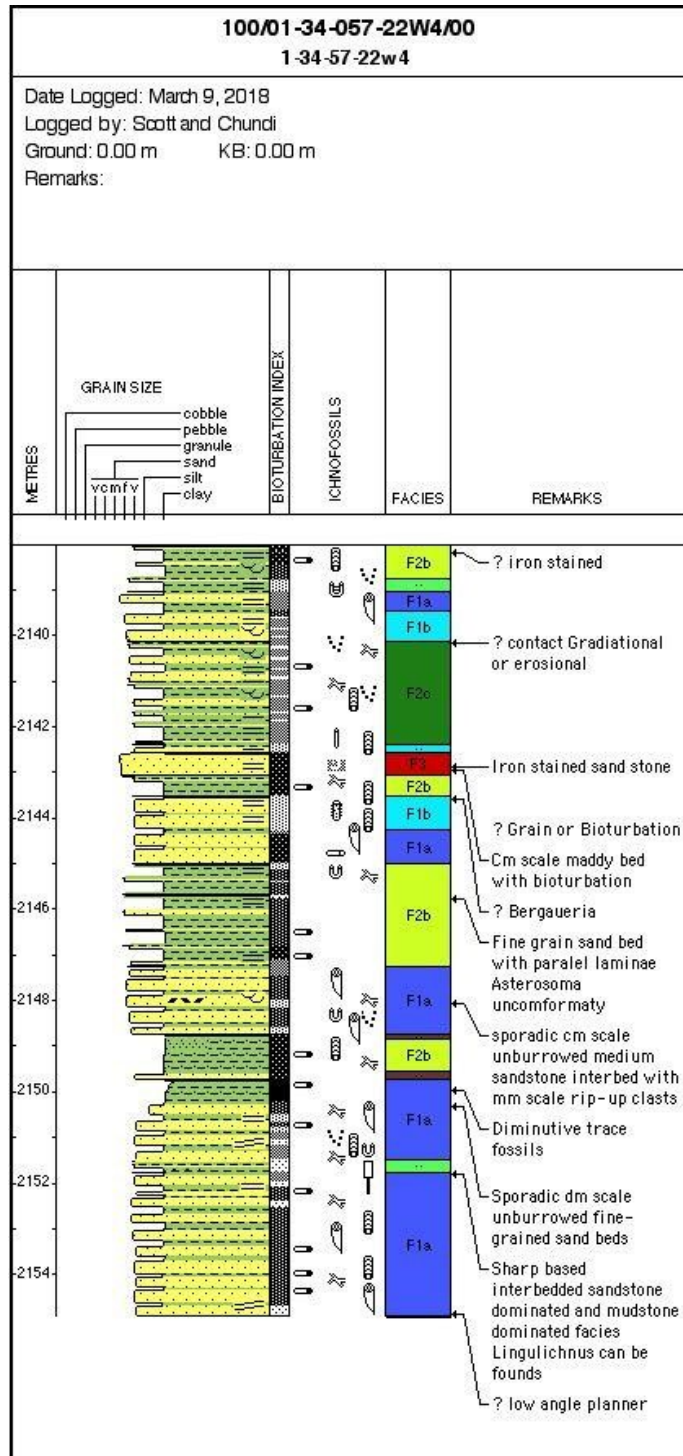


Figure 29. Strip log illustrating the sedimentological and ichnological characteristics of Well 01-34-057-22W4. It is dominated by is sandstone interbedded with mudstone (F1) and mudstone interbedded with very fine sand (F2). The Bioturbation shows low diversity and high intensity.

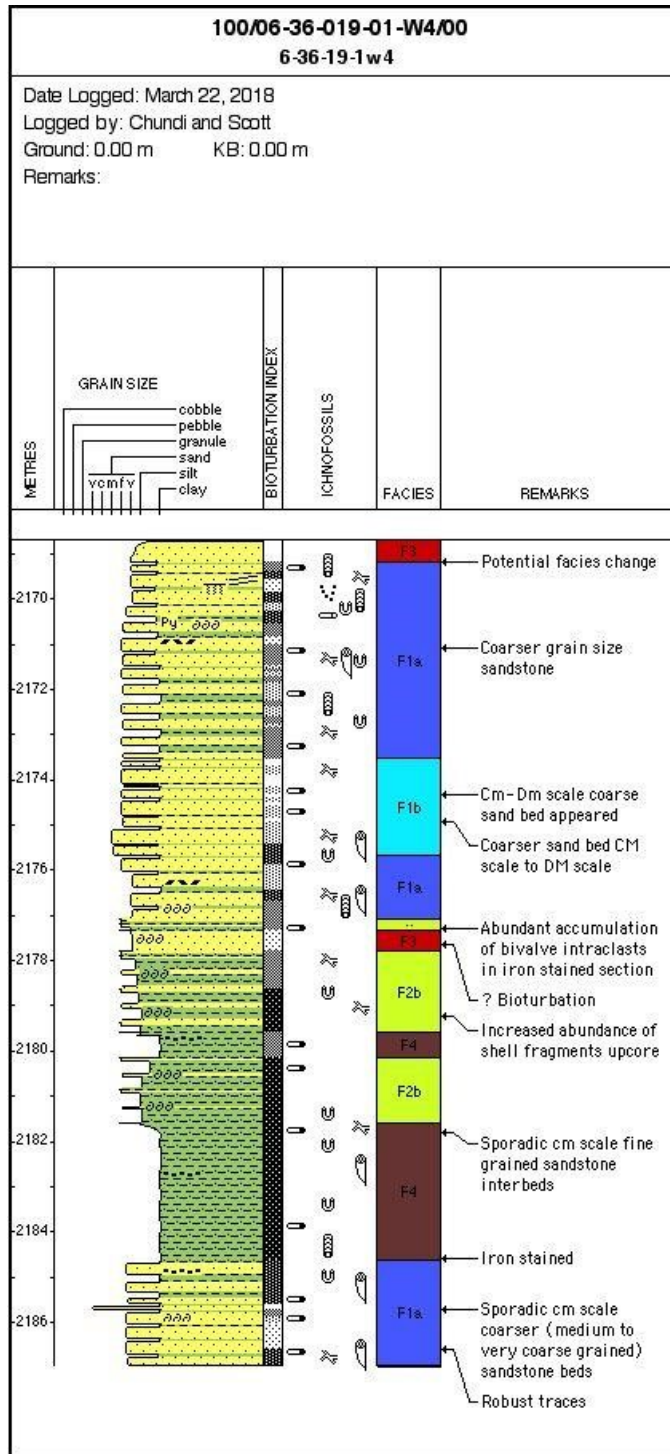


Figure 30. Strip log illustrating the sedimentological and ichnological characteristics of Well 06-36-019-01W4. It is dominated by sandstone interbedded with mudstone (F1) and heavily burrowed sandy mudstone (F4). The bioturbation shows low diversity and high intensity.

including ichnofossil species, diversity, burrow size, BI, and SDI based on Gingras (2011), is presented in Table 5 to Table 7, in the appendix. The analysis identified a total of nine facies, which are summarized in Table 3. These cores were deposited in various sub-environments ranging from shoreface to offshore. The ichnological data indicates a relatively low to moderate diversity, with eight ichnospecies identified, and most burrows having a small average size of 1 cm. The amount of bioturbation, as described by the BI, was moderate to high (BI 3-5) in most facies.

Figure 31 displays the basic features of sample 19233, which was extracted from well 1-34-57-2W4, under both PPL and XPL. The minerals identified are primarily sub-rounded quartz grains with moderate sorting. Likewise, sample 15903, collected from well 1-16-38-15W4, is composed mostly of sub-rounded quartz and glauconite grains with good sorting (Fig. 32). Sample 15962, extracted from well 6-36-19-1W4, mainly consists of sub-angular to sub-rounded quartz with good sorting (Fig. 33). All three thin sections belong to Facies 3 (Fine to medium Massive Sandstone).

3.2 Geochemical Result

Table 6 (in the appendix) presents the comprehensive results of element concentration obtained through HF digestion, while Table 8, 9, and 10 (in the appendix) provide a summary of selected elements and bioturbation information for each core. The average recovery rate for the selected elements ranges from 70% to 90%, indicating that the data is of good quality for analysis.

3.3 Relationship between elemental and ichnology data

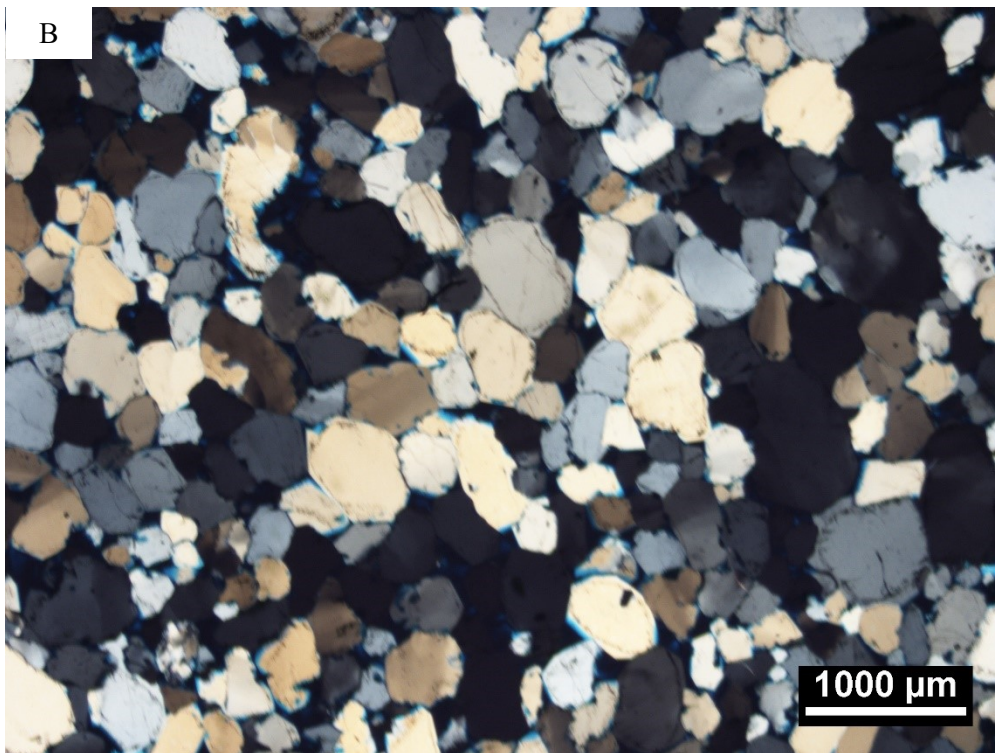
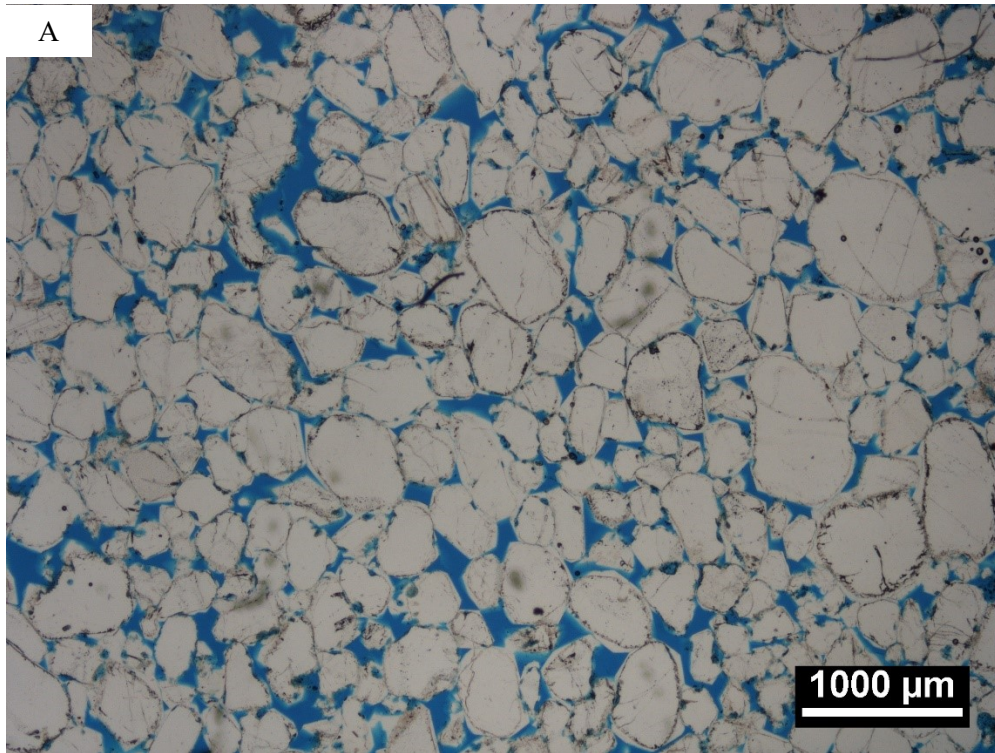


Figure 31. Thin sections under A) PPL and B) XPL of sample 19233 with 20X magnification. It has sub rounded quartz grain with moderate sorting.

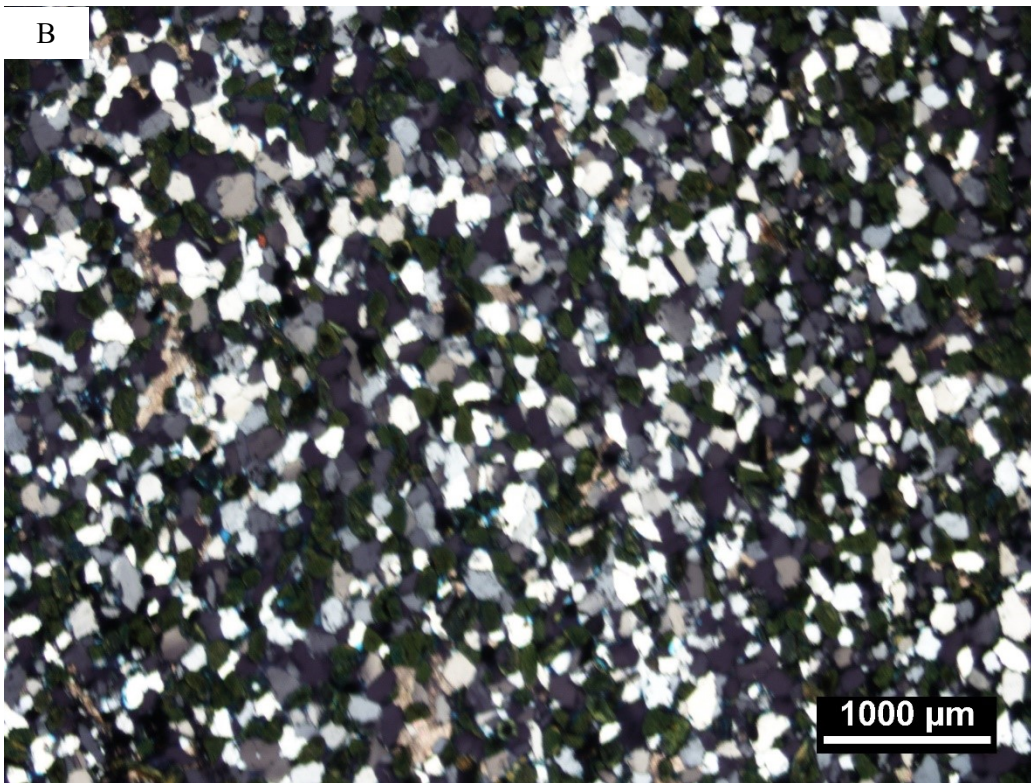
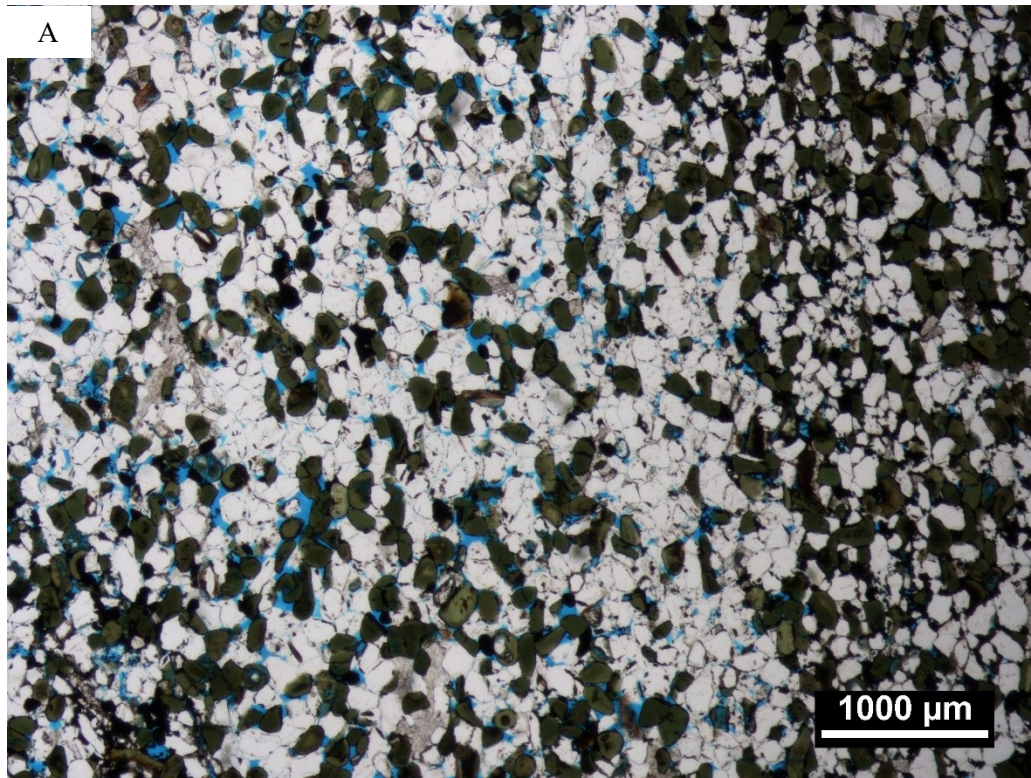


Figure 32. Thin sections under A) PPL and B) XPL of sample 15903 with 20X magnification. It has sub rounded quartz and glaucanite grain with good sorting.

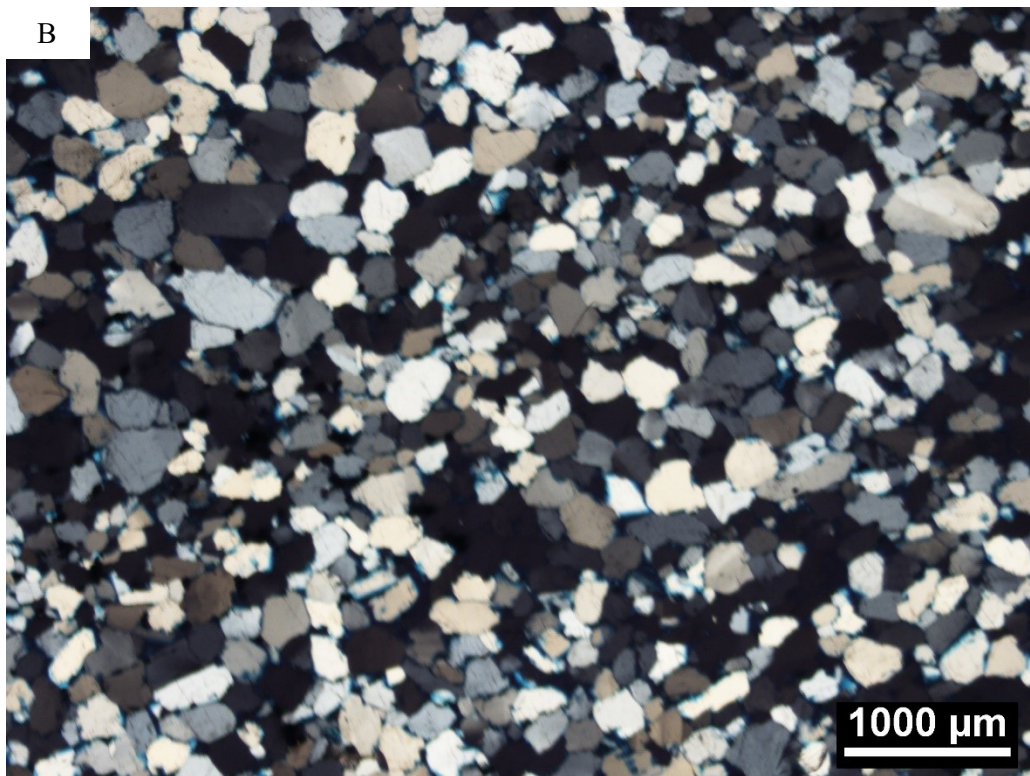
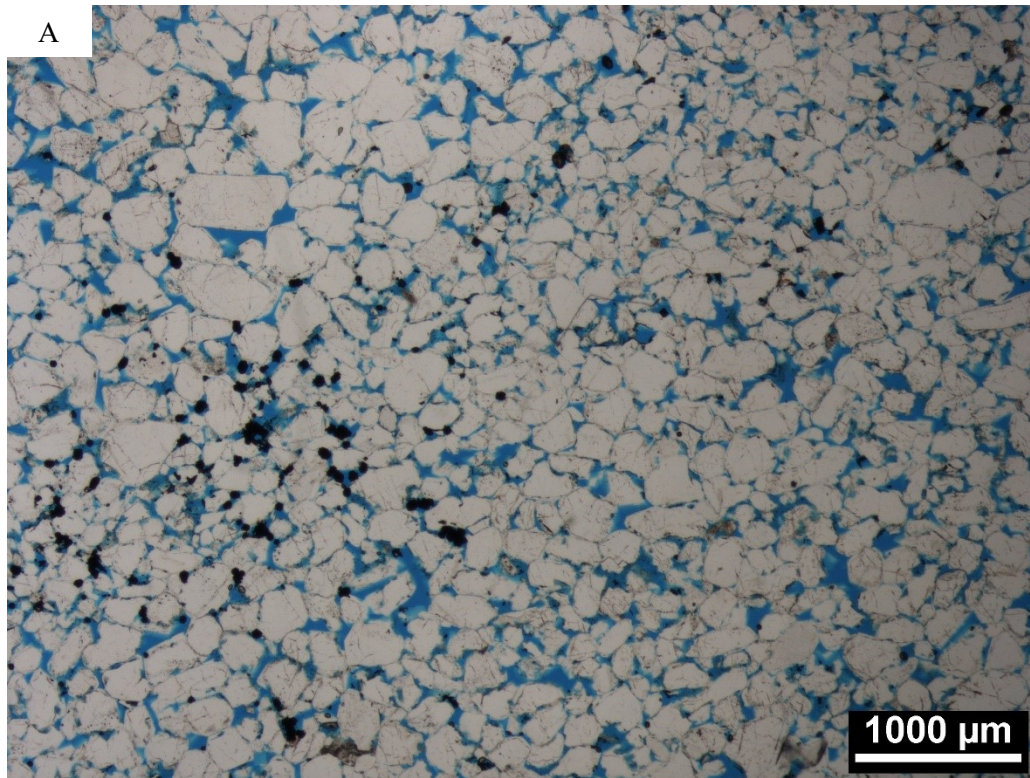


Figure 33. Thin sections under A) PPL and B) XPL of sample 15962 with 20X magnification. It has sub rounded quartz grain with good sorting.

Figures 34 through 39 depict the relationship between redox-sensitive elements and bioturbation data, represented by the Bioturbation Index (BI) and Size and Diversity Index (SDI). However, upon comparison of the elemental data to bioturbation indices, it is evident that there is no correlation between the concentration of redox-sensitive elements and bioturbation. The data points within each figure are widely dispersed in a disorderly pattern, and there is no apparent similarity between the different figures. Conversely, Figures 40, 41 and 42 demonstrate a range of trends between plots of Fe concentration and Ichnology Data as depth increases, further emphasizing the absence of any correlation between redox-sensitive elements and bioturbation.

3.4 Principal Component Analysis

Figures 43 through 45 display the outcomes of Principal Component Analysis (PCA) and illustrate the relationship between selected elements and SDI data (Appendix Table 11-14). While the wells exhibit some similarities, each well has a distinctive distribution. For example, in Well I 1-34-57-22W4, S is in the first quadrant, P, Si, and U are in the second quadrant, Zn, Ba, Ca, and Na are in the third quadrant, and Sr, V, Al, Cd, Mo, and SDI are in the fourth quadrant. In well 6-36-19-1W4, Na, Cd, S, Zn, V, Ba, and Al are in the first quadrant, Mo, U, and Si are in the second quadrant, Ca is in the third quadrant, and P, Fe, Sr, and SDI are in the fourth quadrant. In the case of well 1-6-38-15W4, Na, Ca, Fe, and Mo are in the first quadrant, Al, S, V, Zn, and Sr are in the second quadrant, Si, Ba, and U are in the third quadrant, and P, Cd, and SDI are in the fourth quadrant.

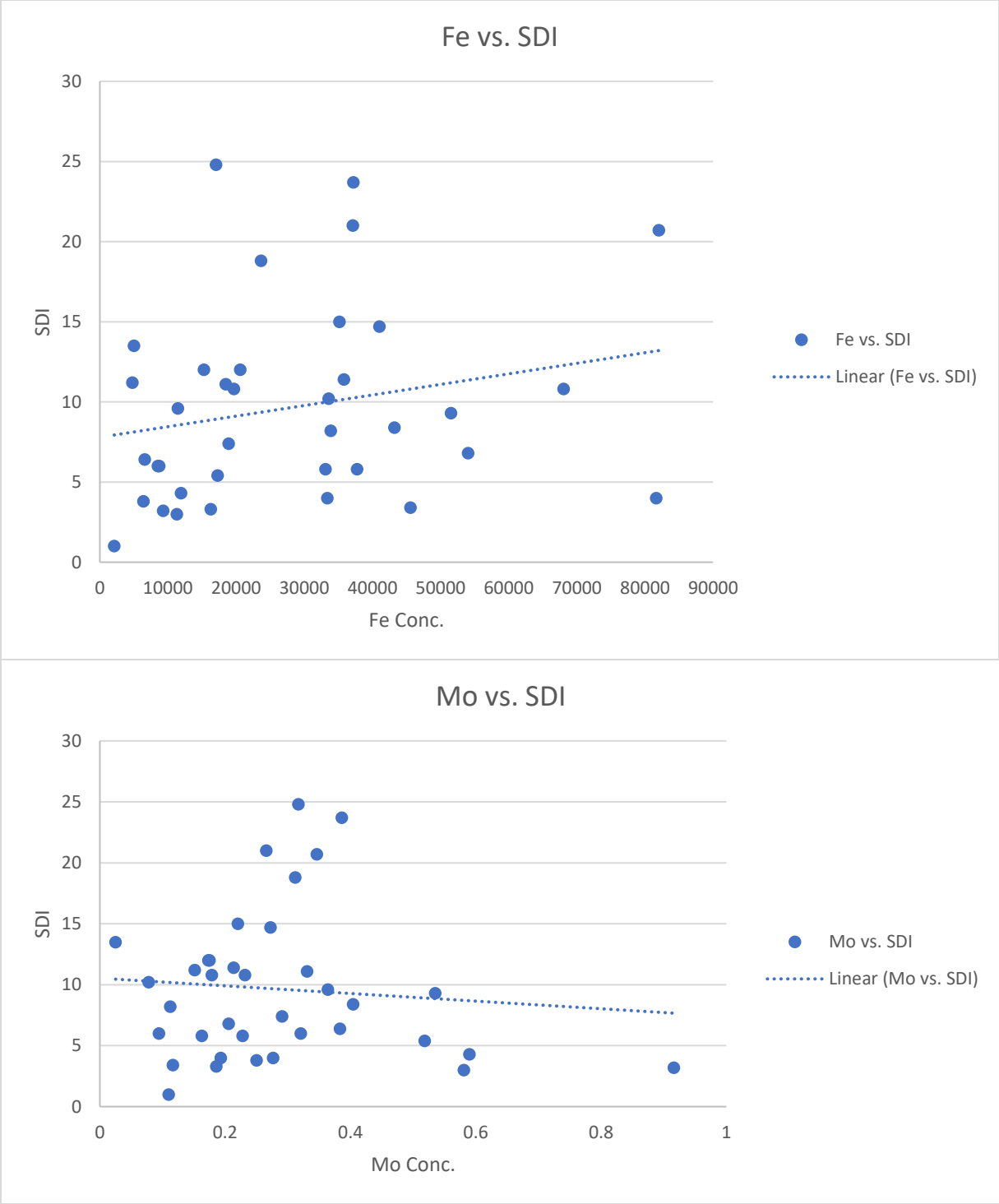


Figure 34. Scatter chart of iron and molybdenum versus Size and Diversity Index (SDI) for well 06-36-019-01W4. The data show a lack of a strong correlation between both elements and SDI values.

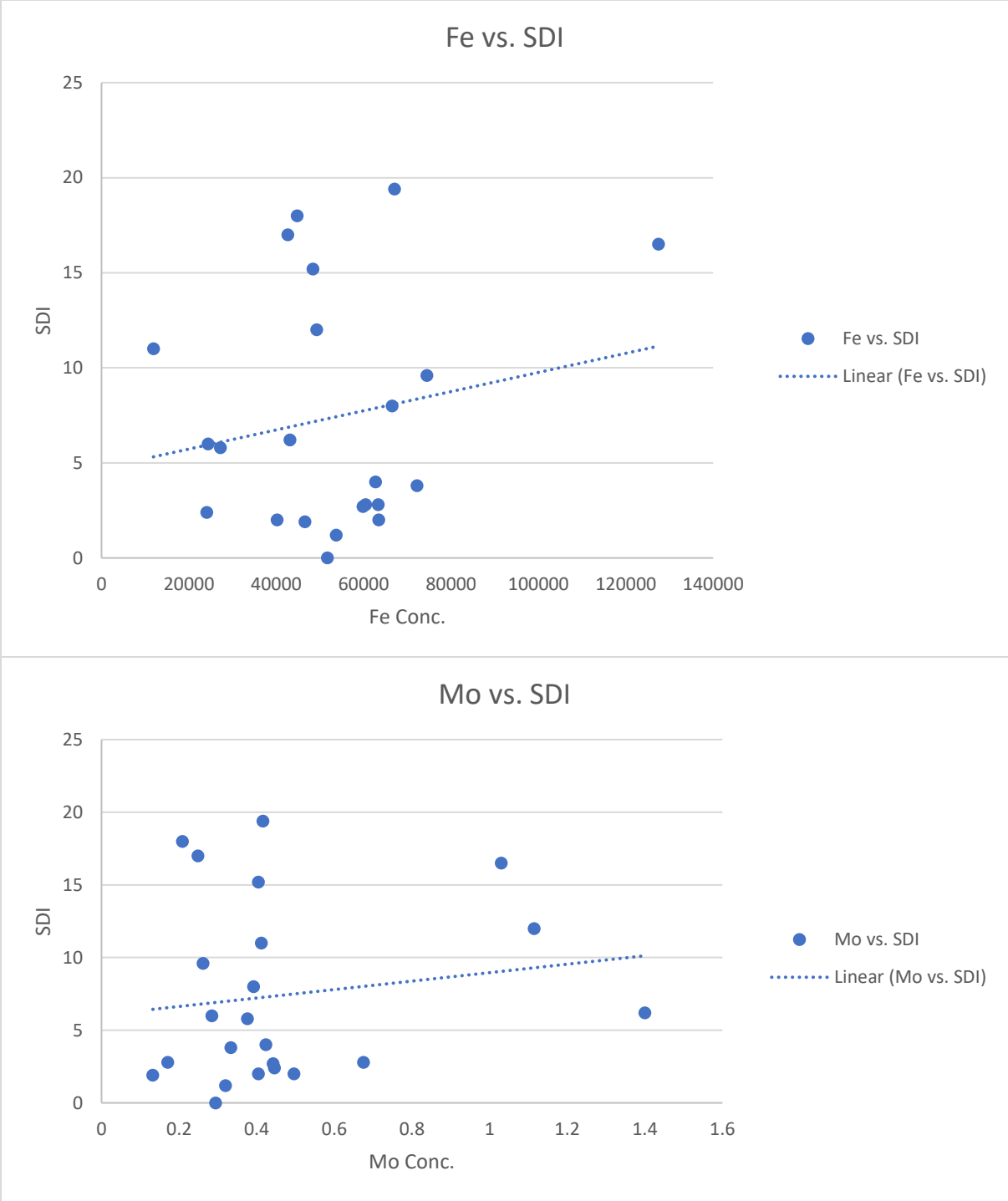


Figure 35. Scatter chart of iron and molybdenum verse Size and Diversity Index (SDI) for well 01-06-038-15W4, which shows a random spread.

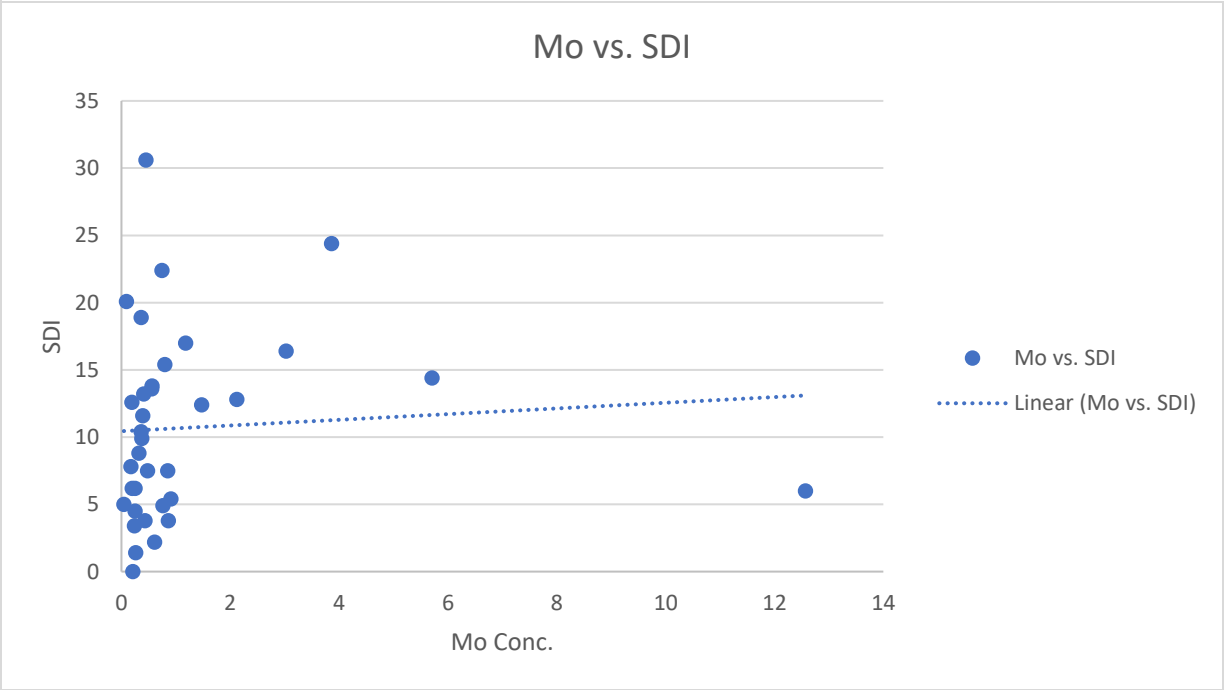
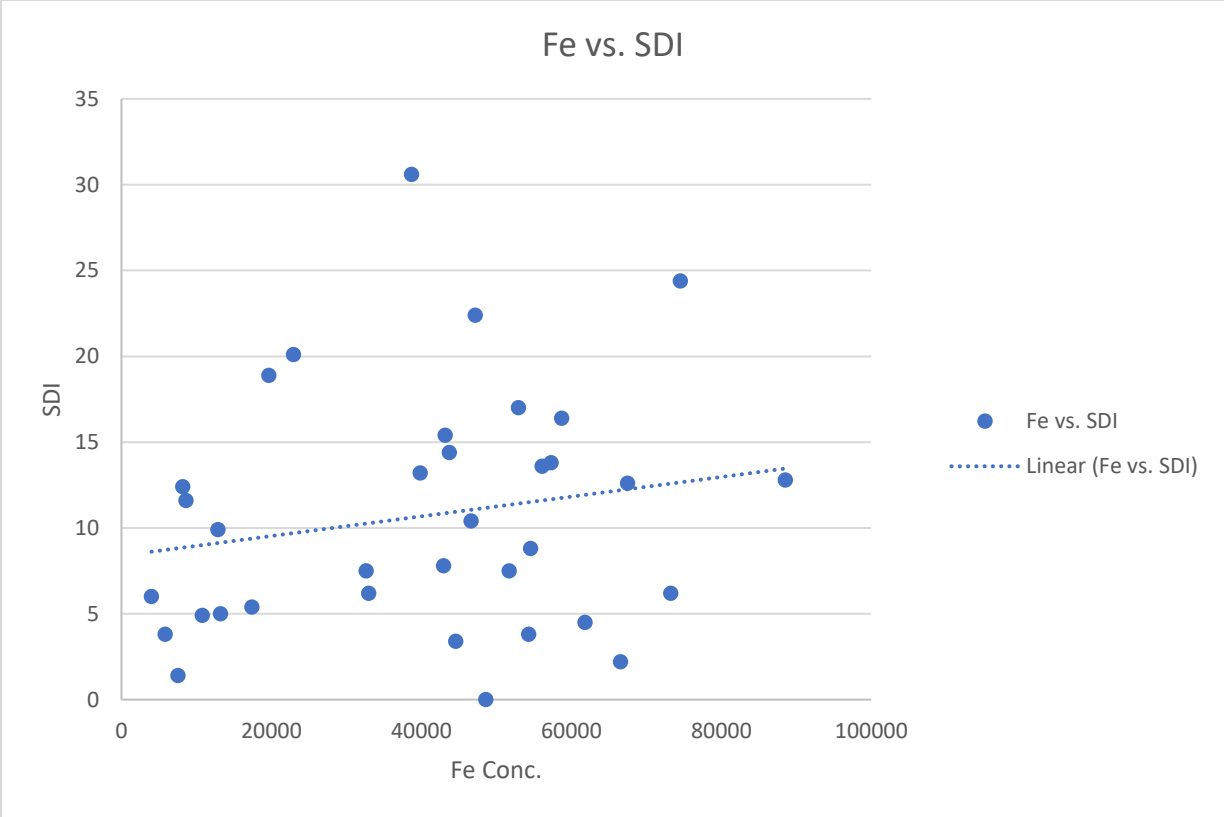


Figure 36. Scatter chart of iron and molybdenum verse Size and Diversity Index (SDI) for well 01-34-057-22W4, which shows a random spread.

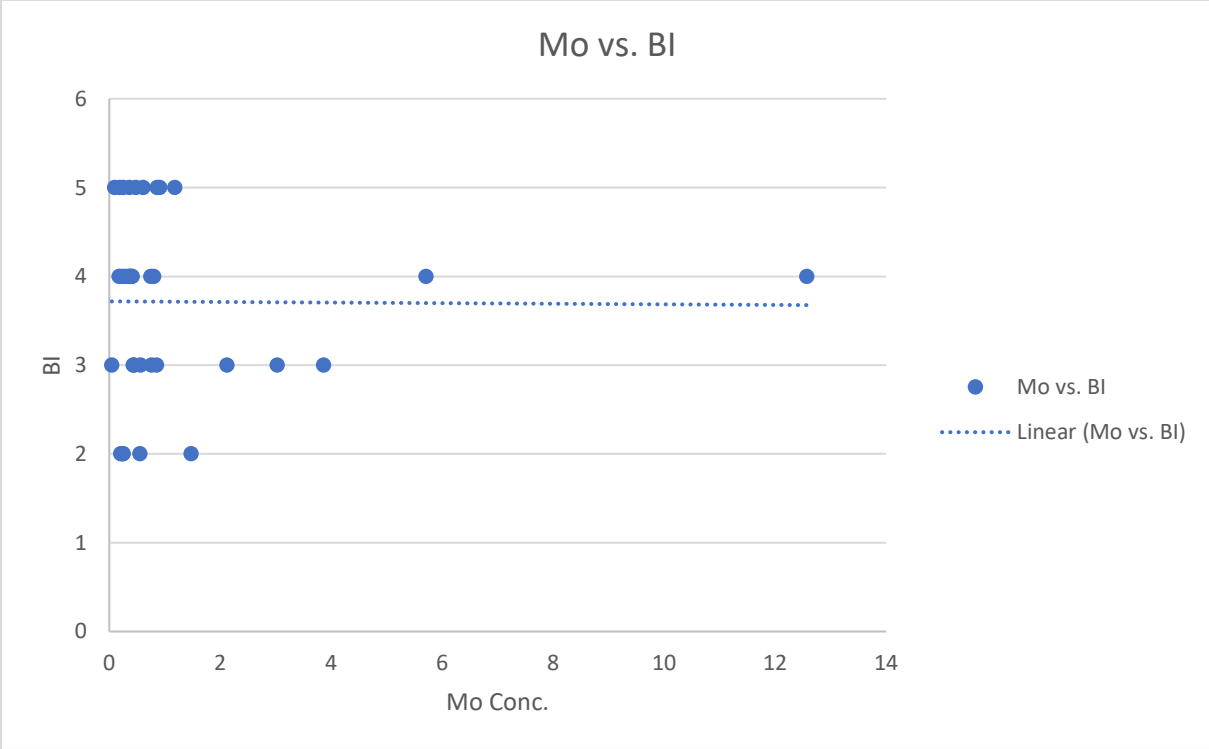
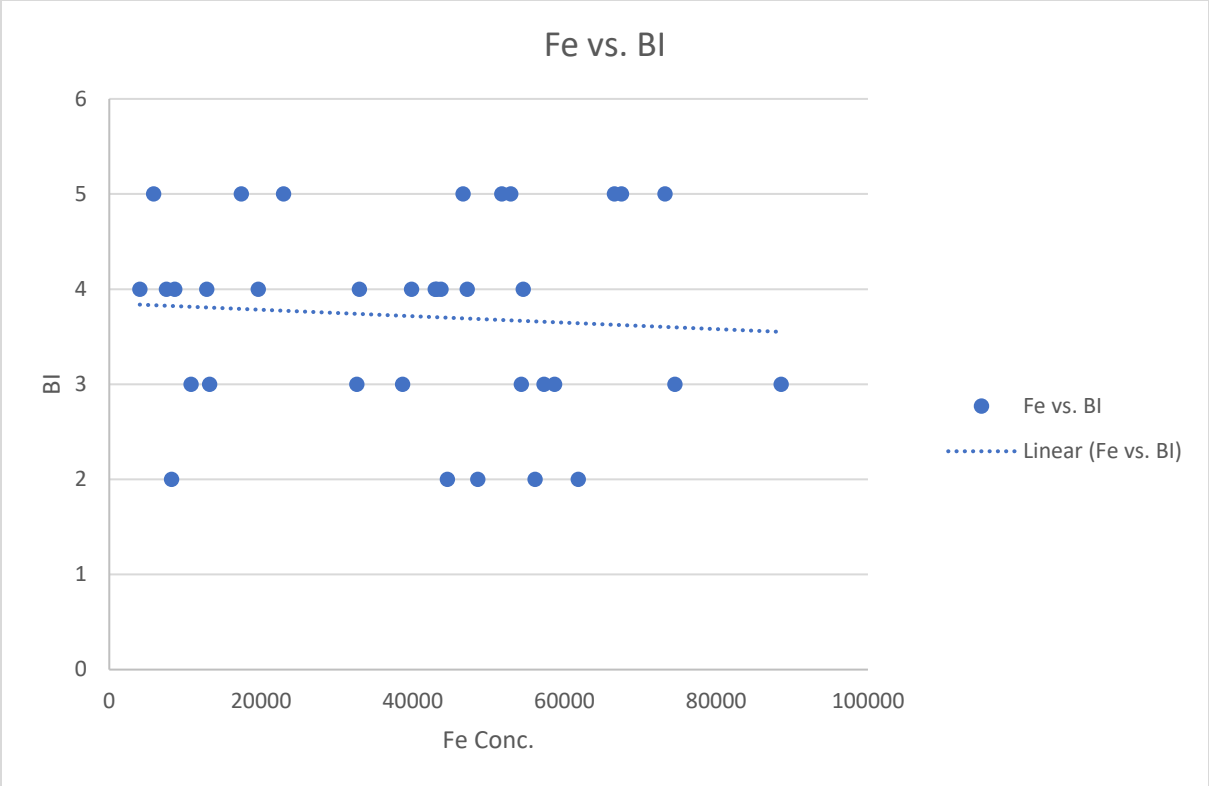


Figure 37. Scatter chart of iron and molybdenum verse Bioturbation Index (BI) for well 01-34-057-22W4, which shows a random spread.

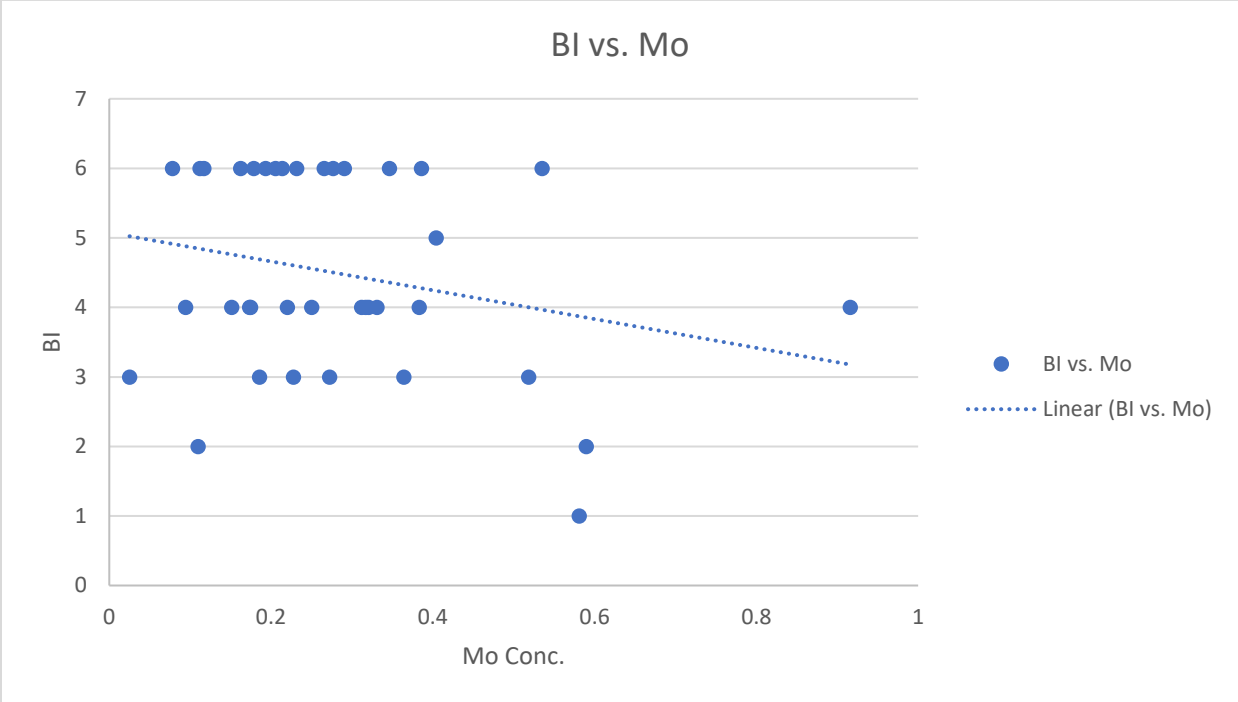
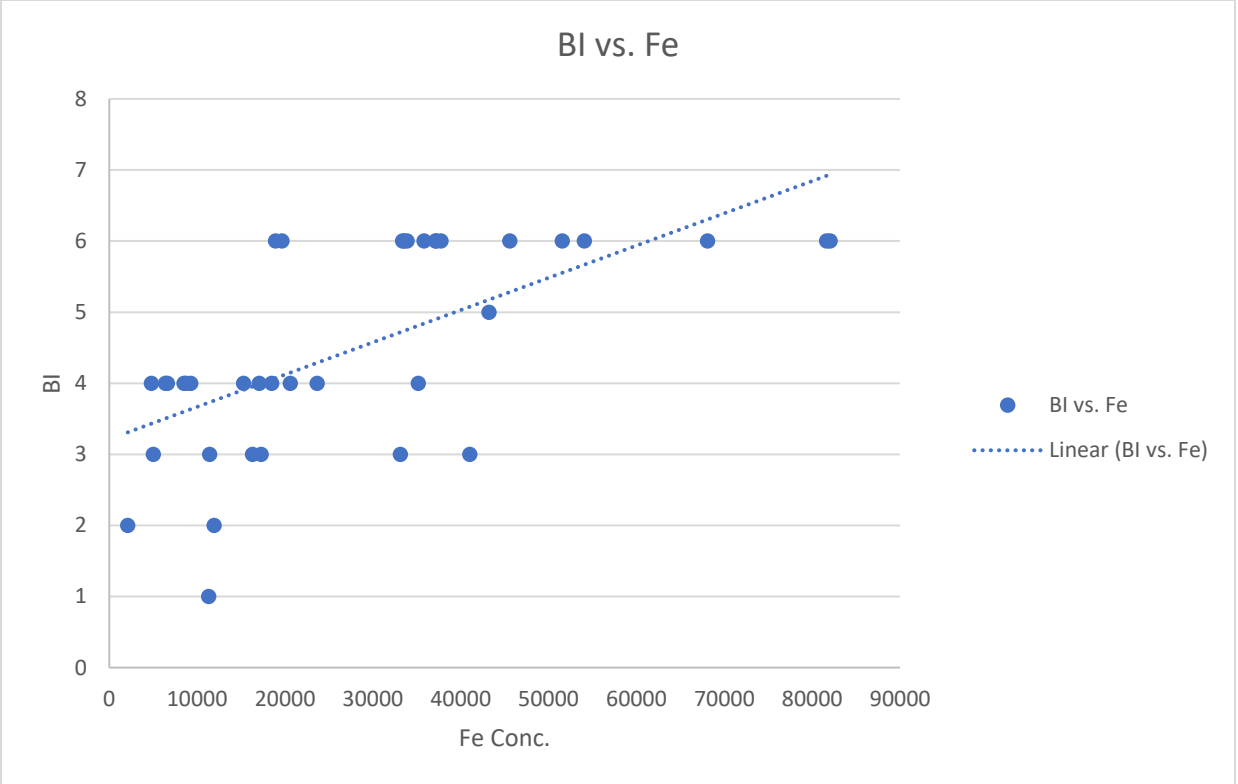


Figure 38. Scatter chart of iron and molybdenum verse Bioturbation Index (BI) for well 06-36-019-01W4, which shows a random spread.

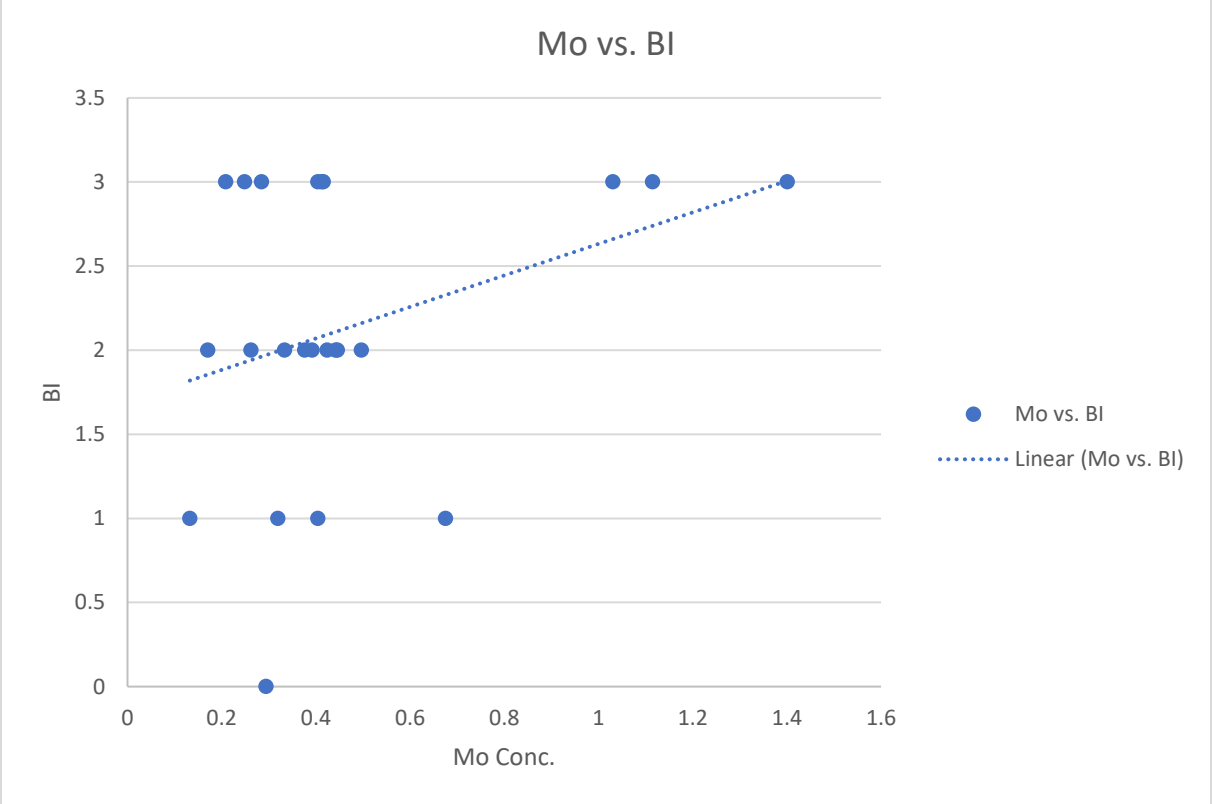
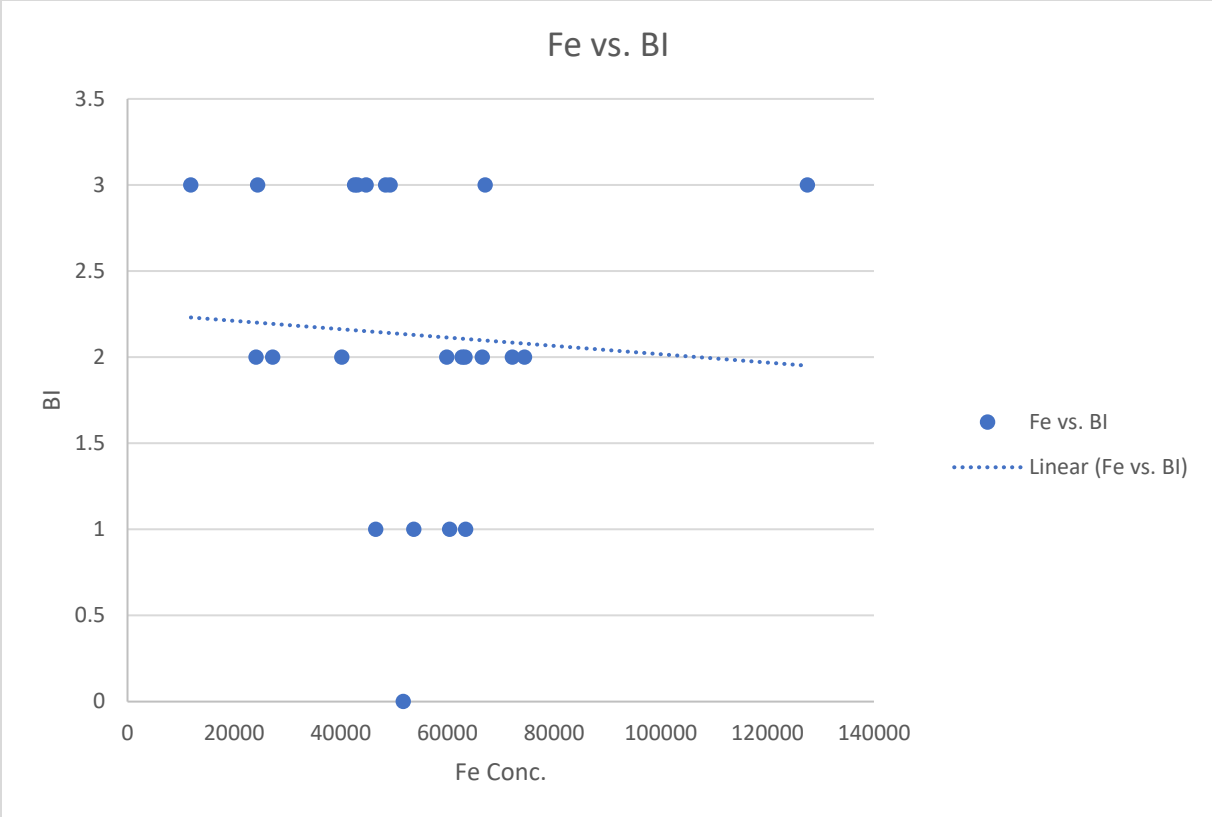


Figure 39. Scatter chart of iron and molybdenum verse Bioturbation Index (BI) for well 01-06-038-15W4, which shows a random spread.

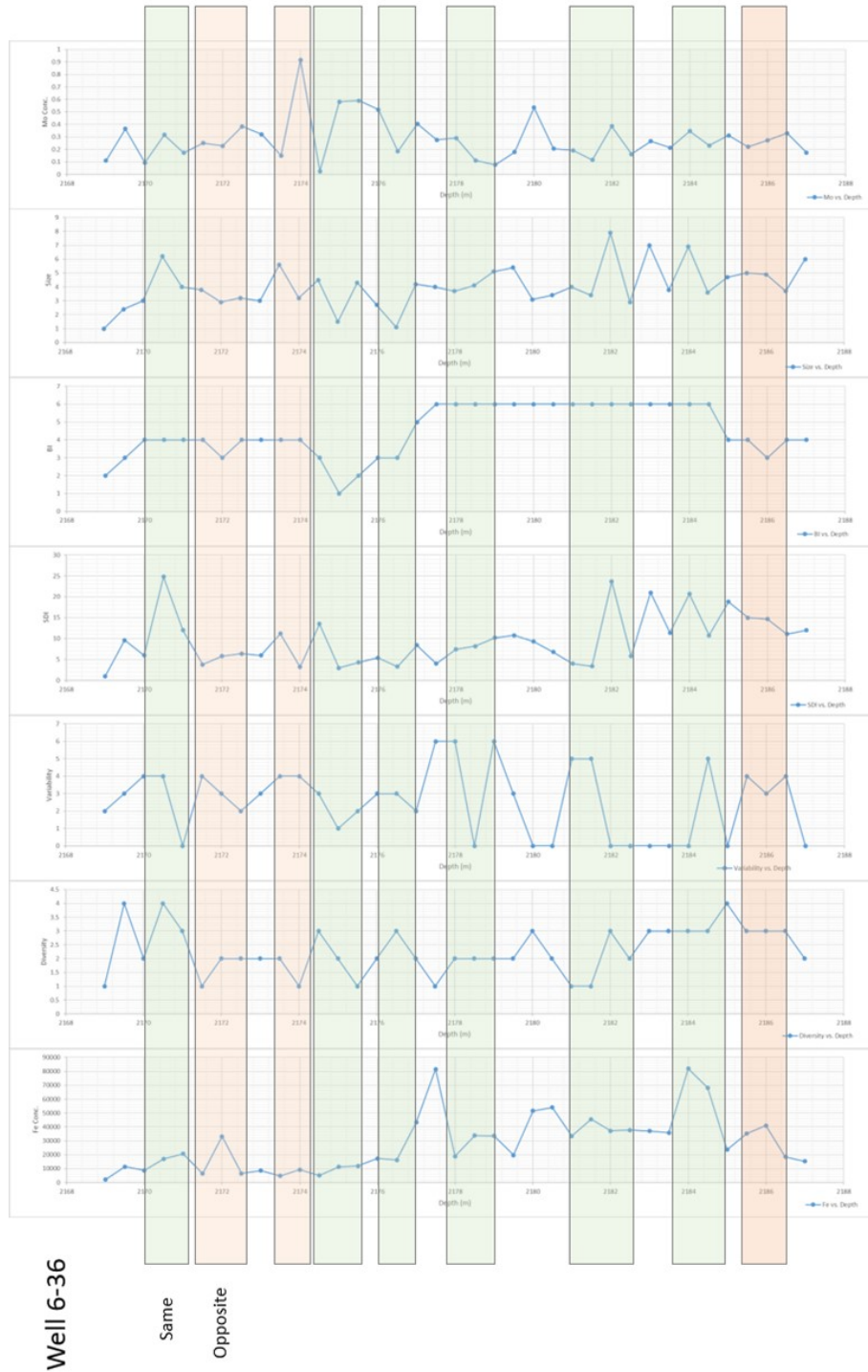


Figure 40. Compare between Fe and Mo concentration versus depth and bioturbation data *versus* depth. The light green color shows the concentration has the same trend with the bioturbation and light orange color shows they have opposite trend. Both trends can be found in the core 06-36-019-01W4.

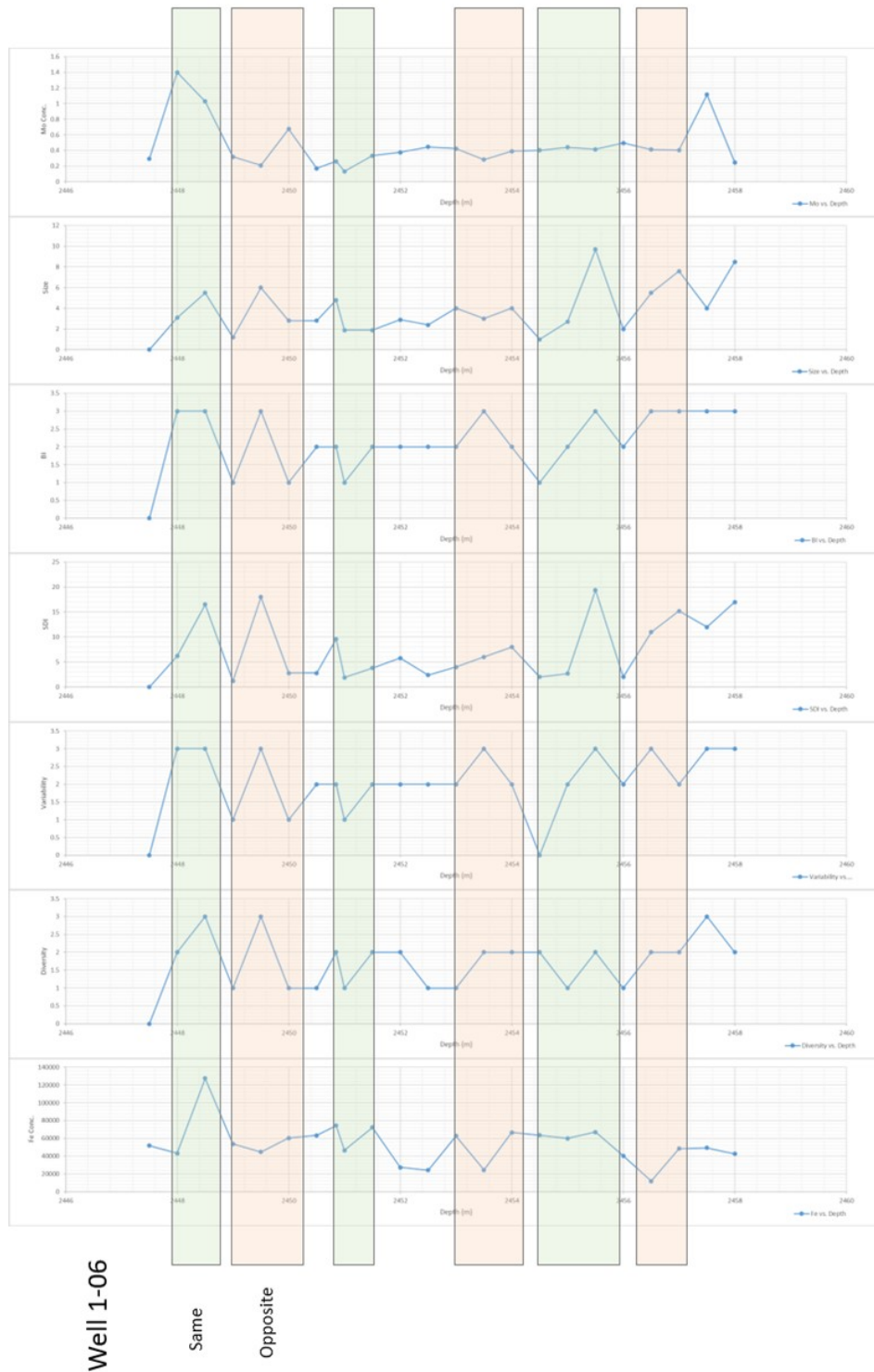


Figure 41. Compare between Fe and Mo concentration versus depth and bioturbation data vs. depth. The lite green color shows the concentration has the same trend with the bioturbation and light orange color shows they have opposite trend. Both trends can be found in the core 01-06-038-15W4.

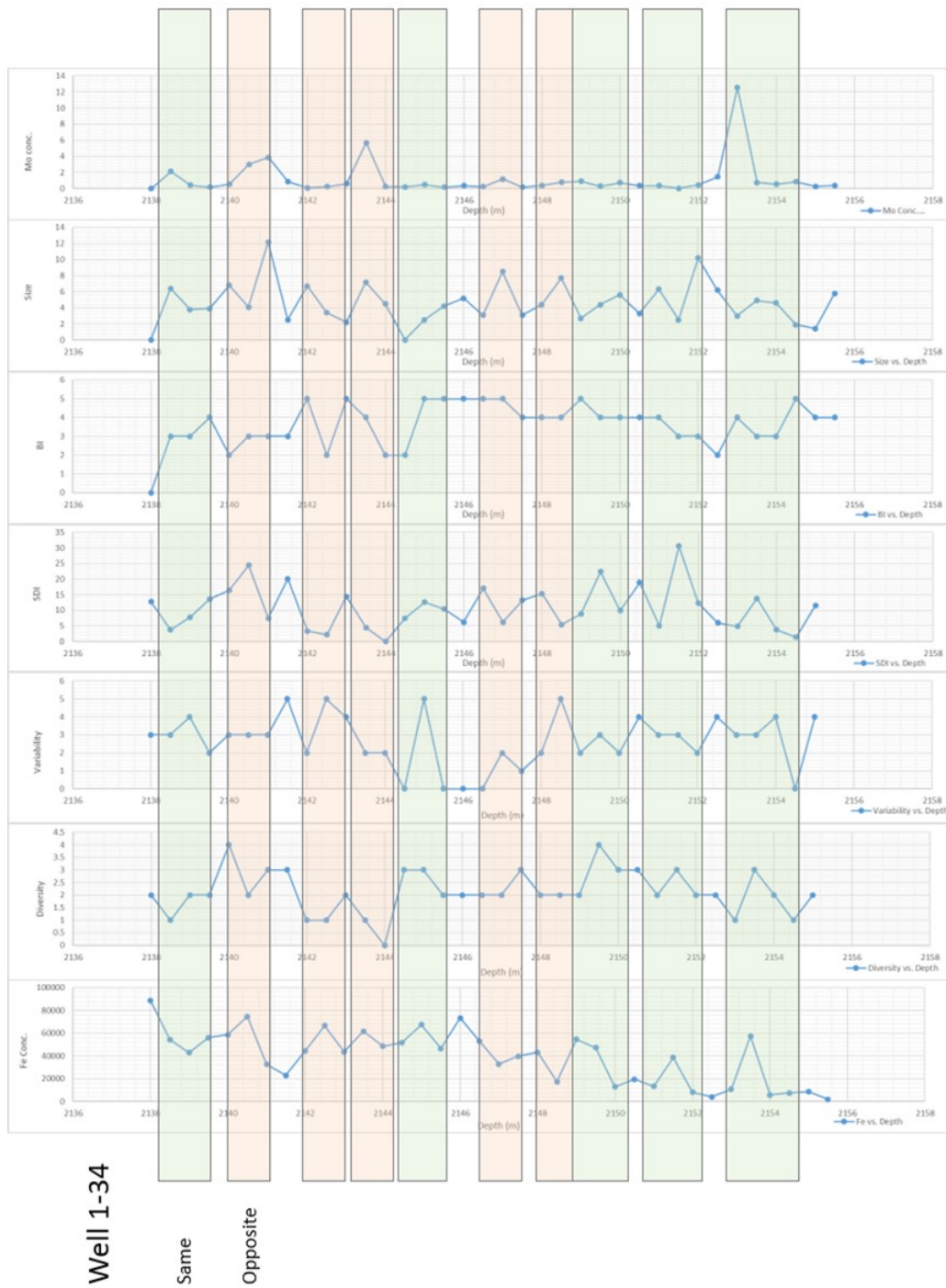


Figure 42. Compare between Fe and Mo concentration versus depth and bioturbation data vs. depth. The lite green color shows the concentration has the same trend with the bioturbation and light orange color shows they have opposite trend. Both trends can be found in the core 01-06-038-15W4.

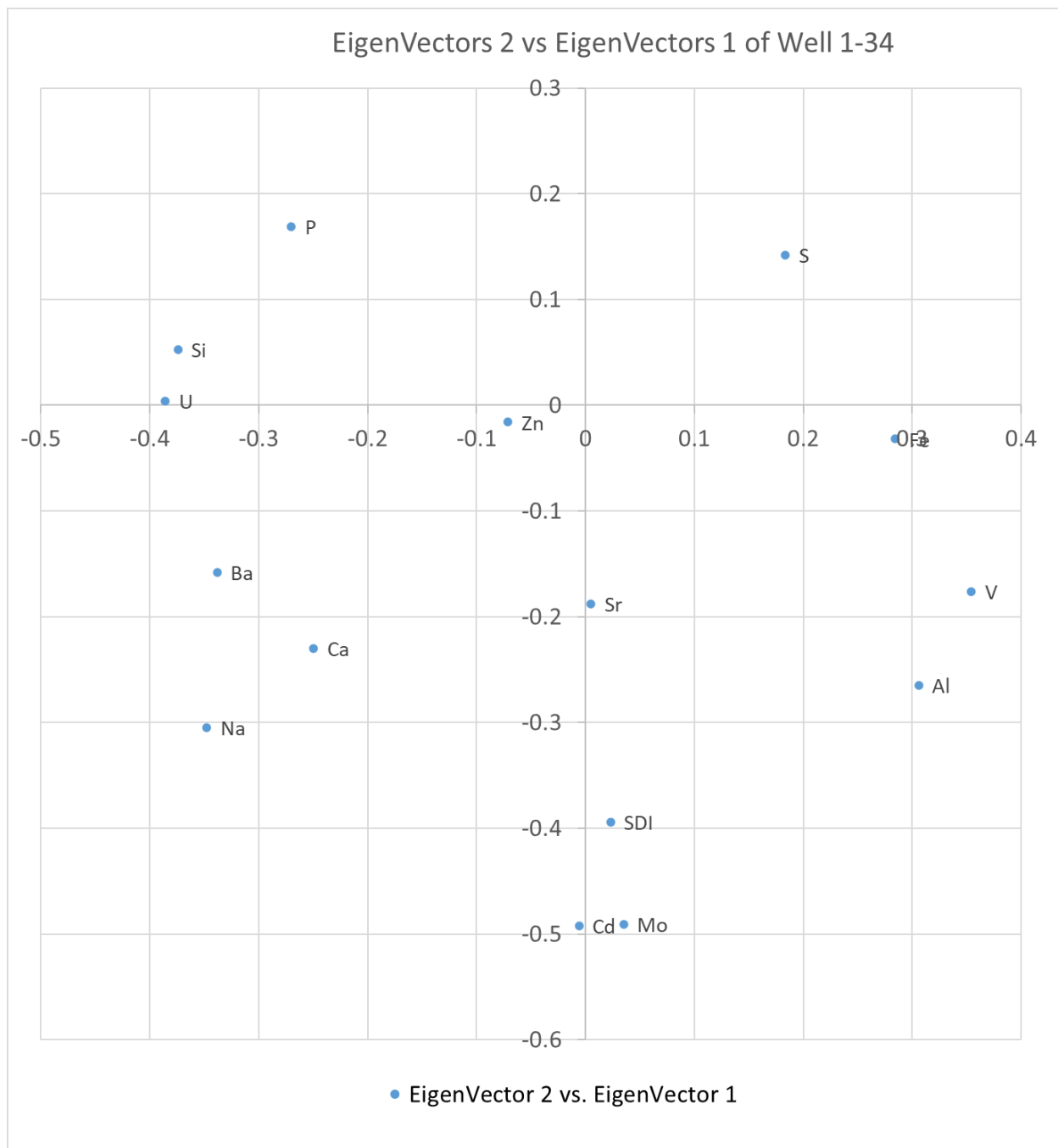
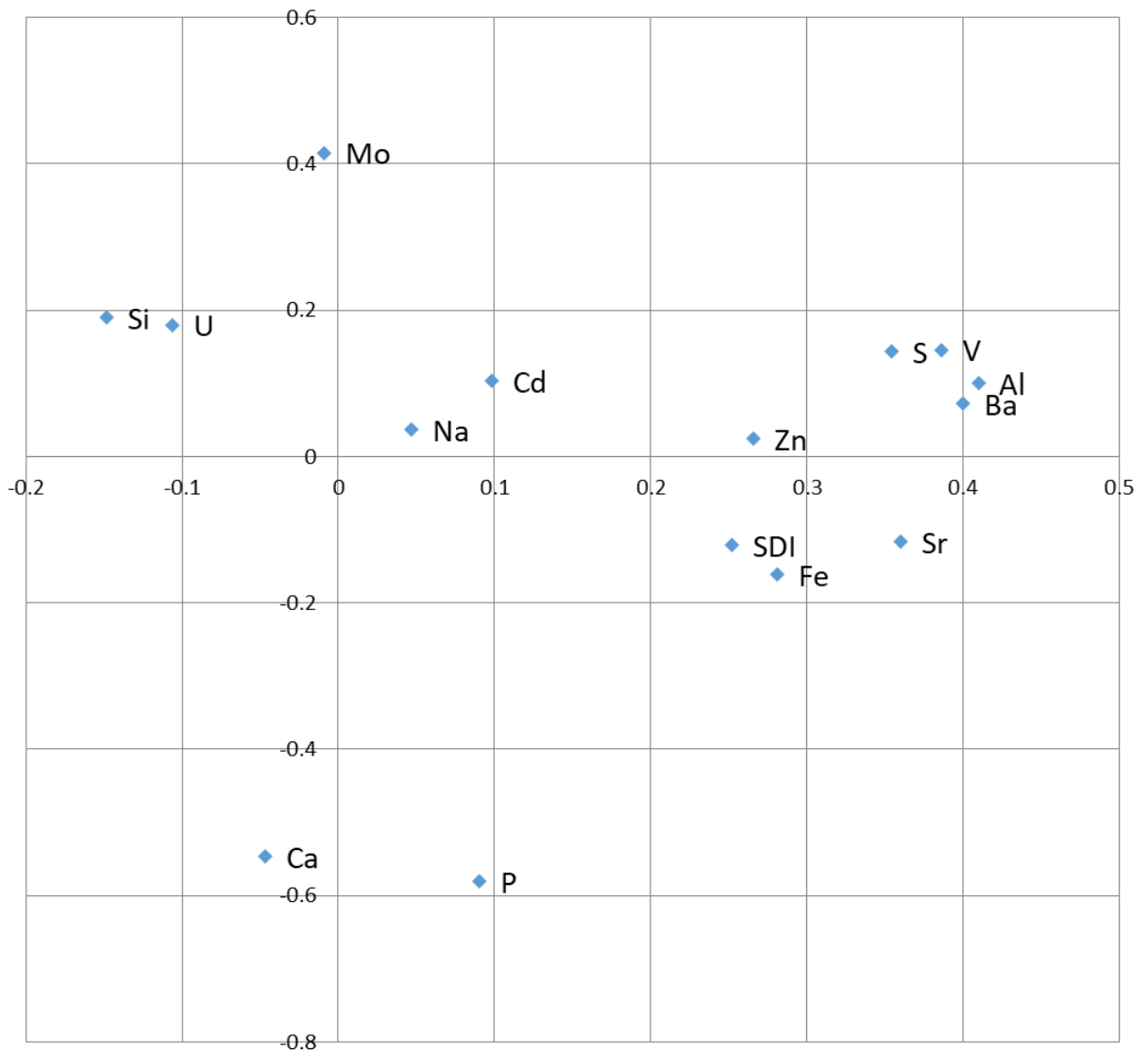


Figure 43. PCA result of Well 1-34-57-22W4 by using Eigenvectors 2 versus Eigenvectors 1. For PCA, the distance between two data points on the X-axis will determine the relationship between data points. Thus, in this well, compared to Mo and Cd, Fe has weaker relationship to SDI.

EigenVectors 2 vs EigenVectors 1 of Well 6-36



◆ EigenVectors 2 vs EigenVectors 1

Figure 44. PCA result of Well 6-36-19-1W4 by using EigenVectors 2 versus EigenVectors 1. For PCA, the distance between two data points on the X-axis will determine the relationship between data points. Thus, in this well, compared to Mo and Cd, Fe has stronger relationship to SDI.

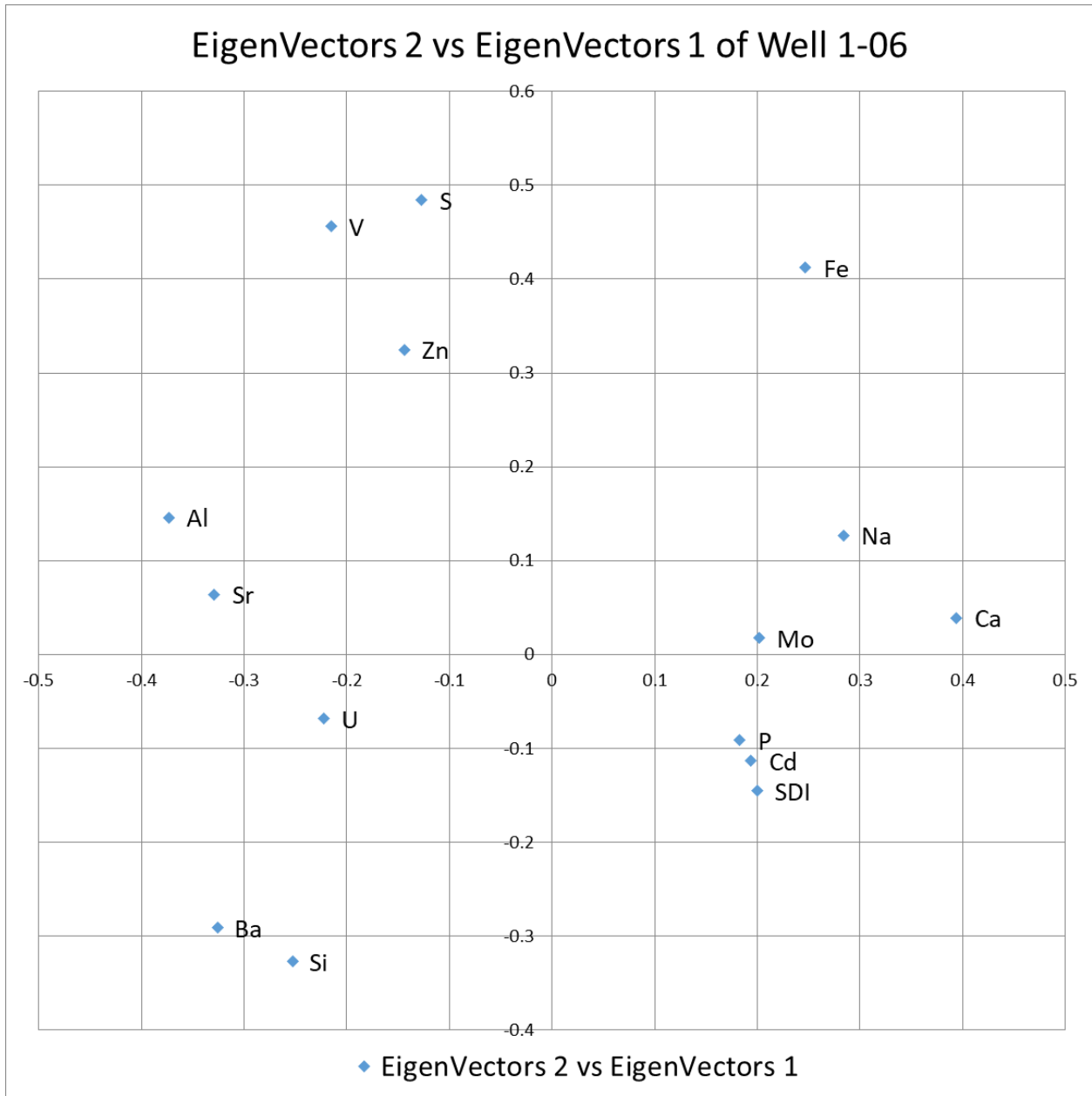


Figure 45. PCA result of Well 1-6-38-15W4 by using Eigenvectors 2 vs Eigenvectors 1. For PCA, the distance between two data points on the X-axis will determine the relationship between data points. Thus, in this well, compared to Mo and Cd, Fe has weaker relationship to SDI.

The proximity of the elements to each other on the scatter plots indicates their co-occurrence. Elements that plot near each other are likely present in the same mineral phase (Ratcliffe et al., 2015). For instance, in Figures 43 and 45, Cd and Mo in the pair of wells 1-34-57-22W4 and 1-6-38-15W4 were more closely associated with SDI than the connection between Fe and SDI. On the other hand, there is a more significant association between Fe and SDI in well 6-36-19-1W4 (Figure 44). In general, Fe displays a correlation with Al in all three wells. Notably, the presence of Si does not appear to maintain a robust relationship with the other elements analyzed across all three wells.

4. Interpretation

4.1 Sedimentology and ichnology interpretation

Facies 1a (F1a) is composed mainly of very fine-grained sandstone with interbedded mudstone, and is characterized by burrowing structures and wavy parallel and low-angle tabular bedding. The dominant ichnofossils include *Teichichnus*, *Cylindrichnus*, *Planolites*, *Arenicolites* and *Lingulichnus*. Bioturbation in this facies ranges from moderate to high, with a BI value of 3-4.

The depositional environment of F1a is interpreted to be lower shoreface, where sedimentary structures are mostly obscured due to moderate to high bioturbation. The presence of low-angle tabular and cross bedding is believed to reflect the influence of temporary high-energy conditions. The Cruziana Ichnofacies is also present in the trace fossil assemblages, supporting this interpretation.

Facies 1b (F1b) is characterized by intermittently burrowed, very fine- to fine-grained sandstone interbedded with mudstone, and is often marked by low angle tabular bedding and

planar bedding. Trace fossils found in this facies include *Teichichnus*, *Cylindrichnus*, *Planolites*, and *Ophiomorpha*, with a bioturbation index (BI) ranging from very low to low (0-3).

The depositional environment of F1b is interpreted to be the middle shoreface, based on the presence of low-angle tabular bedding and planar bedding, which suggests high hydraulic conditions. The low BI indicates high environmental stress. The assemblage of trace fossils found in F1b is consistent with the *Skolithos* Ichnofacies (Pemberton and MacEachern, 1995).

Facies 2a (F2a) is characterized by mudstone interbedded with lightly burrowed very fine sand. The dominant sedimentary structure in this facies is planar bedding. Trace fossils in F2a are limited to *Planolites*, and the Bioturbation Index is very low at 1. Based on these observations, F2a is interpreted as having been deposited in an upper offshore environment with low oxygen levels. The presence of abundant mud suggests a low energy environment, while the very low BI suggests high environmental stress. Planar bedding is likely a result of tempestites generated during temporary high energy events.

Facies 2b (F2b) is characterized by interbedded burrowed mudstone or sandy mudstone and sandstone, with a grain size of mud and very fine sand. This facies lacks sedimentary structures and appears mostly massive. A high bioturbation index (3-5) and a diverse assemblage of trace fossils including *Teichichnus*, *Cylindrichnus*, *Planolites* and *Arenicolites* are identified. The high BI suggests a low-stress environment with low energy, and the ichnofossils indicate the *Cruziana* Ichnofacies (MacEachern et al., 2008). Sedimentary structures are rare, suggesting a low-energy environment with the presence of only a few planar beds possibly representing tempestites. These characteristics suggest that this facies was deposited in a fair-weather dominated offshore transition zone.

Facies 2c (F2c) is a unit consisting of planar bedded mudstone interbedded with sandstone, sporadically burrowed by *Teichichnus* and *Planolites*. Both sedimentary structures, such as cross bedding and planar bedding, and biogenic structures are identified in this facies. The grain size ranges from mud to very fine sand. The Bioturbation Index varies from 0 to 4.

The depositional environment for this facies is interpreted to be a storm-dominated offshore transition. The presence of *Cruziana* Ichnofacies supports this interpretation. The high mud content indicates a low-energy environment, and the sporadically high BI suggests periods of low environmental stress. However, the discovery of planar beds with a very low BI in this unit is interpreted as tempestites.

Facies 3 (F3) is characterized by fine to medium sandstone that appears massive with no distinct sedimentary or biogenic structures. F3 appears between a very fine grain size sediment unit. This erosional contact may represent a transgressive surface of erosion. Shell fragments are present in this unit. The well-sorted fine to medium sand grain size and lack of bioturbation suggest a high-energy environment and high-stress conditions for organisms, likely due to high sedimentation rates and exposure to air. All of these characteristics lead to the interpretation that F3 was deposited in a foreshore environment.

Facies 4 (F4) consists of heavily burrowed sandy mudstone without identifiable sedimentary structures. The high to very high bioturbation index (4-6) suggests a low energy and low stress environment where biogenic structures replace primary structures. The dominant ichnofossils in F4 are *Teichichnus*, *Cylindrichnus*, *Planolites*, and *Arenicolites*, indicating the presence of the *Cruziana* Ichnofacies (MacEachern et al., 2008). These characteristics suggest that F4 was deposited in a fair-weather dominated upper offshore environment.

Facies 5 (F5) is composed of anhydrite dolostone and lacks both biogenic and sedimentary structures. This facies is only found in Well 1-6-38-15W4. Due to its lithology and the presence of block anhydrite, it is possible that F5 was deposited in a lagoon environment.

Facies 6 (F6) is bioclastic sandstone and lacks sedimentary structures. It is also found in Well 1-6-38-15W4. The bioturbation index is 0-1, with the minor presence of *Arenicolites*. The most notable feature of this facies is the presence of a shell bed matrixed with sand, indicating deposition in a beach (foreshore) environment.

Although the nine facies in these cores do not fully represent all sub-environments within the shoreface model, they can still be interpreted within a shoreface model framework. This model includes lower to upper shoreface, upper offshore, and foreshore environments. While all three cores exhibit similar depositional environments, well 1-6-38-15W4 appears to have been deposited in shallower environments due to the presence of the lagoon and foreshore environments.

Despite the limited trace fossil diversity and small burrow size (diameter) in most parts of these cores, the moderate to high BI suggests that the oxygen level was sufficient for animal colonization. The small size and low diversity of the trace fossil suites indicate a relatively high degree of chemical/physical stress (Gingras et al., 2011).

Overall, there is not a significant difference in the ichnology between the Mount Whyte Formation and the Stephen and Cathedral formations.

4.2 Interpretation from Geochemical dataset

The goal of this study was to examine the connection between redox-sensitive elements and bioturbation. However, it is difficult to establish a clear relationship between the chosen

elements and bioturbation by simply combining ichnological factors and PCA analysis data. The data points in Figures 33 to 39 are highly scattered, and the trend line indicates that the correlation between bioturbation and geochemical data is very poor. Some plots exhibit a positive correlation while others show a negative correlation. Additionally, the comparative plots provide a straightforward understanding that positive and negative correlations can coexist within the same well. As a result, Principal Component Analysis is a more appropriate method for investigating the relationship.

Overall, the PCA analysis suggests that there is not a strong relationship between the redox-sensitive elements and bioturbation in these sedimentary environments. While some elements, such as Mo and Cd, may indicate higher oxygen levels in the sediment, the relationship is not consistent across all wells and the fluctuations in oxygen levels may not have been large enough to affect burrowing infauna. Elevated Fe is often observed in association with high SDI (heavily burrowed) and other redox-sensitive elements, but the PCA-distance between Fe and those factors is further, indicating that Fe is not a reliable indicator of redox conditions. The distance between Si and SDI suggests that Si may have originated from a continental environment, and is not strongly correlated with redox conditions or bioturbation. In short, no strong relationship exists between redox-sensitive elements and bioturbation in the studied core.

Thin sections from these three wells shows that the mineralogy is dominated by quartz; the sphericity is from sub-angular to sub-rounded and the grain sizes of the sand grain are roughly equal. This indicates that the sand is mature (Folk, 1951). In well 1-6-38-15W4, Fe is close to the SDI, which suggests the hematite may be related to organic material in Stephen and Cathedral formation. It may also indicate that oxidizing conditions can happen. Important prerequisites for this are low organic productivity and a rapid rate of oxidation of organic

material (Turner, 1979). For the reddish material in well 1-34-57-22W4 and well 6-36-19-1W4 (Mount Whyte formation), because the distance between Fe and clay and detrital element indicator Al (Playter et al., 2018) is generally far in all three well, the reddish material should not be derived from either weathered source areas, sediments previously deposited (Lajoie and Chagnon, 1973; Ziegler and McKerrow, 1975), but may formed by a replacement of hematite (Turner, 1979).

Therefore, based on the PCA analysis and the mineralogical characteristics of the sediment, it can be inferred that the red bed was likely formed through a diagenetic process rather than as a result of the original depositional environment. The weak relationship between Fe and redox-sensitive elements further supports this interpretation. The replacement of detrital grains by clay and other minerals during diagenesis is a common process that can lead to the formation of Fe minerals, including hematite, which may explain the presence of Fe in the red bed.

5. Conclusion

In summary, a total of nine facies have been identified in wells 1-6-38-15W4, 1-34-57-22W4, and 6-36-19-1W4, with a shoreface environment being interpreted as the depositional environment. The relationship between redox sensitive elements and bioturbation distribution is not strong, and there is no clear relationship between the concentration of elements such as Mo and Cd and bioturbation. Ultimately, the weak relationship between iron and bioturbation, which should directly indicate the presence of H_2 in the depositional bottom waters, suggests that the formation of the red bed was caused by diagenesis.

CHAPTER 4: SUMMARY AND CONCLUSIONS

The Mount Whyte, Cathedral, and Stephen Formations in Alberta were reconstructed through the analysis of drill cores, geological reports, and field data. The Middle Cambrian sediment package was then categorized into offshore, shoreface, and foreshore depositional systems using lithostratigraphic and ichnological methods. Two separate studies presented in this thesis offer insight into the depositional environment of the Middle Cambrian sediment package in Alberta.

Chapter 2 of the thesis focuses on the high-resolution facies analysis of the Mount Whyte formation in the Nordegg area of southwestern Alberta, located in the southern Rocky Mountains. The study is based on fieldwork of three outcrops, where data such as color, grain size, sedimentary structure, bioturbation, bedding thickness, contact, and sedimentary accessory features were recorded. Based on this data, six facies were identified, which formed a coherent succession from an offshore transit to shoreface depositional system. Additionally, the process ichnology study indicates a fully marine environment with low levels of physical and chemical stress.

In Chapter 3, the focus is on a comprehensive facies analysis of the Mount Whyte Formation using drill cores (1-6-38-15W4, 1-34-57-22W4, and 6-36-19-1W4) located in the Western Canada Sedimentary Basin of eastern Alberta. The study documented lithology, contacts, sedimentary structures, lithologic accessories, body fossils, and grain-size, as well as ichnological observations of individual trace fossils, distribution, burrow size, diversity, intensity, and trace fossil assemblages. The lithological and ichnological interpretations led to the identification of 9 facies representing depositional environments ranging from offshore to foreshore. Additionally, geochemical methods were utilized to investigate the relationship

between redox sensitive elements and bioturbation, as well as the formation of red beds. The findings suggest that the weak relationship between iron and redox environment indicates that the formation of the red bed was due to diagenesis.

REFERENCES

- Aitken, J. D. (1997). Stratigraphy of the Middle Cambrian platformal succession, southern Rocky Mountains. *Bulletin 398, Geological Survey of Canada.*
- Christie, R. L., Embry, A. F., & Van Dyck, G. A. (1981). *Lexicon of Canadian stratigraphy.* Canadian Society of Petroleum Geologists.
- Eren, M., & Kadir, S. (2013). Colour origin of red sandstone beds within the Hüdai Formation (Early Cambrian), Aydıncık (Mersin), southern Turkey. *Turkish Journal of Earth Sciences, 22(4), 563-573.*
- Folk, R. L. (1951). Stages of textural maturity in sedimentary rocks. *Journal of Sedimentary Research, 21(3), 127-130.*
- Lajoie, J., & Chagnon, A. (1973). Origin of red beds in a Cambrian flysch sequence, Canadian Appalachians, Quebec. *Sedimentology, 20, 91-103.*
- Hauck, T. E., et al. (2009). Brackish-water ichnological trends in a microtidal barrier island embayment system, Kouchibouguac National Park, New Brunswick, Canada. *Palaios, 24(8), 478-496.*
- Herbers, D. S., MacNaughton, R. B., Timmer, E. R., & Gingras, M. K. (2016). Sedimentology and ichnology of an Early-Middle Cambrian storm-influenced barred shoreface succession, Colville Hills, Northwest Territories. *Bulletin of Canadian Petroleum Geology, 64(4), 538-554.*
- Gingras, M. K., MacEachern, J. A., & Dashtgard, S. E. (2011). Process ichnology and the elucidation of physico-chemical stress. *Sedimentary Geology, 237(3), 115-134.*

- MacEachern, J. A., Stelck, C. R., & Pemberton, S. G. (1999). Marine and marginal marine mudstone deposition: Paleoenvironmental interpretations based on the integration of ichnology, palynology and foraminiferal paleoecology.
- MacEachern, J. A., Bann, K. L., Bhattacharya, J. P., & Howell, C. D., Jr. (2005). Ichnology of deltas: Organism responses to the dynamic interplay of rivers, waves, storms, and tides.
- MacEachern, J. A., Pemberton, S. G., Gingras, M. K., & Bann, K. L. (2010). Ichnology and facies models. In N. P. James & R. W. Dalrymple (Eds.), *Facies Models 4. GEOText 6*. Geological Association of Canada, 19-58.
- MacEachern, J. A., & Bann, K. L. (2008). The role of ichnology in refining shallow marine facies models.
- MacEachern, J. A., & Pemberton, S. G. (1992). Ichnological aspects of Cretaceous shoreface successions and shoreface variability in the Western Interior Seaway of North America.
- Mossop, G. D., & Shetsen, I. (1994). Introduction to the geological atlas of the Western Canada Sedimentary Basin. In G. Mossop & I. Shetsen (Eds.), *Geological Atlas of the Western Canada Sedimentary Basin*. Canadian Society of Petroleum Geologists and Alberta Research Council, 159-275.
- Pemberton, S. G., MacEachern, J. A., & Ranger, M. J. (1992). Ichnology and event stratigraphy: The use of trace fossils in recognizing tempestites. In S. G. Pemberton (Ed.), *Applications of Ichnology to Petroleum Exploration: A Core Workshop*. Society of Economic Paleontologists and Mineralogists Core Workshop 17, 85-117.

- Pemberton, S. G. (2001). *Ichnology & sedimentology of shallow to marginal marine systems: Ben Nevis & Avalon reservoirs, Jeanne d'Arc Basin*. Geological Association of Canada.
- Pemberton, S. G., MacEachern, J. A., Dashtgard, S. E., Bann, K. L., Gingras, M. K., & Zonneveld, J. P. (2012). Shorefaces. In *Developments in sedimentology* (Vol. 64, pp. 563-603). Elsevier.
- Pemberton, S. G., & MacEachern, J. A. (1995). The sequence stratigraphic significance of trace fossils: Examples from the Cretaceous foreland basin of Alberta, Canada.
- Pemberton, S. G., MacEachern, J. A., Brett, C. E., & Baird, G. C. (1997). The ichnological signature of storm deposits: the use of trace fossils in event stratigraphy. In *Paleontological Events: Stratigraphic, ecological and evolutionary implications* (pp. 73-109). Columbia University Press.
- Pemberton, S. G., & MacEachern, J. A. (1995). The sequence stratigraphic significance of trace fossils: Examples from the Cretaceous Foreland Basin of Alberta, Canada.
- Playter, T., Corlett, H., Konhauser, K., Robbins, L., Rohais, S., Crombez, V., ... & Zonneveld, J. P. (2018). Clinof orm identification and correlation in fine-grained sediments: A case study using the Triassic Montney Formation. *Sedimentology*, 65(1), 263-302.
- Ratcliffe, K. T., Wilson, A., Payenberg, T., Rittersbacher, A., Hildred, G. V., & Flint, S. S. (2015). Ground truthing chemostratigraphic correlations in fluvial systems. *AAPG Bulletin*, 99(1), 155-171.
- Seilacher, A. (1962). Paleontological studies in turbidite sedimentation and erosion. *Journal of Geology*, 70, 227-234.

Seilacher, A. (1978). Use of trace fossil assemblages for recognizing depositional environments.

In B. Basan (Ed.), *Trace Fossil Concepts: Society of Economic Paleontologists and Mineralogists: Short Course*, 5, 167-181.

Slind, O. L., Andrews, G. D., Murray, D. L., Norford, B. S., Paterson, D. F., Salas, C. J., &

Tawadros, E. E. (n.d.). Chapter 8 – Middle Cambrian to Lower Ordovician Strata.

Retrieved from <https://ags.aer.ca/publications/chapter-8-middle-cambrian-to-lower-ordovician-strata.htm>

Sommers, M. (2018). *Subsurface Analysis and Correlation of Cambrian Formations beneath the Colville Hills, Northern Mainland, Northwest Territories*.

Turner, P. (1979). Diagenetic origin of Cambrian marine red beds: Caerfai Bay shales, Dyfed, Wales. *Sedimentary Geology*, 24(3-4), 269-281.

Wignall, P. B., & Myers, K. J. (1988). Interpreting benthic oxygen levels in mudrocks: A new approach. *Geology*, 16(5), 452-455.

Wilson, M. A., Burt, R., & Lee, C. W. (2006). Improved elemental recoveries in soils with heating boric acid following microwave total digestion. *Communications in Soil Science and Plant Analysis*, 37(3-4), 513-524. <https://doi.org/10.1080/00103620500449377>

Ziegler, A. M., & McKerrow, W. S. (1975). Silurian marine red beds. *American Journal of Science*, 275, 31-56.

APPENDIX I: OBSERVATION OF OUTCROP ONE (OUTCROP CS200806A)

Table 4. Observation of outcrop one (Outcrop CS200806A)

Thickness (m)	Formation	Lithology	Grain size	Structure	Bioturbation	Bioturbation index (BI)	Color	Remarks
18	Mount Whyte	Shale/Mudstone	Clay/silty clay to fine sand	Cm scale planar bedding	No observation	N/A	Greenish grey	Nodulized surface
17	Mount Whyte	Shale/Mudstone	Clay/silty clay to fine sand	Cm scale planar bedding	No observation	N/A	Greenish grey	Nodulized surface
16	Mount Whyte	Shale/Mudstone	Clay/silty clay to fine sand	Cm scale planar bedding	No observation	N/A	Greenish grey	Nodulized surface
15	Mount Whyte	Sandstone	Upper fine sand	Parallel wavy lamination	Pl, Sk, Di,	4	Brown	Massive
14	Mount Whyte	Sandstone	Fine to upper fine sand	Wavy bedding	Di, Te	4-5	Brown to grey	Mostly massive and may have cryptical bioturbation
13	Mount Whyte	Shale/Mudstone	Clay/silty clay to fine sand	Cm scale planar to wavy bedding	No observation	N/A	Reddish brown to grey	N/A
12	Mount Whyte	Shale/Mudstone	Clay/silty clay to fine sand	Cm scale planar to wavy bedding	No observation	N/A	Reddish brown to grey	May have trace fossil
11	Mount Whyte	Shale/Mudstone	Clay/silty clay to fine sand	Cm scale planar to wavy bedding	No observation	N/A	Reddish brown to grey	Nodulized surface
10	Mount Whyte	Shale/Mudstone	Clay/silty clay to fine sand	Massive	No observation	N/A	Greenish grey	N/A
9	Mount Whyte	Sandstone	Fine to upper fine sand	Rarely appeared mm scale planar lamination	No observation	N/A	Grey to brown	Mostly massive may have cryptical bioturbation
8	Mount Whyte	Shale/Mudstone	Silty clay to fine sand	Cm scale planar bedding	No observation	N/A	Greenish grey	Nodulized surface

Table 4 (Continued)

7	Mount Whyte	Shale/Mudstone	Clay/silty clay to fine sand	Cm scale planar bedding	No observation	N/A	Greenish grey	Nodulized surface
6	missing	Missing	Missing	Missing	Missing	Missing	Missing	N/A
5	Mount Whyte	Sandstone	Fine to upper fine sand	no observation/massive	Di, Te and Unknown hook-like trace	4	Reddish brown and grey	N/A
4	Mount Whyte	Sandstone	Fine to upper fine sand	Mm-dm scale planar lamination/bedding	Di, Ar, Sk, Pl, Te	3	Reddish brown and greenish grey	Sharp base with the planar bedding
3	Mount Whyte	Sandstone	Fine to upper fine sand	Mm scale planar lamination/bedding	Rh, Di, Te Unknown hook-like trace	4	Reddish brown and greenish grey	Generally massive
2	Mount Whyte	Sandstone	Fine to upper fine sand	Mm-dm scale planar lamination/bedding	Cy, Ar, Sk, Te, Pl, Di, Rh Unknown hook-like trace	4	Reddish brown and greenish grey	Generally massive
1	Mount Whyte	Sandstone	Fine to upper fine sand	Mm-dm scale planar lamination/bedding mm scale crossbedding	Cy, Ar, Sk, Unknown hook-like trace	4-5	Pale greenish grey	Nodulized surface
0	Gog	Sandstone	Fine to upper fine sand	Mm-dm scale planar lamination/bedding	Sk on top view	1-2	Pale reddish brown to pale green	Sharp contact with Mount Whyte formation on the top

APPENDIX II: ICHNOLOGY DATA COLLECTION FORMS

Table 5 in appendix refers to Table 5. Ichnology data collection forms of 1-6-38-15W4.xlsx in the supplementary material.

Table 6 in appendix refers to Table 6. Ichnology data collection forms of 6-36-19-1W4.xlsx in the supplementary material.

Table 7 in appendix refers to Table 7. Ichnology data collection forms of 1-34-57-22W4.xlsx in the supplementary material.

APPENDIX III: GEOCHEMISTRY RESULT

Table 8 in appendix refers to Table 8. Complete results of elements concentration by HF digestion.xlsx in the supplementary material.

Table 9 in appendix refers to Table 9. Summarized table of geochemistry and ichnology data of well 6-36-19-1W4.xlsx in the supplementary material.

Table 10 in appendix refers to Table 10. Summarized table of geochemistry and ichnology data of well 1-6-38-15W4.xlsx in the supplementary material.

Table 11 in appendix refers to Table 11. Summarized table of geochemistry and ichnology data of well 1-34-57-22W4.xlsx in the supplementary material.

APPENDIX IV: EIGENVECTORS TABLES

Table 12 in appendix refers to Table 12. EigenVectors table for PCA of well 1-34-57-22W4.xlsx in the supplementary material.

Table 13 in appendix refers to Table 13. EigenVectors table for PCA of well 6-36-19-1W4.xlsx in the supplementary material.

Table 14 in appendix refers to Table 14. EigenVectors table for PCA of well 1-6-38-15W4.xlsx in the supplementary material.